Aus dem Institut für Medizinische Mikrobiologie und Krankenhaushygiene

Direktor: Prof. Dr. Michael Lohoff

des Fachbereichs Medizin der Philipps-Universität Marburg

The manifold roles of immunoproteasome and short-chain fatty acids in shaping the anti-tumor immune responses

Die vielfältigen Auswirkungen des Immunoproteasoms und kurzkettiger Fettsäuren auf die Anti-Tumor-Immunität

Kumulative Dissertation zur Erlangung des Doktorgrades der Naturwissenschaften (Dr. rer. nat.)

dem Fachbereich Medizin der Philipps-Universität Marburg

vorgelegt von

Hanna Katharina Leister

aus Bad Homburg

Marburg, 2023

Angenommen vom Fachbereich Medizin der Philipps-Universität Marburg am: 13.02.2023

Gedruckt mit Genehmigung des Fachbereichs Medizin

Dekanin: Prof. Dr. Hilfiker-Kleiner

Referent: Prof. Dr. Alexander Višekruna

Korreferent: PD. Dr. Till Adhikary

“It’s the questions we can’t answer that teach us the most. They teach us how to think. If you give a man an answer, all he gains is a little fact. But give him a question and he’ll look for his own answers. That way, when he finds the answers, they’ll be precious to him. The harder the question, the harder we hunt. The harder we hunt, the more we learn. An impossible question…”

Patrick Rothfuss, The Wise Man’s Fear

Inhalt

1 Abbreviations 4
2 Abstract 5
3 Zusammenfassung 6
4 Introduction 7
4.1 T cells 7
4.1.1 T cell subtypes 7
4.2 B cells 8
4.3 Dendritic cells 8
4.4 The proteasome: a major checkpoint in cellular regulation 9
4.4.1 Ubiquitin-proteasome pathway 9
4.4.2 Constitutive proteasome 9
4.4.3 Immunoproteasome 9
4.4.4 Thymoproteasome 10
4.4.5 Immunoproteasome and Immune System 10
4.5 Transcriptional and epigenetic gene regulation 12
4.5.1 Histone tail modifications and SCFAs 12
5 Aim of the present work 14
6 Results 15
6.1 Pro- and anti-tumorigenic capacity of immunoproteasomes in shaping the tumor microenvironment 15
6.2 Regulation of the effector function of $CD8^+$ T cells by gut microbiota-derived metabolite butyrate 17
6.3 Microbial short-chain fatty acids modulate $CD8^+$ T cell responses and improve adoptive immunotherapy for cancer 20
7 Discussion 24
7.1 The role of immunoproteasome in NF-κB pathway and antigen presentation during immune responses 24
7.2 Gut microbial SCFAs modulate $CD8^+$ T cell response and improve anti-cancer immunity of CAR T cells 25
8 References 28
9 Apendix 39
9.1 Curriculum vitae ..... **Fehler! Textmarke nicht definiert.**
9.2 Publications 39
9.3 Academic teachers 40
9.4 Acknowledgement 40

1 Abbreviations

APC	antigen presenting cell
bp	base pair
BMDCs	bone marrow derived DCs
CAC	colitis-associated carcinogenesis
CAR	chimeric antigen receptor
CD	cluster of differentiation
cP	constitutive proteasome
COX	cyclooxygenase
cTECs	cortical thymic epithelial cells
CTL	cytotoxic T lymphocytes
DCs	dendritic cells
2-DG	2-deoxyglucose
DNA	deoxyribonucleic acid
ER	endoplasmatic reticulum
ERAD	endoplasmic-reticulum-associated protein degradation
ERK	extracellular-signal regulated kinases
Foxp3	Forkhead-Box-Protein P3
HATs	histone acetyltransferases
HDACs	histone deacetylases
ICI	immune checkpoint inhibitory
iP	immunoproteasome
IBD	inflammatory bowel disease
IκBα	inhibitor of kappa B protein
IKK	I-KB kinase
ILCs	innate lymphoid cells
IFN-γ	Interferon-gamma
IL	interleukin
LPS	lipopolysaccharides
MHC	major histocompatibility complex
mLN	mesenteric lymph node
NF-κB	nuclear factor 'kappa-light-chain-enhancer' of activated B-cells
ROR1	receptor tyrosine kinase-like orphan receptor 1
RORγt	RAR-related orphan receptor gamma-t
ROS	reactive oxygen species
POMP	recombinant proteasome maturation protein
ROR-γt	retinoic acid-related orphan receptor
SCFAs	short-chain fatty acids
STAT	Signal transducer and activator of transcription
TAP	transporter associated with antigen processing
TCR	T cell receptors
Tfh	T follicular helper cells
Th	T helper
tP	thymoproteasome
TLR	Toll-like receptor
TME	tumor microenvironment
TNF	tumor necrosis factor
TGF	transforming growth factor
TF	transcription factor
TKO	Triple knockout
TSA	trichostatin A
UPP	ubiquitin-proteasome pathway
WT	wild type

2 Abstract

The mucosal immune system is shaped by tight interactions between immune cells and host microbiota. However, the factors contributing to the development of a functional immune system with a finely regulated homeostasis remain poorly understood. Here, we demonstrated the impact of the microbial metabolites SCFAs on the effector function of immune cells by modulation of metabolic state, as well as epigenetic regulation via HDAC inhibition. Especially the physiologically abundant SCFAs butyrate and pentanoate elicited beneficial effects on the effector function of $CD8^+$ T cells and might be considered for anti-cancer therapy implementation. In the second part of this study, we discovered that the proteasome, as a main checkpoint in cellular function, displays opposing roles in tumor development. As an activator of NF-κB, the immunoproteasome impacts on the expression of pro-inflammatory mediators. Consequently, the immunoproteasome exhibits pro-tumorigenic capacity in an inflammatory-driven carcinogenesis, such as colitis-associated cancer, by enhancing the expression of cytokines and chemokines, contributing to immune cell infiltration and inflammation. On the other side, the immunoproteasome might generate neo-antigens for presentation via MHC class I molecules, thereby enabling cytotoxic T cell response against solid tumors. We demonstrated that the lack of immunoproteasome subunits (LMP7, LMP2 and MECL-1) protects mice against the development of colitis-associated carcinogenesis, but in melanoma microenvironement, high expression of immunoproteasome is required to induce an efficient anti-tumor response.

3 Zusammenfassung

Das mukosale Immunsystem wird durch eine enge Wechselwirkung zwischen Immunzellen und der Mikrobiota des Wirts geformt. Die Faktoren, die zur Entwicklung eines funktionierenden Immunsystems beitragen, sind jedoch noch weitgehend unverstanden. Wir konnten zeigen, dass microbielle Metabolite wie kurzkettige Fettsäuren die Effektorfunktion von Immunzellen durch Modulation von metabolischen sowie epigenetischen Faktoren maßgeblich beeinflussen. Besonders die kurzkettigen Fettsäuren Butyrat und Pentanoat zeigten eine positive Wirkung auf die Effektorfunktion von $CD8^+$ T-Zellen und könnten für die Implementierung einer Anti-Krebs-Therapie in Betracht gezogen werden. Im zweiten Teil der Arbeit entdeckten wir, dass das Proteasom abhängig von der Umgebung gegensätzliche Rollen bei der Tumorprogression spielt. Mittels der Aktivierung von NF-κB reguliert das Immunoproteasom die Expression entzündungsfördernder Mediatoren. Folglich zeigt das Immunoproteasom pro-tumorigene Kapazität in einer entzündungsgetriebenen Karzinogenese, indem es die Expression von Zytokinen und Chemokinen verstärkt, welche die Infiltration von Immunzellen und Entzündungen verursacht. Auf der anderen Seite reguliert das Immunoproteasom die Präsentation von Antigenen über MHC Klasse I Moleküle. Demnach wäre es möglich, dass es ebenfalls zur Präsentation von tumoreigenen Antigenen beiträgt und die Wahrscheinlichkeit einer Erkennung durch das Immunsystem mit anschließender zytotoxischer T-Zellantwort gegen solide Tumore entscheidend erhöht. Wir konnten nachweisen, dass das Fehlen von Immunoproteasom-Untereinheiten Mäuse vor der Entwicklung einer Colitis-assoziierten Karzinogenese schützt. Allerdings ist in der Tumorumgebung eines malignen Melanoms eine hohe Expression des Immunoproteasoms erforderlich, um eine effiziente Antitumorantwort zu induzieren.

4 Introduction

The immune system is a complex, interactive network of various immune cell types defending its host against pathogens (e.g. bacteria or viruses) and malignant cells. At the most basic level, the distinction of „self“ from „non-self“ is required to prevent self-destruction. A synergy of adaptive and innate immunity defines the main lines of defense.

The evolutionary conserved innate immune system provides immediate but unspecific (antigen-independent) immune response by anatomical barriers (skin, mucosa), as well as cellular (neutrophils, macrophages, dendritic cells) and humoral components (complement, cytokines).

Cells of the adaptive immune system, which undergo a selection process, show an antigen-specific response and result in immunological memory (Murphy and Weaver 2018). The function of adaptive immunity is mainly based on T and B lymphocytes which are derived from hematopoietic stem cells.

4.1 T cells

Maturation and development of T cells takes place in the thymus where T cell receptors (TCR) have to interact with antigens presented by major histocompatibility complex (MHC) molecules. CD (cluster of differentiation) surface molecules (CD4 or CD8) define two different subsets of T cells and interact with either MHC class I or MHC class II molecules. An affinity for MHC class I, which is expressed on all nucleated cells, results in the development of $CD8^+$ cytotoxic T cells (CTL) which are capable of directly killing infected or tumor cells (Murphy and Weaver 2018). MHC class II is expressed on antigen presenting cells (APCs). The recognition of this complex drives the development of $CD4^+$ T helper cells.

4.1.1 T cell subtypes

Naive $CD4^+$ T cells that passed thymic selection process migrate to the secondary lymphoid organs to encounter their appropriate antigen presented by APCs. Recognition of the specific antigen, together with a costimulatory molecule, leads to differentiation into a distinct subset of T helper (Th) cell. The cytokine milieu in which the priming takes place is decisive for the differentiation process and shapes the immune response. Every Th subset is characterised by a specific cytokine profile and specific master transcription factor (TF). Consequently, every subset fulfils a specific function and is required for distinctive immune responses. Th1 cells for example are essential to combat intracellular pathogens and tumors. Activated APCs stimulate them to produce interferon-gamma (IFN-γ) by secreting interleukin (IL-)12. Th1 cells promote the maturation of CTLs and macrophages (Fields et al. 2002). Th2 cells in contrast are required for the defense against parasites and worms and they initiate the B cell class switch towards immunoglobulin (Ig)E antibodies (Schmitt et al. 2014). Besides their protective role in immunity, they are together with IL-9-secreting Th9 cells implicated in the development of inflammatory disease like allergy and asthma. Another Th subset involved in autoimmune disease as well as the defense against extracellular bacteria are Th17 cells. Mainly the cytokines IL-6, IL-21 and

transforming growth factor (TGF)-β drive the polarisation of these IL-17 A-producing cells (Lee et al. 2012). One of the main functions of Th cells is the recruitment of cells such as neutrophils and macrophages and orchestrating the immune response. Apart from this, they are crucial for the activation of B cells to undergo class switch and induce antibody production. T follicular helper cells (Tfh) especially provide help for B cells to produce high-affinity antibodies (Baumjohann and Ansel 2015).

As immune homeostasis is essential to prevent chronic inflammation, the regulatory T cells (Tregs) play an essential role in suppressing inflammation and act as counterpart to the Th cells. The differentiation into Tregs depends on the cytokine TGF-β. Their TF Forkhead-Box-Protein P3 (Foxp3) is inhibited by IL-6, meaning there is a balanced regulation between the polarisation towards Th17 or Treg cells depending on the surrounding cytokine milieu and especially on the abundance of IL-6. Th17 TF retinoic acid-related orphan receptor (ROR)-γt and Foxp3 are tightly regulated by each other.

Tregs can either develop in thymus (nTregs) upon interaction of high-affinity TCRs with MHC class II molecules presenting self-antigens (doi.org/10.4049/jimmunol.162.9.5317) or in the periphery (iTregs) where naïve T cells encounter their appropriate antigens in presence of TGF-β or microbial metabolites such as short-chain fatty acids (SCFA) (Smith et al. 2013). They are required to maintain a state of immune tolerance, as absence results in autoimmunity or chronic inflammation.

4.2 B cells

B cells belong to the lymphoid linage of immune cells. They originate from the bone marrow and finalize their maturation process in the B-cell follicles of the spleen (Murphy and Weaver 2018). During a process called VDJ recombination, an immunoglobulin-related antigen-specific B cell receptor is generated (Brack et al. 1978). Binding of the appropriate antigen leads to the internalization of the receptor-ligand complex and an MHC class II-mediated presentation of the respective antigen (Parker 1993b). The additional activation via Tfh cell binding offers further B cell activation with costimulatory molecules and mediates the maturation into antibody-secreting plasma cells (Parker 1993a). This class switch induces the formation of antibodies with changed constant region (Fc part), meaning they can lead to opsonisation and complement activation (Shimizu and Honjo 1984; Flannagan et al. 2012; Klasse and Sattentau 2002).

As for T cells, there is also a regulatory counterpart (Bregs) dampening inflammatory processes by secreting the anti-inflammatory cytokine IL-10. In context of infection, strong activation of Toll-like receptor (TLR) signalling leads to the development of regulatory B cells (Bregs) (Korniotis et al. 2016).

4.3 Dendritic cells

Dendritic cells (DCs) originate either from myeloid or lymphoid progenitor cells. Immature DCs are phagocytic cells that enter the tissue to encounter potential pathogens. The take up of a pathogen leads to their activation. Afterwards, they present pathogen-antigens to T lymphocytes thereby

inducing adaptive immune system. They build the bridge between innate and adaptive immunity. Furthermore, the secretion of IL-12 consisting of IL-12p40 and IL-12p35 drives the activation of Th cells as well as innate lymphoid cells (ILCs) (Murphy and Weaver 2018).

4.4 The proteasome: a major checkpoint in cellular regulation

4.4.1 Ubiquitin-proteasome pathway

The ubiquitin-proteasome pathway (UPP) has a central role in the selective degradation of intracellular proteins. More than 80% of the protein turnover is regulated by this pathway to maintain cellular homeostasis and cell viability (Crawford et al. 2011). Consequently, UPP regulates the levels of numerous proteins and therefore, affects multiple cellular functions, like transcription, cell cycle, inflammatory processes and the induction of apoptosis (Zollner et al. 2002). Dysfunction of the UPP is implicated in several autoimmune and neurodegenerative disease, although the exact mechanisms remain poorly understood (Basler et al. 2014; Dantuma and Bott 2014; Schmidt et al. 2010). The key step of this pathway, the degradation of proteins, is achieved by the proteasome.

4.4.2 Constitutive proteasome

The proteasome is a multi-subunit protease complex present in archaea, some bacteria and mammals. Two sub-complexes, 20S core proteasome and two 19S regulatory complex components form the 26S or constitutive proteasome (cP) (Krüger et al. 2001). The 20S core proteasome is the catalytic part of this multi-subunit complex. Its barrel-shaped structure consisting of seven membered stacked protein rings (two α- and two β-rings) enables the selective degradation of marked proteins. While the outer α-rings have scaffold-like function and seal the central channel, the inner β-rings contain the catalytic protein function (Groll et al. 2000). The three catalytic subunits (β1, β2 and β5) have distinct proteolytic activities (β1=caspase-like, β2=trypsin-like, β5=chymotrypsin-like) determining the generation of a specific repertoire of cleaved peptides for antigen presentation via MHC class I molecules. Recently, a mechanism was proposed in which the catalytic activities allosterically regulate each other, further accelerating the degradation of proteins inside the proteasome (Kisselev et al. 1999).

Apart from the important role of protein degradation by the catalytic part of the proteasome, the 19S regulatory complex accomplishes the unwinding and transfer of ubiquitinated proteins into the core complex in an ATP dependent manner (Kloetzel 2001).

4.4.3 Immunoproteasome

While cPs are ubiquitously located in nuclei and cytoplasm of all eukaryotes to degrade ubiquitinated proteins and maintain cellular homeostasis, other proteasome isoforms are exclusively present in specific tissues (Kniepert and Groettrup 2014). In mammals, the best-characterized isoform, apart from cP is the immunoproteasome (iP), which is optimized for efficient presentation of antigens via MHC class I molecules (Kloetzel and Ossendorp 2004). The exchange of the constitutive catalytic subunits by iP catalytic subunits: β1i (LMP2), β2i (MECL-1) and β5i (LMP7) can be induced in every nucleated

cell upon type I and type II IFNs stimulation (Ebstein et al. 2013; Heink et al. 2005). Apart from a higher protein turnover rate, iP subunits exhibit different cleavage specificities (β1i = chymotrypsin-like, β2i = trypsin-like, β5i = chymotrypsin-like) to generate peptides with a higher binding affinity for MHC class I complex. This circumstance allows an optimized antigen presentation, which is crucial in regard of a viral or bacterial infection to enable a rapid immune response (Khan et al. 2001; Kincaid et al. 2011). Upon infection with viruses or intracellular bacteria, the expression of iP in infected tissue is induced by IFN-γ. Simultaneously to the substitution of cP with iP subunits, the 19S regulatory complex is replaced by 11S regulator, composed of proteasome activator α (PA28α) and β (PA28β) (Basler et al. 2011; Kimura et al. 2015). Recently, additional isoforms of proteasomes like the spermatoproteasome and the thymoproteasome (tP) were identified (Belote and Zhong 2009; Murata et al. 2007).

4.4.4 Thymoproteasome

To circumvent auto reactivity, lymphocytes development requires thymic selection. Newly generated TCRαβ$^+$CD4$^+$CD8$^+$ cells are positively and negatively selected according to their TCR peptide-MHC complex interaction (Takahama et al. 2012). Positive selection takes place in the cortical thymus where the immature T cells must interact with a peptide-MHC complex with low-affinity binding. Upon this interaction the cells receive a survival signal and become single positive (CD4$^+$CD8$^-$/ CD4$^-$CD8$^+$) T cells. They migrate to the thymic medulla where they undergo negative selection. Lymphocytes with strongly self-reactive receptors are eliminated to prevent autoimmune reactions and develop self-tolerance (Palmer 2003).

Recent identification of the tP, which is exclusively expressed in cortical thymic epithelial cells (cTECs), has advanced our understanding of positive selection and how positive selection contributes to the establishment of the immune system. The tP consists of the subunits β1i and β2i together with the specialized catalytic protein β5t. In contrast to cP and iP, tP generates peptides with a lower binding affinity for MHC class I molecules. It is conceivable that peptides generated by tP are quite different from those generated by cP or iP. Consequently, cTECs display a unique repertoire of low affinity MHC class I-associated peptides, which facilitate positive selection of CD8$^+$ T cells. The number of CD4$^-$CD8$^+$ T cells in mice lacking β5t subunit is decreased to approximately 20-30% of that in normal mice, underlying the relevance of tP for positive selection of CD8$^+$ T cells (Nitta et al. 2010; Murata et al. 2018).

4.4.5 Immunoproteasome and Immune System

4.4.5.1 Infection

IP are constitutively expressed in immune cells like APCs or T lymphocytes (McCarthy and Weinberg 2015). The altered specificities (less caspase-like, more chymotrypsin-like) favour the formation of hydrophobic peptides that display a higher binding affinity for MHC class I molecules, facilitating antigen presentation (Driscoll et al. 1993). The degradation of foreign or tumor antigens for antigen

presentation by MHC class I molecules is crucial for the induction of a potent $CD8^+$ T cell response. Intracellular pathogens or mutated proteins are degraded by the proteasome, afterwards they are transported by the protein transporter associated with antigen processing (TAP) into the endoplasmatic reticulum (ER), where endoplasmic-reticulum-associated protein degradation (ERAD) loads them onto MHC class I molecules to guide them on the cell surface mediating MHC I-peptide-TCR interaction for $CD8^+$ T cell activation (Heink et al. 2006). Proteasome assembly is efficiently achieved by competitive integration of the catalytic subunits. The high affinity of iP subunits to assembling proteins facilitates the replacement of cP subunits. Especially LMP7 interaction with recombinant proteasome maturation protein (POMP) (a chaperone that binds selectively to precursor subunits) promotes proteasome assembly and increases the amount of iP in infected cells (Heink et al. 2005). Under inflammatory conditions, activated CTLs produce IFN-γ, thereby further increasing the expression of iP and consequently antigen presentation. The lack of iP subunits in mice reduced $CD8^+$ T cell mediated immune responses during viral infections (Chen et al. 2001; Moebius et al. 2010; Robek et al. 2007). Furthermore, combined deficiency of all three iP subunits abrogated the development of an effective host resistance against *Trypanosoma cruzi* in mice, leading to significantly impaired *T. cruzi*-specific $CD8^+$ T cell responses (Ersching et al. 2016). In general, the lack of iP limits the repertoire of peptides for antigen presentation, resulting in a 50% lower MHC class I surface presentation in mice-deficient for iP. Additionally those mice reject skin transplants or splenic cells from wild type (WT) animals, suggesting that the set of peptides presented in WT and iP-deficient animals markedly differs (Kincaid et al. 2011; Toes et al. 2001).

4.4.5.2 Chronic inflammation and colitis-associated carcinogenesis (CAC)

Besides the obvious impact of the proteasome on antigen presentation, the proteasome is involved in multiple cellular regulations. We and others have shown that iP activity in the inflamed intestine promotes the production of pro-inflammatory cytokines, like IL-6, tumor necrosis factor (TNF)-a, IL-17A and IL-23 (Basler et al. 2010; Schmidt et al. 2010; Visekruna et al. 2006). These cytokines are the integral part of a signalling network, which synergistically activates nuclear factor 'kappa-light-chain-enhancer' of activated B-cells (NF-κB) and signal transducer and activator of transcription *(*STAT)3 (Simone et al. 2015). NF-κB not only regulates inflammatory responses, but is also involved in various tumor-related processes, such as suppression of apoptosis and induction of proliferation, angiogenesis and migration (Kubiczkova et al. 2014). By masking its nuclear localization site, inhibitor of kappa B protein (IκBα) keeps NF-κB dimers sequestered in the cytoplasm in an inactive state. In case of an NF-κB activation signal, I-KB kinase (IKK) phosphorylates IκBα, which further becomes ubiquitinated by an E3 ligase and afterwards degraded by the proteasome. The proteasomal degradation of IκBα is a crucial step in the activation of inflammatory NF-κB signalling cascade leading to expression of pro-inflammatory cytokines like IL-6, TNF-α and IL-17A, as well as chemokines (CXCL-1, -2, -3), which are

involved in the recruitment of inflammatory leucocytes (West et al. 2015). Infiltrating neutrophils as well as other immune cells cause tissue damage chronic cellular stress and further support tumorigenesis (Greten et al. 2004). The activation of NF-κB and the expression of pro-inflammatory cytokines are crucially implicated in the onset of inflammation-associated carcinogenesis (CAC) in the gut. Patients suffering from inflammatory bowel disease (IBD) excessively produce pro-inflammatory cytokines contributing to the development of CAC (Karin 2009; Neurath 2014; West et al. 2015). The specific inhibition of iP subunit LMP7, as well as the non-specific inhibition of the proteasome with bortezomib, supressed the expression of pro-inflammatory cytokines and prevented the development of colitis in mice (Kalim et al. 2012; Schmidt et al. 2010). Pharmacological inhibition of iP subunit LMP7 has been shown to limit inflammation and inflammation-associated carcinogenesis (Vachharajani et al. 2017).

4.5 Transcriptional and epigenetic gene regulation

The human genome comprises around three mega-base pairs (bp) and over the last decades about 20.000 to 25.000 genes have been identified to encode for essential proteins (International Human Genome Sequencing Consortium 2004). Apart from that, the question arises how differentiation processes and transcription of those are regulated, as a tightly controlled expression of specific factors is essential to enable the appropriate immune responses.

Currently it is assumed, that epigenetic modifications enable a precise regulation, despite genetic homogeneity. Histone modifications are meanwhile accepted to impact on transcriptional control. Additionally, in recent years several new histone modifications, besides the very well accepted DNA methylation and phosphorylation, have been described. Therefore, epigenetic modifications might be the key mechanisms involved in fine tuning gene expression. The genome in all eukaryotic cells is arranged in chromatin, a macromolecular complex composed of DNA and protein. The DNA is wrapped around histone complexes, consisting of dimers of four histone proteins (H2A, H2B, H3 and H4) which together form the nucleosomes, that allow a 10.000 to 20.000-fold compression (Zentner and Henikoff 2013). The term chromatin remodelling describes changes at nucleosomes such as posttranslational modifications of the histone tails like acetylation, ubiquitinylation, sumoylation or methylation and contributes to the encoding of epigenetic information (Ryu and Hochstrasser 2021).

4.5.1 Histone tail modifications and SCFAs

The posttranslational modification of histone tails has been highly investigated in recent years. The stability of nucleosomes is supported by the interaction of positively charged lysine residues of histones and the negatively charged DNA phosphate backbone. Acetylation of a lysine residue has been shown to decrease this interaction, contributing to higher accessibility of the DNA for transcription (Dion et al. 2005). The two antagonistic enzyme-classes histone acetyltransferases (HATs) and histone

deacetylases (HDACs) are responsible for acetylation and deacetylation of lysine residues (Alabert et al. 2017). Apart from acetylation, histone methylation of lysine residues at histone H3 or H4 by methyltransferases has been described to silence or activate gene expression, determined by the position and number of methyl groups (Kanno et al. 2012). Interestingly, recent research identified even larger posttranslational modifications like propionylation and butyrylation, indicating, that SCFAs might be potential substrates for histone modification (Kebede et al. 2017).

The human microbiota consists of six main phyla and is dominated by the phyla *Bacteroides* and *Firmicutes*. The generation of bacterial metabolites has been associated with various effect on the immune system. For instance, these metabolites have been described to impact and shape the immune cells via surface receptor interaction or even intracellularly.

Dietary fibres are indigestible for humans therefore they pass the upper part of the gastrointestinal tract and are metabolized by bacteria mainly in the caecum and colon. Gut commensal bacteria like *Clostridia* and *Prevotella* are enzymatically equipped to generate SCFAs apart from other bacterial metabolites (El Kaoutari et al. 2013). The most abundant SCFAs generated by gut commensals are acetate, propionate and butyrate, but also branched SCFAs like isobutyrate have been identified in the human gut (Koh et al. 2016). As they are able to cross the epithelial barrier, they are capable to directly shape the mucosal immune response. The oral administration of SCFAs has been shown to have beneficial protective effects in experimental models of colitis, multiple sclerosis, type 1 diabetes, allergic airway inflammation and food allergy (Berndt et al. 2012; Haghikia et al. 2016; Trompette et al. 2014; Tan et al. 2016; Mariño et al. 2017). Interestingly, it has been shown that SCFAs interact with receptor GPR43, which is selectively expressed on colonic regulatory T cells (Smith et al. 2013). Additionally, the uptake of SCFAs by mucosal T cells induced the differentiation of peripheral Tregs. SCFAs acted as HDAC inhibitors and enhanced expression of Foxp3 TF (Furusawa et al. 2013; Arpaia et al. 2013).

5 Aim of the present work

Activation of innate and adaptive immunity as well as inflammatory signalling are tightly regulated by the NF-κB signalling. A crucial step in NF-κB activation is mediated by the proteasome, which is itself a main checkpoint of cellular function and is implicated in the differentiation of T cells via the regulation of cytokine expression. By activating NF-κB signalling, the proteasome directly affects pro-inflammatory gene expression. The lack of LMP7 subunit has been described to protect mice against the development of inflammation-driven carcinogenesis. As LMP7 is only one of three iP subunits, we wondered whether the complete knockout of all three iP subunits has the same beneficial effects against the development of inflammation-driven disease. Furthermore, we intended to analyse the role of iP in the tumor microenvironment (TME) of melanoma.

The immune system is a complex network shaped by environmental factors like the gut microbiota. Bacterial metabolites directly affect the differentiation of immune cells and establish a state of tolerance by supporting the inhibitory potential of Tregs. A dysregulation of this finely balanced homeostasis leads to the development of disease. One aim of this study was to elucidate the mechanisms on how microbial-derived SCFAs affect $CD8^+$ T cells. We specifically focused on their function as epigenetic modulators and their impact on the metabolic state of T cells, deciphering if they could be used as a potential therapeutic agent.

6 Results

6.1 Pro- and anti-tumorigenic capacity of immunoproteasomes in shaping the tumor microenvironment

Hanna Leister#, Maik Luu#, Daniel Staudenraus, Aleksandra Lopez Krol, Hans-Joachim Mollenkopf, Arjun Sharma, Nils Schmerer, Leon N. Schulte, Wilhelm Bertrams, Bernd Schmeck, Markus Bosmann, Ulrich Steinhoff, Alexander Visekruna

Cancer Immunol Res. 2021 June ; 9(6): 682–692. doi:10.1158/2326-6066.CIR-20-0492

In this study, we described the opposing roles of iP in regulating the tumor microenvironment (TME). The function of the iP is to optimize $CD8^+$ T cell response during viral and intracellular bacterial infection. We hypothesized, that the presentation of neo-antigens might also depend on proteasome composition, as the isoform and expression of the proteasome dictates the peptide repertoire in a cell. As solid tumors like melanoma are independent of chronic inflammation, we wondered whether the expression of the iP in such tumors might play a role in the modulation of the immune response and the tumor progression, as well as in the modulation of TME.

The immunoproteasome is involved in presentation of tumor antigens to $CD8^+$ T cells (Vigneron et al. 2017; Groettrup et al. 2010). However, the role of iP in the onset of melanoma was largely unknown. We examined the expression of iP subunit LMP7 (*PSMB8*), LMP2 (*PSMB9*) and MECL-1 (*PSMB10*) in TCGA datasets from 470 patients suffering from skin cutaneous melanoma. Indeed, we observed a significant correlation of a better overall survival and a high expression of all three iP subunits, suggesting that iP might be a prognostic marker for melanoma patients (Fig. 1A).

As the effect of cP and iP on the TME were only poorly characterized, we analysed WT mice and mice lacking all three iP subunits (*Triple knockout* (TKO) mice) implanted with B16-F10 melanoma tumors. We observed a significantly higher increase in tumor volume and weight in TKO mice compared to WT animals, suggesting that iP contributes to anti-tumor response in this model (Fig. 1B-D). Additionally, TKO mice recruited less IFN-γ^+ $CD8^+$ cytotoxic T cells (CTLs) into the tumor and the tumor draining lymph nodes at day 15 after tumor cell injection, resulting in less IFN-γ in the TME (Fig. 1E-G).

As TKO mice completely lack iP subunits, they are unable to build complete tP (β5t, LMP2 and MECL-1). The tP is crucial for positive selection of immature thymocytes (Nitta et al. 2010). Consequently, naïve TKO mice have reduced frequencies and cell numbers of CD8 single positive thymocytes and $CD8^+$ T cells in the periphery compared to WT mice (sF. S3) (Kincaid et al. 2011). LMP7-deficient animals at steady state displayed normal level of $CD8^+$ T cells, suggesting that the lack of the iP subunits LMP2 and MECL-1, which are part of the tP, might be responsible for this defect (sF. S4).

To exclude that the observed effects were mediated by the partial lack of $CD8^+$ T cells in TKO mice, we assessed the impact of LMP7-deficiency on melanoma growth. We injected B16-F10 cells subcutaneously into WT and LMP7-deficient mice. LMP7 KO mice showed like TKO mice progressively increased tumor growth compared to WT mice. Although the frequency of $CD4^+$ and $CD8^+$ T cells in

tumors and tumor draining lymph nodes of LMP7-deficient mice was comparable to WT animals, they showed reduced numbers of IFN-γ$^+$ T lymphocytes (Fig. 2C-D, sFig. S5). In absence of LMP7 subunit, CD4$^+$ T cells isolated from the tumors showed a reduced expression of IFN-γ and IL 17A cytokines (Fig. 2E). Similarly, tumor-derived CTLs from LMP7 KO mice produced less IFN-γ than WT mice (Fig. 2F). Additionally, the expression of TNF-α and IL-12 in the TME was significantly reduced in LMP7-deficient mice (Fig. 2G), indicating that the absence of LMP7 subunit affects the cytokine expression in APC as well. As these cytokines induce the production of IFN-γ in T cells, this might partially explain this effect. *In vitro* generated bone marrow derived DCs (BMDCs) of LMP7-deficient and TKO mice, in contrast to WT animals, were not able to upregulate IL-12 expression upon stimulation with LPS (sFig. S6). Collectively, these results highlight the important role of iP in shaping CTL, CD4$^+$ T cell and APC anti-tumor activity.

Further, we could show, that in absence of the iP the cytokines and chemokines produced in TME were not able to induce the expression of iP subunit LMP7 in tumors (B16 melanoma cells express iP subunits) of LMP7-deficient and TKO animals compared to WT animals (sFig. S7). This implies that the expression of IFN-γ in immune cells of WT mice directly induce the expression of iPs in tumor cells and enhances the neo-antigen presentation. This was also confirmed in *in vitro* experiments, as the treatment with IFN-γ directly induced the expression of iP subunits in B16-F10 cells (sFig. S7). Furthermore, the overexpression of iP in human melanoma cells has been shown to have a clear tendency to increase their immunogenic antigen repertoire (Kalaora et al. 2020).

Apart from the role in antigen presentation, we and others could show that pharmacological inhibition of the iP efficiently inhibits the development of colitis and colitis-associated cancer (CAC) (Schmidt et al. 2010; Koerner et al. 2017; Vachharajani et al. 2017). Additionally, other laboratories could demonstrate that iPs orchestrate the onset of inflammation driven disease like Crohn's disease and rheumatoid arthritis (Muchamuel et al. 2009; Visekruna et al. 2006). To better understand the role of the iP on the TME during inflammation driven carcinogenesis, we treated mice lacking iP (TKO) and WT animal with AOM/DSS. WT mice after 80 days developed cancer-associated neoplasia, indicated by weight loss, colon shortening and tumor development. TKO mice exhibited less weight loss and shortening of the colon, as well as almost no detectable tumors compared to WT mice. H&E staining showed infiltration of immune cells and tissue damage in WT but not TKO mice (Fig 3A-D).

At day 30 after induction of AOM/DSS-mediated carcinogenesis lower percentage of CD4$^+$ IFN-γ and IL-17A producing cells, along with reduced tumor numbers and lower frequencies of infiltrating neutrophils, were found in TKO lamina propria compared to WT mice (Fig. 4A-C). RT-qPCR confirmed a reduced expression of pro-inflammatory cytokines such as IL-6, IL-1β and cyclooxygenase (COX)-2, an enzyme that directly enhances the proliferative capacity of epithelia cells. Additionally, the expression of the chemokines CXCL1, CXCL2 and CXCL3, attracting neutrophil infiltration, were

downregulated in TKO mice (Fig. 4D). The production of IL-1β and reactive oxygen species (ROS) by activated neutrophils directly contributes to tissue damage, thereby aggravating the pathogenesis of CAC through induction of DNA damage in epithelial cells (Shang et al. 2012; Wang et al. 2014). As the maturation of neutrophils in the bone marrow of TKO mice was normal (sFig. S8), we concluded that the recruitment must be impaired in the absence of iP. Lipopolysaccharides (LPS)/IFN-γ treated APCs lacking iP showed partially defective activation of extracellular-signal regulated kinases (ERK) and NF-κB signalling pathways (sFig. S9). These signalling pathways are essentially involved in the transcription of pro-inflammatory mediators, which are associated with CAC development. It is known that their optimal function is dependent on proteasome/ubiquitin system (Sun and Ley 2008). We could demonstrate that NF-κB pathway in thymocytes of naïve TKO mice was not affected, indicating that only inflammation-driven chronic activity of NF-κB is impaired in the absence of iP (sFig. S9).

Ulcerative colitis is a chronic inflammatory disease with a high risk to develop colorectal cancer (CRC) (Neurath 2014). As iP-induced factors play an essential role in the development of chronic inflammation and CRC, we performed micro array analysis of UC patients. This data revealed that UC, but not Crohn's disease patients had a pronounced signature of genes associated with the recruitment of innate immune cells, including neutrophil attracting chemokines CXCL1, CXCL2 and CXCL3 (Fig. 5A). Genes characteristic for adenoma/adenocarcinoma were significantly enriched compared to control colonic tissue (Fig. 5B). Interestingly, also the iP expression was significantly upregulated in chronically inflamed tissues of UC patients (Fig. 5C). It was completely unknown if malignant epithelial cells were able to express iP. We could demonstrate that the treatment of HT29 cells, a human colorectal adenocarcinoma cell line, with IFN-γ led to the expression of iP in those cells. Additionally, the combined treatment with IFN-γ, TNF-α and IL-1β significantly induced the expression of CXCL1 to 3 and was completely abrogated upon the additional treatment with the iP inhibitor ONX 0914 (Fig. 5E). Thus, the iP are not only important in shaping the TME, but also actively promote the recruitment of innate immune cells and thereby support inflammation-driven carcinogenesis. Together, our data provided insight in the pathogenesis of CAC and furthermore it could be suggested that the treatment of UC patients with proteasome inhibitor might reduce the risk of developing cancer.

For this work I contributed in planning and carrying out the experiments leading to the figures 1, 3, 4 and 5, as well as the supplementary figures. I helped in redacting and revising the manuscript (text and figures).

6.2 Regulation of the effector function of $CD8^+$ T cells by gut microbiota-derived metabolite butyrate

Maik Luu, Katharina Weigand, Fatana Wedi, Carina Breidenbend, **Hanna Leister**, Sabine Pautz, Till Adhikary & Alexander Visekruna

Bacterial fermentation of non-digestible, complex carbohydrates such as dietary fibres generates SCFAs. While the anti-inflammatory capacity of SCFAs has been extensively investigated, recent findings revealed an impact on $CD4^+$ effector T cells (Park et al. 2015; Luu et al. 2017). SCFAs are able to modulate the function and phenotype of numerous immune cells such as neutrophils, macrophages and DCs (Kim et al. 2013; Singh et al. 2014; Meijer et al. 2010). Nevertheless, the effects on $CD8^+$ T cell-mediated anti-tumor immunity remained largely unknown. We were able to show that the treatment of $CD8^+$ T cells induced a switch towards CTL phenotype and enhanced anti-tumor effector cytokine expression by HDAC inhibition.

We examined the effects of the SCFAs propionate, acetate and butyrate on CTLs and Tc17 cells *in vitro* and observed an increase in the frequency of IFN-γ^+ cells compared to the untreated control. Of note, butyrate treatment exerted the strongest effects. Additionally, the treatment with butyrate reduced the production of IL-17A in Tc17 cells, shifting their cytokine profile from producing mainly IL-17A towards IFN-γ (Fig 1A-F). To test whether treatment with SCFAs could alter IFN-γ production of $CD8^+$ T cells *in vivo* we treated WT mice for three weeks orally with SCFAs and examined the frequency of IFN-γ-producing $CD4^+$ and $CD8^+$ T cells afterwards via flow cytometry analysis. We observed a slight but reproducible increase in IFN- γ^+ $CD8^+$ T cells in mesenteric lymph nodes (mLN) but not in the spleen (Fig 1g, h). In contrast, the treatment with butyrate had no effect on $CD4^+$ T cells (sFig. 1A-B).

Apart from IFN-γ, CTLs produce the effector molecule granzyme B, mediating cytotoxicity. *In vitro* treatment with butyrate significantly increased the frequency of IFN-γ^+ granzyme B^+ $CD8^+$ T cell population (Fig 2A-B). Interestingly, this effect turned out to be long lasting. Pre-treatment with butyrate increased the frequency of IFN-γ^+ cells and was still measurable 3 days after the withdrawal of the SCFAs. Similarly, the adoptive transfer of $Ly5.1^+$ CTLs pre-treated with butyrate, into untreated $Ly5.2^+$ host mice, maintained high level of T-bet and IFN-γ (sFig 2B).

We also revealed that the treatment with butyrate completely changed the expression profile of Tc17 cells. Normally these cells have a high expression of IL-17A RORγt, with low levels of granzyme B, perforin, T-bet and Eomes. Upon treatment granzyme B levels as well as the expression of CTL-associated genes *Tbx21*, *Eomes* and *Prf1* significantly increased and the expression of Tc17 specific TF RORγt was significantly downregulated (Fig. 2C-E).

To understand the underlying mechanism and the role of TF T-bet, we treated Tc17 cells and CTLs derived from WT mice and mice deficient for T-bet (*Tbx21-/-*) with SCFAs. *Tbx21-/-* cells treated with butyrate displayed only a partially defective production of IFN-γ and an incomplete switch towards CTL phenotype (Fig. 3A-B). The TF Eomes is essential for the optimal expression of granzyme B, IFN-γ and perforin in $CD8^+$ T cells (Intlekofer et al. 2005; Araki et al. 2008). Regarding this, it is conceivable that butyrate-mediated induction of Eomes, apart from T-bet might be required for phenotypical alterations within the $CD8^+$ T cell subset.

As mentioned before, SCFA-mediated effects include the direct interaction with surface receptors such as GPR41 and GPR43, as well as the inhibition of HDAC enzymes. Both mechanisms affect the gene expression. To examine the cellular pathways involved in the regulation of $CD8^+$ T cells treated with butyrate, we investigated whether the effects are mediated by the receptors GPR41 and GPR43. CTLs and Tc17 cells deficient for those receptors showed no differences in the frequencies of IFN-γ. *In vivo* the treatment of mice deficient for GPR41 and GPR43 (*Ffar2-/-Ffar3-/-)* showed similarly to WT mice an increase in the percentage of IFN-γ^+CD8^+ T cells in the mLN (sFig. 3D). These data demonstrated that the surface molecules are dispensable for butyrate-mediated effects on $CD8^+$ T cells.

On the other hand, we investigated the role of butyrate as HDAC inhibitor in $CD8^+$ T cells. Western blot analysis revealed an increase in acetylation of histone H4 by butyrate treatment in CTLs (Fig. 3C). Quantitative Chip analysis of histone H4 in $CD8^+$ T cells revealed that the treatment with butyrate enhanced acetylation at *Tbx21* and *IFNγ* promoters in CTLs (Fig. 3D).

A fluorometric HDAC activity assay clearly indicated that butyrate, as well as valproate exerted a strong HDAC inhibitory effect, similar to the effect of trichostatin A (TSA), a pan-HDAC inhibitor. In contrast, acetate did not show an inhibitory effect to the enzymatic activity of HDACs derived from $CD8^+$ T cell lysates (Fig. 4A). Interestingly, butyrate displayed the same inhibitory capacity to cell lysates derived from *Ffar2-/-Ffar3-/-* CTLs, indicating, that the effects of SCFAs are mediated via HDAC inhibition (sFig. 3E). Furthermore, treatment of CTLs and Tc17 cells with HDAC inhibitor TSA and valproate also significantly increased IFN-γ production and mediated a switch towards CTL phenotype, similar to butyrate treatment. In addition, the frequencies of granzyme B^+ IFN-γ^+ T cells were increased compared to untreated cells (Fig. 4B-H). Together, these results suggest that physiological HDAC inhibitor butyrate induces enhanced histone acetylation, thereby supporting a CTL-associated phenotype in $CD8^+$ T cells.

Recent studies revealed an increase in $Foxp3^+CD4^+$ Treg differentiation upon butyrate treatment (Smith et al. 2013; Furusawa et al. 2013; Arpaia et al. 2013). A high prevalence of unusual $Foxp3^+CD8^+$ regulatory T cells has been associated with immunosuppressive microenvironment of colorectal cancer (Chaput et al. 2009). Interestingly, we observed that combined treatment of $CD8^+$ T cells under Treg-inducing condition with butyrate or TSA induced a switch towards CTL phenotype and increased the expression of T-bet and IFN-γ. As *Tbx21-/-* cells were not able to downregulate Foxp3 expression in contrast to WT cells, this effect partially depends on T-bet (sFig. 4A-D). Together, our findings indicate that in $CD8^+$ T cells the effect of butyrate is triggered via HDAC inhibitory activity and not GPR41 and GPR43 receptors.

Furthermore, treatment with 25mM of acetate mediated comparable increases in IFN-γ production as 1mM butyrate (Fig. 5C-D). As previously described acetate treatment is associated with enhanced AKT/mTOR pathway (Park et al. 2015). Rapamycin treatment, the inhibitor of mTor, downregulated

IFN-γ expression in acetate but not butyrate treated CTLs, suggesting that acetate enhances IFN-γ production by acting as a metabolic substrate and butyrate primarily acts as HDAC inhibitor to increase expression of IFN-γ in $CD8^+$ T cells.

For this work I contributed in carrying out the flow cytometry experiments and I helped in analysing the data.

6.3 Microbial short-chain fatty acids modulate $CD8^+$ T cell responses and improve adoptive immunotherapy for cancer

Maik Luu, Zeno Riester, Adrian Baldrich, Nicole Reichardt, Samantha Yuille, Alessandro Busetti, Matthias Klein, Anne Wempe, **Hanna Leister**, Hartmann Raifer, Felix Picard, Khalid Muhammad, Kim Ohl , Rossana Romero, Florence Fischer, Christian A. Bauer, Magdalena Huber, Thomas M. Gress, Matthias Lauth, Sophia Danhof, Tobias Bopp, Thomas Nerreter, Imke E. Mulder, Ulrich Steinhoff, Michael Hudecek & Alexander Visekruna

Several studies recently demonstrated that the intestinal microbiota directly affects the efficacy of cancer immune therapies (Sivan et al. 2015). Adoptive transfer of tumor specific $CD8^+$ cytotoxic T cells as well as immune checkpoint inhibitory (ICI) therapy have been shown to be influenced by the composition of microbiota (Wang et al. 2018). Previous studies have revealed SCFAs to promote the expansion of Tregs, protect against autoimmune disease, and enhance the effector function of T cells (Arpaia et al. 2013; Furusawa et al. 2013; Park et al. 2015; Kespohl et al. 2017; Mariño et al. 2017). Interestingly, SCFA pentanoate induced strong production of effector molecules in CTLs and chimeric antigen receptor (CAR) T cells, resulting in an enhanced anti-tumor immunity (Luu et al. 2019).

In this work, we demonstrated that the SCFAs butyrate and pentanoate enhance anti-tumor activity of CTLs and CAR T cells through metabolic and epigenetic reprograming. Enhanced mTOR activity combined with the inhibition of class I HDAC activity resulted in elevated production of effector molecules and significantly improved anti-tumor response in syngeneic murine melanoma and pancreatic cancer models.

As mentioned before, it is well established, that commensal microbiota generates SCFAs by degradation of non-digestible fibres. While most commensals generate high amounts of acetate and formate, we observed that some few like *Faecalibacterium prausnitzii* and *Anaerostipes hadrus* synthesized high amounts of butyrate (Fig. 1A). Furthermore, we demonstrated that the low abundant bacteria *Megasphera massiliensis* was able to produce high amounts of the SCFA pentanoate. We observed that the treatment of CTLs with supernatants of *M. massiliensis* markedly increased the frequencies of IFN-γ^+ TNF-α^+ $CD8^+$ T cells (Fig. 1B). To elucidate the direct effect of those SCFAs, we performed control treatment with the pure SCFAs and observed the same phenomenon (Fig 1.C-D). We decided to perform further analysis with pentanoate and butyrate as they had the strongest effects on CTLs.

SCFAs are known to inhibit HDAC activity, thereby epigenetically modulating the fate of eukaryotic cells (Koh et al. 2016). Among the 16 tested commensal strains, we discovered that the pentanoate and butyrate-producing bacteria *M. massiliensis, M. elsdenii, F. prausnitzii* and *A. hadrus* specifically exhibited pan-HDAC inhibitory capacity. Particularly HDAC class I was inhibited by those but not by other bacteria (Fig. 2A). Cell lysates generated from CTLs treated with butyrate and pentanoate exhibited similar inhibition of HDAC activity (Fig. 2B). Further, we observed an increase in the production of TNF-α and IFN-γ by CTLs treated with pentanoate and butyrate. Interestingly, also treatment with the HDAC class I inhibitor mocetinostat increased the percentage of IFN-γ^+ TNF-α^+ $CD8^+$ T cells. TMP-195, a specific HDAC class II inhibitor in contrast showed no significant changes in the cytokine expression profile (Fig. 2C-E). These results suggested a specific inhibition of HDAC class I modulates the effector function of CTLs. It is well established, that the expression of IFN-γ as well as the effector function of T cells is dependent on the glycolytic metabolic pathway (Luu et al. 2019; Chang et al. 2013; Peng et al. 2016; Qiu et al. 2019; Cham and Gajewski 2005). Consequently, the inhibition of glycolysis by the glucose analogue 2-deoxyglucose (2-DG) or inhibition of mTOR complex by rapamycin resulted in a decrease of IFN-γ production (sFig. 4A). T cells can utilize SCFAs for their metabolic demand (Kim et al. 2016; Balmer et al. 2016). We demonstrated that SCFA pentanoate is capable of increasing mTOR complex activity, a key regulator of cell growth and metabolism, as well as its downstream target S6 ribosomal protein. As the HDAC inhibitors mocetinostat and TMP-195 had no effect on mTOR and S6 phosphorylation, the impact of butyrate and pentanoate on metabolic status of T cells seemed to be HDAC independent (Fig. 2F). SCFAs also act via the binding of G-protein-coupled receptors (GPR41 and GPR43). Therefore, we validated if the lack of those receptors affected the expression of IFN-γ in CTLs and observed no effects. We concluded that the expression of IFN-γ and effector molecules in CTLs might be mediated via metabolic modulation and HDAC inhibition and not *via* G-protein-coupled receptors (sFig. 5C).

Next, we examined the anti-tumor reactivity of SCFAs treated CTLs *in vivo*. OT-I CTLs pre-treated with pentanoate or butyrate showed significantly increased anti-tumor activity against s.c. injected B16OVA melanoma cells, indicated by decreased tumor volume (Fig 3A-C). On day 10 after adoptive transfer, higher percentages of pre-treated CTLs were present in the LNs and expressed higher levels of IFN-γ and TNF-α compared to untreated CTLs (Fig. 3D-G). Similar effects were mediated by the pre-treatment of CTLs with supernatant of *M. massiliensis* (Fig. 3B-G). HDAC class I inhibition elicited similar effects on adoptively transferred CTLs, but to a lesser extent than butyrate and pentanoate treatment. In contrast, HDAC inhibitor TMP-195 did not enhance the anti-tumor immune responses (Fig. 3B-G).

PancO2 cells expressing OVA protein (PancOVA) are used for an aggressive pancreatic tumor model. We assessed the anti-tumor capacity of pentanoate-treated CTLs in this model and demonstrated that the adoptive transfer of low numbers ($7.5x10^5$) of pentanoate-treated $CD45.1^+$ OT-I $CD8^+$ T

lymphocytes was sufficient to significantly abrogate the tumor growth in CD45.2$^+$ recipient animals compared to untreated CTLs (Fig. 3H-J). Of note, while the untreated cells on day 23 after tumor inoculation were hardly found, pentanoate-treated cells were persistent and had a high expression of IFN-γ within the LNs and spleen of recipient mice even 10 days after first achievement of remission (Fig. 3J, sFig. 6A-B). It should be mentioned, that *in vivo* administration with pentanoate did not enhance anti-tumor immunity. Additionally, pentanoate had no beneficial effect on anti-PD-1 therapy (sFig. 7A-B). A recent study revealed that systemic treatment with butyrate limited the effect of CTLA-4 blockade by inhibiting upregulation of CD80 and CD86 on DCs (Coutzac et al. 2020).

In order to investigate the role of pentanoate in survival and persistence of CD8$^+$ T cells, we injected Rag1-deficient mice a mixture of pentanoate treated CTLs (CD45.2$^+$) and control CTLs (CD45.1$^+$) at ratio 1:1. To mimic tumor microenvironment we additionally transferred Tregs (CD45.2$^+$ from FIR x tiger reporter mice), which are frequently present in solid tumors. As a source of IL-2 we co-transferred Foxp3-CD4$^+$ T cells (sFig. 8A-B). Interestingly, CFSE labelling displayed a higher proliferation of pentanoate-treated cells (sFig. 8C-D). Furthermore, these cells exhibited a strong expression of CD25 compared to untreated control cells (sFig. 8F-G). Apart from the upregulation of CD25, pentanoate substantially increased IL-2-induced STAT5 phosphorylation (sFig. 8H-I). The pharmacological inhibition of glycolysis with 2-DG completely abrogated the upregulation of CD25 by pentanoate treatment (sFig. 8H). Pentanoate treatment prolonged the production of IL-2 production, thereby sustaining an autocrine loop. Taken together the upregulation of CD25, in combination with the higher production of IL-2 seemed to contribute to the persistence of pentanoate-treated CTLs *in vivo*.

To further investigate, if our findings could help to improve potential therapeutic implementation, we used genetically engineered chimeric antigen receptor (CAR) T cells recognizing receptor tyrosine kinase-like orphan receptor 1 (ROR1) (Fig. 4A). ROR1 is frequently expressed in epithelial tumors and some B cell malignancies (Srivastava et al. 2019).

Similar to the previous observed effects on CTLs, pentanoate and butyrate-treated ROR1-CAR T cells had a significantly increased expression of CD25, IFN-γ and TNF-α compared to untreated cells (Fig. 4A-D). To test the anti-tumor efficacy of SCFA treated ROR1-CAR T cells *in vivo*, we generated ROR1-expressing Panc02 tumor cells (Panc02/ROR1). On day 5 after s.c injection of this tumor cells in WT mice, we adoptively transferred pentanoate-treated or untreated ROR1-CAR T cells and observed a substantially diminished tumor weight on day 10 in mice that received pentanoate-treated CAR T cells (Fig. 4 A, E, F). Additionally, we observed a higher frequency and absolute number of IFN-γ$^+$ TNF-α$^+$ pentanoate-pre-treated CAR T cells (Fig. 4G).

In a complementary approach, we tested the effect of pre-treatment with pentanoate on human ROR1-CAR T cells for 4 days. Subsequently, we analysed the cytokine production. The effects mediated by pentanoate mimicked those observed in mouse CAR T cells. CD25 expression and secretion of IL-2

were upregulated (Fig. 5C-D). Co-culture of ROR1-CAR T cells with ROR1-expressing K562 cancer cells resulted in significantly elevated levels of CTL-related cytokines IFN-γ and TNF-α upon pre-treatment with pentanoate (Fig. 5E). Furthermore, proliferation was stronger compared to the control cells (Fig. 5F). Collectively, these data showed that the pre-treatment with pentanoate or butyrate had beneficial effects on the effector function and survival of mouse and human ROR1-specific CAR T cells.

For this work I contributed in performing *in vitro* experiments and I helped in analysing the data.

7 Discussion

7.1 The role of immunoproteasome in NF-κB pathway and antigen presentation during immune responses

Canonical NF-κB pathway is involved in multiple aspects of adaptive and innate immune responses. The formation of heterodimers consisting of RelA/p50 or c-Rel/p50 upon bacterial infection and chronic inflammation is crucial for the activation of inflammatory gene expression and induction of immune responses (Ciechanover 1998; Wolf and Hilt 2004). Recently, we could demonstrate that apart from NF-κB protein p50, c-Rel is required for the induction of protective antibacterial responses (Luu et al. 2020).

The TF NF-κB has recently been identified as a major factor in the development of inflammation-driven carcinogenesis due to its role in regulating the expression of pro-inflammatory mediators like IL-6, TNF-α and IL-17A as well as of chemokines recruiting more immune cells to the tissue (Arkan and Greten 2011; McAllister et al. 2014). Proteasomal degradation of inhibitory molecule IκBα is a key step in this activation process. The role of iP in cancer development is not as well understood as in the regulation of innate immunity and in cytokine production. One report described that the lack of LMP7 in breast cancer cells suppressed tumor invasion and metastasis (Li et al. 2019). Another report revealed a better response to treatment with immune checkpoint inhibitors in combination with high expression of iP in human melanoma (Kalaora et al. 2020). Recently, novel findings suggested a contribution on neo-antigen presentation (Vigneron et al. 2017). We revealed opposing roles for the iP in shaping TME. We observed a pro-tumorigenic role for the iP during chronic colonic inflammation as it supported the colonic tumor progression by elevating the production of pro-tumorigenic factors in immune and cancer cells. The enhanced secretion of chemokines further induced the recruitment of innate immune cells to the inflamed gut. The capacity to alter the TME likely results from the upregulation of iP in the gut epithelial cells but also from post-transcriptional regulation of key TFs like NF-κB, STAT3 and IRF4 (Muchamuel et al. 2009; Kalim et al. 2012). Our experiments with colon cancer cells demonstrated that iPs are not only active in immune cells but also in neoplastic epithelial cells during CAC development. The lower expression of pro-tumorigenic chemokines CXCL1-3 in TKO compared to WT mice, provided evidence that the iP acts as a link between chronic inflammation and cancer development in the large intestine.

In contrast to inflammation-driven carcinogenesis, we observed that the lack of iP subunits led to enhanced growth of melanoma tumors, caused by lower expression of pro-inflammatory cytokines and an inefficient CTL mediated anti-tumor immunity. Impaired NF-κB activation in iP deficient APCs caused a reduction in IL-12 and TNF-α secretion *in vivo*. Also *in vitro* generated BMDCs lacking LMP7 or all iP subunits failed to upregulate IL-12 expression following LPS stimulation. IL-12 is necessary for the activation of T cells to produce IFN-γ, which itself induces the expression of iP. Importantly, the iP

generates peptides for antigen presentation. The reduced IFN-γ levels in the TME of TKO mice led to impaired antigen presentation via MHC class I in B16 melanoma cells. The presentation of tumor epitopes to tumor infiltrating $CD8^+$ T cells is crucial to induce an effective anti-tumor response. Mice lacking iP subunits showed significantly higher increase in tumor volume and tumor weight, as well as reduced frequencies and numbers of tumor infiltrating CTLs and $CD8^+$ T cells in tumor draining lymph nodes compared to WT counterparts suggesting that the iP exhibits anti-tumor effects in this model.
Mice lacking iP subunits LMP2 and MECL-1 have an impaired positive selection of $CD8^+$ T cells as the tP consisting of β5t, LMP2 and MECL-1 cannot be assembled. The tP generates peptides with a lower binding affinity, thereby enabling a better positive selection of immature thymocytes to become $CD8^+$ T cells. This defect in positive selection causes a reduction of $CD8^+$ T cells to approximately 50% for mice lacking LMP2 and MECL-1 subunit (Nitta et al. 2010; Takahama et al. 2012). Mice lacking LMP7 subunit consequently have no impaired positive selection as they can build a complete tP. However, mice exclusively lacking LMP7 subunit showed comparable tumor growth as TKO mice. Although numbers of tumor infiltrating lymphocytes were not reduced compared to WT animals, LMP7-deficient mice had less IFN-γ^+ T cells, as well as lower frequencies of IL-17A and IFN-γ expressing $CD4^+$ T cells, suggesting that LMP7 subunit is crucial for the activation of pro-inflammatory signalling and orchestrating of an efficient immune response.
Collectively, the role of iP depends on the tumor-specific environment. By upregulating the gene expression of pro-inflammatory mediators and recruiting innate immune cells, the iP perpetuates inflammatory reactions leading to development of CAC. In contrast, in tumors that arise independently of chronic inflammation, iPs have an anti-tumorigenic function by supporting APC and T cell immunity (Fig.6). Our findings indicate that the role of iP should be considered in a more differentiated way. Further studies will be needed to elucidate the role of the iP in different cancer types in order to develop adequate therapies.

7.2 Gut microbial SCFAs modulate $CD8^+$ T cell response and improve anti-cancer immunity of CAR T cells

SCFAs like acetate, butyrate and propionate are generated by bacterial fermentation in the small intestine. These gut microbiota derived metabolites have the highest concentration in the caecum and decrease from the proximal to the distal colon (Haenen et al. 2013). They directly affect immune cells by interacting with surface receptors, manipulating gene expression via HDAC inhibition or changing the metabolic demand by acting as metabolic substrate. Several studies described an impact on the suppressor function of Tregs in diverse experimental settings of autoimmune and inflammatory disorders (Mariño et al. 2017; Haghikia et al. 2016). Additionally, butyrate induced epigenetic reprogramming by enhancing the acetylation of H3 on *Foxp3 locus* (Furusawa et al. 2013). On the other side, some reports demonstrated an effect of SCFAs on the effector function of $CD4^+$ and $CD8^+$ T cells,

indicating that the influence of microbial composition and bacterial metabolites might be more complex than previously thought (Park et al. 2015; Kespohl et al. 2017; Trompette et al. 2018; Bachem et al. 2019). It was demonstrated that T cells require aerobic glycolysis for IFN-γ production (Chang et al. 2013). Accordingly, we observed a reduction in IFN-γ production upon inhibition of glycolysis with 2-DG. Our data suggest a strong involvement of epigenetic regulation in the expression of IFN-γ, since HDAC inhibition, mediated by TSA or SCFAs butyrate or propionate significantly increased the expression of this cytokine in $CD8^+$ T cells. Further, we observed differences among the ability of SCFAs to impact on the gene expression of CTLs and Tc17 cells. All SCFAs induced a phenotypic switch towards CTL-like phenotype by enhancing the expression of effector molecules. Nevertheless, acetate predominantly exerted its effect upon the activity of mTOR complex by serving as a metabolic substrate. In contrast, butyrate mediated its profound effect by its HDAC inhibitory activity, since it induced increased acetylation of histone H3 of *Tbx21* and *Ifnγ*. Interestingly, enhanced intestinal butyrate synthesis has been shown to attenuate the development of CAC (Singh et al. 2014). Our data provide new insights into the understanding of how SCFAs might exert anti-cancer effects by increasing effector cytokine production of CTLs.

Furthermore, we investigated if butyrate and pentanoate treatment could enhance anti-tumor activity of CTLs and CAR T cells through metabolic and epigenetic reprogramming. We identified that the relatively low-abundant human gut bacterial strain *M. massiliensis* was able to produce high amounts of pentanoate (Yuille et al. 2018). Previously, we showed that pentanoate acted as HDAC inhibitor and substantially influenced $CD4^+$ T cells by additionally modulating cellular metabolism through the activation of mTOR (Luu et al. 2019). *In vitro* treatment of CTLs and CAR T cells with pentanoate or butyrate increased mTOR activity, which is a central cellular sensor and significantly enhanced anti-tumor activity by elevating the production of CD25, IFN-γ and TNF-α. These CTL-associated effector molecules were further upregulated by epigenetic reprogramming caused by the inhibition of class I histone deacetylase activity. These results were also confirmed *in vivo*, as ROR1-targeting CAR T cells treated with pentanoate showed significantly better anti-tumor activity in syngeneic murine melanoma and pancreatic cancer models compared to control. Our recent collaborative work further demonstrated that the T cell specific deletion of HDAC1 and HDAC2 triggered the expression of CTL-associated effector molecules even in $CD4^+$ T cells (Preglej et al. 2020). As also the treatment of human $CD4^+$ T cells with pentanoate induced the differentiation towards CTL-like phenotype, HDAC inhibitory capacity seems to dominate over metabolic effects in T cells. Interestingly, also the pan-HDAC inhibitor TSA exerted effects on mTOR by increasing its activity, suggesting an interdependence between HDAC inhibition and metabolic effects, although HDAC inhibitors mocetinostat and TMP-195 did not affect mTOR activity (Park et al. 2015).

SCFAs mediate their effects also by binding to cognate receptors on the cell surface. GPR41 and GRP43 are mainly expressed on intestinal Tregs and epithelial cells. Binding of SCFAs mediates activation of mitogen-activated protein kinase signalling and induces the secretion of cytokines and chemokines (Smith et al. 2013; Kim et al. 2013). Treatment of *in vitro* differentiated CTLs lacking those receptors with pentanoate showed no detectable difference to WT pentanoate treated CTLs. This might be caused by a low expression of the surface receptors as they were isolated from the spleen. Only $CD4^+$ T cells derived from the intestine have been shown to have a high expression of these receptors (Park et al. 2015).

Treatment of CTLs with pentanoate increased the secretion of IL-2. As activated T cells consume IL-2 in an autocrine manner, the enhanced secretion might have an impact on the proliferation and longevity of adoptively transferred CTLs in the microenvironment of solid tumors. Interestingly, the inhibition of glycolysis with 2-DG completely abrogated the enhanced expression of CD25, indicating that pentanoate-mediated enhanced glycolysis might be responsible for the enhanced expression of CD25. Furthermore, recent findings described that CD25 activated mTOR signalling, suggesting a possible positive feedback (Ray et al. 2015).

The genetic modification of T cells with a specific antigen target enables a more precise and efficient elimination of cancer cells, further minimising side effects. Orphan receptor ROR1 is expressed on epithelial tumor cells and is recognized by CAR T cells (Srivastava et al. 2019; Mestermann et al. 2019). We demonstrated that bacterial metabolite SCFAs have beneficial effects on the efficacy of CAR T cells by increasing their effector molecules and enhancing their longevity, suggesting that SCFAs could be therapeutically employed. However, the clinical implementation of SCFAs will require further careful investigations to determine the optimal route and dose in order to achieve the most advantageous effector function.

8 References

Publication bibliography

Alabert, Constance; Jasencakova, Zuzana; Groth, Anja (2017): Chromatin Replication and Histone Dynamics. In *Advances in experimental medicine and biology* 1042, pp. 311–333. DOI: 10.1007/978-981-10-6955-0_15.

Araki, Yasuto; Fann, Monchou; Wersto, Robert; Weng, Nan-Ping (2008): Histone acetylation facilitates rapid and robust memory CD8 T cell response through differential expression of effector molecules (eomesodermin and its targets: perforin and granzyme B). In *Journal of immunology (Baltimore, Md. : 1950)* 180 (12), pp. 8102–8108. DOI: 10.4049/jimmunol.180.12.8102.

Arkan, Melek C.; Greten, Florian R. (2011): IKK- and NF-κB-mediated functions in carcinogenesis. In *Current topics in microbiology and immunology* 349, pp. 159–169. DOI: 10.1007/82_2010_97.

Arpaia, Nicholas; Campbell, Clarissa; Fan, Xiying; Dikiy, Stanislav; van der Veeken, Joris; deRoos, Paul et al. (2013): Metabolites produced by commensal bacteria promote peripheral regulatory T-cell generation. In *Nature* 504 (7480), pp. 451–455. DOI: 10.1038/nature12726.

Bachem, Annabell; Makhlouf, Christina; Binger, Katrina J.; Souza, David P. de; Tull, Deidra; Hochheiser, Katharina et al. (2019): Microbiota-Derived Short-Chain Fatty Acids Promote the Memory Potential of Antigen-Activated CD8+ T Cells. In *Immunity* 51 (2), 285-297.e5. DOI: 10.1016/j.immuni.2019.06.002.

Balmer, Maria L.; Ma, Eric H.; Bantug, Glenn R.; Grählert, Jasmin; Pfister, Simona; Glatter, Timo et al. (2016): Memory CD8(+) T Cells Require Increased Concentrations of Acetate Induced by Stress for Optimal Function. In *Immunity* 44 (6), pp. 1312–1324. DOI: 10.1016/j.immuni.2016.03.016.

Basler, Michael; Beck, Ulrike; Kirk, Christopher J.; Groettrup, Marcus (2011): The antiviral immune response in mice devoid of immunoproteasome activity. In *Journal of immunology (Baltimore, Md. : 1950)* 187 (11), pp. 5548–5557. DOI: 10.4049/jimmunol.1101064.

Basler, Michael; Dajee, Maya; Moll, Carlo; Groettrup, Marcus; Kirk, Christopher J. (2010): Prevention of experimental colitis by a selective inhibitor of the immunoproteasome. In *Journal of immunology (Baltimore, Md. : 1950)* 185 (1), pp. 634–641. DOI: 10.4049/jimmunol.0903182.

Basler, Michael; Mundt, Sarah; Muchamuel, Tony; Moll, Carlo; Jiang, Jing; Groettrup, Marcus; Kirk, Christopher J. (2014): Inhibition of the immunoproteasome ameliorates experimental autoimmune encephalomyelitis. In *EMBO molecular medicine* 6 (2), pp. 226–238. DOI: 10.1002/emmm.201303543.

Baumjohann, Dirk; Ansel, K. Mark (2015): Tracking early T follicular helper cell differentiation in vivo. In *Methods in molecular biology (Clifton, N.J.)* 1291, pp. 27–38. DOI: 10.1007/978-1-4939-2498-1_3.

Belote, J. M.; Zhong, L. (2009): Duplicated proteasome subunit genes in Drosophila and their roles in spermatogenesis. In *Heredity* 103 (1), pp. 23–31. DOI: 10.1038/hdy.2009.23.

Berndt, Bradford E.; Zhang, Min; Owyang, Stephanie Y.; Cole, Tyler S.; Wang, Teresa W.; Luther, Jay et al. (2012): Butyrate increases IL-23 production by stimulated dendritic cells. In *American journal of physiology. Gastrointestinal and liver physiology* 303 (12), G1384-92. DOI: 10.1152/ajpgi.00540.2011.

Brack, Christine; Hirama, Minoru; Lenhard-Schuller, Rita; Tonegawa, Susumu (1978): A complete immunoglobulin gene is created by somatic recombination. In *Cell* 15 (1), pp. 1–14. DOI: 10.1016/0092-8674(78)90078-8.

Cham, Candace M.; Gajewski, Thomas F. (2005): Glucose availability regulates IFN-gamma production and p70S6 kinase activation in CD8+ effector T cells. In *Journal of immunology (Baltimore, Md. : 1950)* 174 (8), pp. 4670–4677. DOI: 10.4049/jimmunol.174.8.4670.

Chang, Chih-Hao; Curtis, Jonathan D.; Maggi, Leonard B.; Faubert, Brandon; Villarino, Alejandro V.; O'Sullivan, David et al. (2013): Posttranscriptional control of T cell effector function by aerobic glycolysis. In *Cell* 153 (6), pp. 1239–1251. DOI: 10.1016/j.cell.2013.05.016.

Chaput, N.; Louafi, S.; Bardier, A.; Charlotte, F.; Vaillant, J-C; Ménégaux, F. et al. (2009): Identification of CD8+CD25+Foxp3+ suppressive T cells in colorectal cancer tissue. In *Gut* 58 (4), pp. 520–529. DOI: 10.1136/gut.2008.158824.

Chen, W.; Norbury, C. C.; Cho, Y.; Yewdell, J. W.; Bennink, J. R. (2001): Immunoproteasomes shape immunodominance hierarchies of antiviral CD8(+) T cells at the levels of T cell repertoire and presentation of viral antigens. In *The Journal of experimental medicine* 193 (11), pp. 1319–1326. DOI: 10.1084/jem.193.11.1319.

Ciechanover, A. (1998): The ubiquitin-proteasome pathway: on protein death and cell life. In *The EMBO journal* 17 (24), pp. 7151–7160. DOI: 10.1093/emboj/17.24.7151.

Coutzac, Clélia; Jouniaux, Jean-Mehdi; Paci, Angelo; Schmidt, Julien; Mallardo, Domenico; Seck, Atmane et al. (2020): Systemic short chain fatty acids limit antitumor effect of CTLA-4 blockade in hosts with cancer. In *Nature communications* 11 (1), p. 2168. DOI: 10.1038/s41467-020-16079-x.

Crawford, Lisa J.; Walker, Brian; Irvine, Alexandra E. (2011): Proteasome inhibitors in cancer therapy. In *Journal of cell communication and signaling* 5 (2), pp. 101–110. DOI: 10.1007/s12079-011-0121-7.

Dantuma, Nico P.; Bott, Laura C. (2014): The ubiquitin-proteasome system in neurodegenerative diseases: precipitating factor, yet part of the solution. In *Frontiers in molecular neuroscience* 7, p. 70. DOI: 10.3389/fnmol.2014.00070.

Dion, Michael F.; Altschuler, Steven J.; Wu, Lani F.; Rando, Oliver J. (2005): Genomic characterization reveals a simple histone H4 acetylation code. In *Proceedings of the National Academy of Sciences of the United States of America* 102 (15), pp. 5501–5506. DOI: 10.1073/pnas.0500136102.

Driscoll, J.; Brown, M. G.; Finley, D.; Monaco, J. J. (1993): MHC-linked LMP gene products specifically alter peptidase activities of the proteasome. In *Nature* 365 (6443), pp. 262–264. DOI: 10.1038/365262a0.

Ebstein, Frédéric; Voigt, Antje; Lange, Nicole; Warnatsch, Annika; Schröter, Friederike; Prozorovski, Timour et al. (2013): Immunoproteasomes are important for proteostasis in immune responses. In *Cell* 152 (5), pp. 935–937. DOI: 10.1016/j.cell.2013.02.018.

El Kaoutari, Abdessamad; Armougom, Fabrice; Gordon, Jeffrey I.; Raoult, Didier; Henrissat, Bernard (2013): The abundance and variety of carbohydrate-active enzymes in the human gut microbiota. In *Nature reviews. Microbiology* 11 (7), pp. 497–504. DOI: 10.1038/nrmicro3050.

Ersching, Jonatan; Vasconcelos, José R.; Ferreira, Camila P.; Caetano, Braulia C.; Machado, Alexandre V.; Bruna-Romero, Oscar et al. (2016): The Combined Deficiency of Immunoproteasome Subunits Affects Both the Magnitude and Quality of Pathogen- and Genetic Vaccination-Induced CD8+ T Cell Responses to the Human Protozoan Parasite Trypanosoma cruzi. In *PLoS pathogens* 12 (4), e1005593. DOI: 10.1371/journal.ppat.1005593.

Fields, Patrick E.; Kim, Sean T.; Flavell, Richard A. (2002): Cutting edge: changes in histone acetylation at the IL-4 and IFN-gamma loci accompany Th1/Th2 differentiation. In *Journal of immunology (Baltimore, Md. : 1950)* 169 (2), pp. 647–650. DOI: 10.4049/jimmunol.169.2.647.

Flannagan, Ronald S.; Jaumouillé, Valentin; Grinstein, Sergio (2012): The cell biology of phagocytosis. In *Annual review of pathology* 7, pp. 61–98. DOI: 10.1146/annurev-pathol-011811-132445.

Furusawa, Yukihiro; Obata, Yuuki; Fukuda, Shinji; Endo, Takaho A.; Nakato, Gaku; Takahashi, Daisuke et al. (2013): Commensal microbe-derived butyrate induces the differentiation of colonic regulatory T cells. In *Nature* 504 (7480), pp. 446–450. DOI: 10.1038/nature12721.

Greten, Florian R.; Eckmann, Lars; Greten, Tim F.; Park, Jin Mo; Li, Zhi-Wei; Egan, Laurence J. et al. (2004): IKKbeta links inflammation and tumorigenesis in a mouse model of colitis-associated cancer. In *Cell* 118 (3), pp. 285–296. DOI: 10.1016/j.cell.2004.07.013.

Groettrup, Marcus; Kirk, Christopher J.; Basler, Michael (2010): Proteasomes in immune cells: more than peptide producers? In *Nature reviews. Immunology* 10 (1), pp. 73–78. DOI: 10.1038/nri2687.

Groll, Michael; Kim, Kyung Bo; Kairies, Norman; Huber, Robert; Crews, Craig M. (2000): Crystal Structure of Epoxomicin:20S Proteasome Reveals a Molecular Basis for Selectivity of α‘,β‘-Epoxyketone Proteasome Inhibitors. In *J. Am. Chem. Soc.* 122 (6), pp. 1237–1238. DOI: 10.1021/ja993588m.

Haenen, Daniëlle; Zhang, Jing; Souza da Silva, Carol; Bosch, Guido; van der Meer, Ingrid M.; van Arkel, Jeroen et al. (2013): A diet high in resistant starch modulates microbiota composition, SCFA concentrations, and gene expression in pig intestine. In *The Journal of nutrition* 143 (3), pp. 274–283. DOI: 10.3945/jn.112.169672.

Haghikia, Aiden; Jörg, Stefanie; Duscha, Alexander; Berg, Johannes; Manzel, Arndt; Waschbisch, Anne et al. (2016): Dietary Fatty Acids Directly Impact Central Nervous System Autoimmunity via the Small Intestine. In *Immunity* 44 (4), pp. 951–953. DOI: 10.1016/j.immuni.2016.04.006.

Heink, Sylvia; Fricke, Benjamin; Ludwig, Daniela; Kloetzel, Peter-M; Krüger, Elke (2006): Tumor cell lines expressing the proteasome subunit isoform LMP7E1 exhibit immunoproteasome deficiency. In *Cancer research* 66 (2), pp. 649–652. DOI: 10.1158/0008-5472.CAN-05-2872.

Heink, Sylvia; Ludwig, Daniela; Kloetzel, Peter-M; Krüger, Elke (2005): IFN-gamma-induced immune adaptation of the proteasome system is an accelerated and transient response. In *Proceedings of the National Academy of Sciences of the United States of America* 102 (26), pp. 9241–9246. DOI: 10.1073/pnas.0501711102.

International Human Genome Sequencing Consortium (2004): Finishing the euchromatic sequence of the human genome. In *Nature* 431 (7011), pp. 931–945. DOI: 10.1038/nature03001.

Intlekofer, Andrew M.; Takemoto, Naofumi; Wherry, E. John; Longworth, Sarah A.; Northrup, John T.; Palanivel, Vikram R. et al. (2005): Effector and memory CD8+ T cell fate coupled by T-bet and eomesodermin. In *Nature immunology* 6 (12), pp. 1236–1244. DOI: 10.1038/ni1268.

Kalaora, Shelly; Lee, Joo Sang; Barnea, Eilon; Levy, Ronen; Greenberg, Polina; Alon, Michal et al. (2020): Immunoproteasome expression is associated with better prognosis and response to checkpoint therapies in melanoma. In *Nature communications* 11 (1), p. 896. DOI: 10.1038/s41467-020-14639-9.

Kalim, Khalid W.; Basler, Michael; Kirk, Christopher J.; Groettrup, Marcus (2012): Immunoproteasome subunit LMP7 deficiency and inhibition suppresses Th1 and Th17 but enhances regulatory T cell

differentiation. In *Journal of immunology (Baltimore, Md. : 1950)* 189 (8), pp. 4182–4193. DOI: 10.4049/jimmunol.1201183.

Kanno, Yuka; Vahedi, Golnaz; Hirahara, Kiyoshi; Singleton, Kentner; O'Shea, John J. (2012): Transcriptional and epigenetic control of T helper cell specification: molecular mechanisms underlying commitment and plasticity. In *Annual review of immunology* 30, pp. 707–731. DOI: 10.1146/annurev-immunol-020711-075058.

Karin, Michael (2009): NF-kappaB as a critical link between inflammation and cancer. In *Cold Spring Harbor perspectives in biology* 1 (5), a000141. DOI: 10.1101/cshperspect.a000141.

Kebede, Adam F.; Nieborak, Anna; Shahidian, Lara Zorro; Le Gras, Stephanie; Richter, Florian; Gómez, Diana Aguilar et al. (2017): Histone propionylation is a mark of active chromatin. In *Nature structural & molecular biology* 24 (12), pp. 1048–1056. DOI: 10.1038/nsmb.3490.

Kespohl, Meike; Vachharajani, Niyati; Luu, Maik; Harb, Hani; Pautz, Sabine; Wolff, Svenja et al. (2017): The Microbial Metabolite Butyrate Induces Expression of Th1-Associated Factors in CD4+ T Cells. In *Frontiers in immunology* 8, p. 1036. DOI: 10.3389/fimmu.2017.01036.

Khan, S.; van den Broek, M.; Schwarz, K.; Giuli, R. de; Diener, P. A.; Groettrup, M. (2001): Immunoproteasomes largely replace constitutive proteasomes during an antiviral and antibacterial immune response in the liver. In *Journal of immunology (Baltimore, Md. : 1950)* 167 (12), pp. 6859–6868. DOI: 10.4049/jimmunol.167.12.6859.

Kim, Myung H.; Kang, Seung G.; Park, Jeong H.; Yanagisawa, Masashi; Kim, Chang H. (2013): Short-chain fatty acids activate GPR41 and GPR43 on intestinal epithelial cells to promote inflammatory responses in mice. In *Gastroenterology* 145 (2), 396-406.e1-10. DOI: 10.1053/j.gastro.2013.04.056.

Kim, Myunghoo; Qie, Yaqing; Park, Jeongho; Kim, Chang H. (2016): Gut Microbial Metabolites Fuel Host Antibody Responses. In *Cell host & microbe* 20 (2), pp. 202–214. DOI: 10.1016/j.chom.2016.07.001.

Kimura, Hiroaki; Caturegli, Patrizio; Takahashi, Masafumi; Suzuki, Koichi (2015): New Insights into the Function of the Immunoproteasome in Immune and Nonimmune Cells. In *Journal of immunology research* 2015, p. 541984. DOI: 10.1155/2015/541984.

Kincaid, Eleanor Z.; Che, Jenny W.; York, Ian; Escobar, Hernando; Reyes-Vargas, Eduardo; Delgado, Julio C. et al. (2011): Mice completely lacking immunoproteasomes show major changes in antigen presentation. In *Nature immunology* 13 (2), pp. 129–135. DOI: 10.1038/ni.2203.

Kisselev, A. F.; Akopian, T. N.; Castillo, V.; Goldberg, A. L. (1999): Proteasome active sites allosterically regulate each other, suggesting a cyclical bite-chew mechanism for protein breakdown. In *Molecular cell* 4 (3), pp. 395–402. DOI: 10.1016/s1097-2765(00)80341-x.

Klasse, P. J.; Sattentau, Q. J. (2002): Occupancy and mechanism in antibody-mediated neutralization of animal viruses. In *The Journal of general virology* 83 (Pt 9), pp. 2091–2108. DOI: 10.1099/0022-1317-83-9-2091.

Kloetzel, P. M. (2001): Antigen processing by the proteasome. In *Nature reviews. Molecular cell biology* 2 (3), pp. 179–187. DOI: 10.1038/35056572.

Kloetzel, Peter Michael; Ossendorp, Ferry (2004): Proteasome and peptidase function in MHC-class-I-mediated antigen presentation. In *Current opinion in immunology* 16 (1), pp. 76–81. DOI: 10.1016/j.coi.2003.11.004.

Kniepert, Andrea; Groettrup, Marcus (2014): The unique functions of tissue-specific proteasomes. In *Trends in biochemical sciences* 39 (1), pp. 17–24. DOI: 10.1016/j.tibs.2013.10.004.

Koerner, Julia; Brunner, Thomas; Groettrup, Marcus (2017): Inhibition and deficiency of the immunoproteasome subunit LMP7 suppress the development and progression of colorectal carcinoma in mice. In *Oncotarget* 8 (31), pp. 50873–50888. DOI: 10.18632/oncotarget.15141.

Koh, Ara; Vadder, Filipe de; Kovatcheva-Datchary, Petia; Bäckhed, Fredrik (2016): From Dietary Fiber to Host Physiology: Short-Chain Fatty Acids as Key Bacterial Metabolites. In *Cell* 165 (6), pp. 1332–1345. DOI: 10.1016/j.cell.2016.05.041.

Korniotis, Sarantis; Gras, Christophe; Letscher, Hélène; Montandon, Ruddy; Mégret, Jérôme; Siegert, Stefanie et al. (2016): Treatment of ongoing autoimmune encephalomyelitis with activated B-cell progenitors maturing into regulatory B cells. In *Nature communications* 7, p. 12134. DOI: 10.1038/ncomms12134.

Krüger, Elke; Kloetzel, Peter-Michael; Enenkel, Cordula (2001): 20S proteasome biogenesis. In *Biochimie* 83 (3-4), pp. 289–293. DOI: 10.1016/s0300-9084(01)01241-x.

Kubiczkova, Lenka; Pour, Ludek; Sedlarikova, Lenka; Hajek, Roman; Sevcikova, Sabina (2014): Proteasome inhibitors - molecular basis and current perspectives in multiple myeloma. In *Journal of cellular and molecular medicine* 18 (6), pp. 947–961. DOI: 10.1111/jcmm.12279.

Lee, Youjin; Awasthi, Amit; Yosef, Nir; Quintana, Francisco J.; Xiao, Sheng; Peters, Anneli et al. (2012): Induction and molecular signature of pathogenic TH17 cells. In *Nature immunology* 13 (10), pp. 991–999. DOI: 10.1038/ni.2416.

Li, Shengnan; Dai, Xiaoqin; Gong, Kunxiang; Song, Kai; Tai, Fang; Shi, Jian (2019): PA28α/β Promote Breast Cancer Cell Invasion and Metastasis via Down-Regulation of CDK15. In *Frontiers in oncology* 9, p. 1283. DOI: 10.3389/fonc.2019.01283.

Luu, Maik; Pautz, Sabine; Kohl, Vanessa; Singh, Rajeev; Romero, Rossana; Lucas, Sébastien et al. (2019): The short-chain fatty acid pentanoate suppresses autoimmunity by modulating the metabolic-epigenetic crosstalk in lymphocytes. In *Nature communications* 10 (1), p. 760. DOI: 10.1038/s41467-019-08711-2.

Luu, Maik; Romero, Rossana; Bazant, Jasmin; Abass, Elfadil; Hartmann, Sabrina; Leister, Hanna et al. (2020): The NF-κB transcription factor c-Rel controls host defense against Citrobacter rodentium. In *European journal of immunology* 50 (2), pp. 292–294. DOI: 10.1002/eji.201948314.

Luu, Maik; Steinhoff, Ulrich; Visekruna, Alexander (2017): Functional heterogeneity of gut-resident regulatory T cells. In *Clinical & translational immunology* 6 (9), e156. DOI: 10.1038/cti.2017.39.

Mariño, Eliana; Richards, James L.; McLeod, Keiran H.; Stanley, Dragana; Yap, Yu Anne; Knight, Jacinta et al. (2017): Gut microbial metabolites limit the frequency of autoimmune T cells and protect against type 1 diabetes. In *Nature immunology* 18 (5), pp. 552–562. DOI: 10.1038/ni.3713.

McAllister, Florencia; Bailey, Jennifer M.; Alsina, Janivette; Nirschl, Christopher J.; Sharma, Rajni; Fan, Hongni et al. (2014): Oncogenic Kras activates a hematopoietic-to-epithelial IL-17 signaling axis in preinvasive pancreatic neoplasia. In *Cancer cell* 25 (5), pp. 621–637. DOI: 10.1016/j.ccr.2014.03.014.

McCarthy, Mary K.; Weinberg, Jason B. (2015): The immunoproteasome and viral infection: a complex regulator of inflammation. In *Frontiers in microbiology* 6, p. 21. DOI: 10.3389/fmicb.2015.00021.

Meijer, Kees; Vos, Paul de; Priebe, Marion G. (2010): Butyrate and other short-chain fatty acids as modulators of immunity: what relevance for health? In *Current opinion in clinical nutrition and metabolic care* 13 (6), pp. 715–721. DOI: 10.1097/MCO.0b013e32833eebe5.

Mestermann, Katrin; Giavridis, Theodoros; Weber, Justus; Rydzek, Julian; Frenz, Silke; Nerreter, Thomas et al. (2019): The tyrosine kinase inhibitor dasatinib acts as a pharmacologic on/off switch for CAR T cells. In *Science translational medicine* 11 (499). DOI: 10.1126/scitranslmed.aau5907.

Moebius, Jacqueline; van den Broek, Maries; Groettrup, Marcus; Basler, Michael (2010): Immunoproteasomes are essential for survival and expansion of T cells in virus-infected mice. In *European journal of immunology* 40 (12), pp. 3439–3449. DOI: 10.1002/eji.201040620.

Muchamuel, Tony; Basler, Michael; Aujay, Monette A.; Suzuki, Erika; Kalim, Khalid W.; Lauer, Christoph et al. (2009): A selective inhibitor of the immunoproteasome subunit LMP7 blocks cytokine

production and attenuates progression of experimental arthritis. In *Nature medicine* 15 (7), pp. 781–787. DOI: 10.1038/nm.1978.

Murata, Shigeo; Sasaki, Katsuhiro; Kishimoto, Toshihiko; Niwa, Shin-Ichiro; Hayashi, Hidemi; Takahama, Yousuke; Tanaka, Keiji (2007): Regulation of CD8+ T cell development by thymus-specific proteasomes. In *Science (New York, N.Y.)* 316 (5829), pp. 1349–1353. DOI: 10.1126/science.1141915.

Murata, Shigeo; Takahama, Yousuke; Kasahara, Masanori; Tanaka, Keiji (2018): The immunoproteasome and thymoproteasome: functions, evolution and human disease. In *Nature immunology* 19 (9), pp. 923–931. DOI: 10.1038/s41590-018-0186-z.

Murphy, Kenneth; Weaver, Casey (2018): Janeway Immunologie. 9. Auflage. Berlin: Springer Spektrum.

Neurath, Markus F. (2014): Cytokines in inflammatory bowel disease. In *Nature reviews. Immunology* 14 (5), pp. 329–342. DOI: 10.1038/nri3661.

Nitta, Takeshi; Murata, Shigeo; Sasaki, Katsuhiro; Fujii, Hideki; Ripen, Adiratna Mat; Ishimaru, Naozumi et al. (2010): Thymoproteasome shapes immunocompetent repertoire of CD8+ T cells. In *Immunity* 32 (1), pp. 29–40. DOI: 10.1016/j.immuni.2009.10.009.

Palmer, Ed (2003): Negative selection--clearing out the bad apples from the T-cell repertoire. In *Nature reviews. Immunology* 3 (5), pp. 383–391. DOI: 10.1038/nri1085.

Park, J.; Kim, M.; Kang, S. G.; Jannasch, A. H.; Cooper, B.; Patterson, J.; Kim, C. H. (2015): Short-chain fatty acids induce both effector and regulatory T cells by suppression of histone deacetylases and regulation of the mTOR-S6K pathway. In *Mucosal immunology* 8 (1), pp. 80–93. DOI: 10.1038/mi.2014.44.

Parker, D. C. (1993a): T cell-dependent B cell activation. In *Annual review of immunology* 11, pp. 331–360. DOI: 10.1146/annurev.iy.11.040193.001555.

Parker, D. C. (1993b): The functions of antigen recognition in T cell-dependent B cell activation. In *Seminars in immunology* 5 (6), pp. 413–420. DOI: 10.1006/smim.1993.1047.

Peng, Min; Yin, Na; Chhangawala, Sagar; Xu, Ke; Leslie, Christina S.; Li, Ming O. (2016): Aerobic glycolysis promotes T helper 1 cell differentiation through an epigenetic mechanism. In *Science (New York, N.Y.)* 354 (6311), pp. 481–484. DOI: 10.1126/science.aaf6284.

Preglej, Teresa; Hamminger, Patricia; Luu, Maik; Bulat, Tanja; Andersen, Liisa; Göschl, Lisa et al. (2020): Histone deacetylases 1 and 2 restrain CD4+ cytotoxic T lymphocyte differentiation. In *JCI insight* 5 (4). DOI: 10.1172/jci.insight.133393.

Qiu, Jing; Villa, Matteo; Sanin, David E.; Buck, Michael D.; O'Sullivan, David; Ching, Reagan et al. (2019): Acetate Promotes T Cell Effector Function during Glucose Restriction. In *Cell reports* 27 (7), 2063-2074.e5. DOI: 10.1016/j.celrep.2019.04.022.

Ray, John P.; Staron, Matthew M.; Shyer, Justin A.; Ho, Ping-Chih; Marshall, Heather D.; Gray, Simon M. et al. (2015): The Interleukin-2-mTORc1 Kinase Axis Defines the Signaling, Differentiation, and Metabolism of T Helper 1 and Follicular B Helper T Cells. In *Immunity* 43 (4), pp. 690–702. DOI: 10.1016/j.immuni.2015.08.017.

Robek, Michael D.; Garcia, Mayra L.; Boyd, Bryan S.; Chisari, Francis V. (2007): Role of immunoproteasome catalytic subunits in the immune response to hepatitis B virus. In *Journal of virology* 81 (2), pp. 483–491. DOI: 10.1128/JVI.01779-06.

Ryu, Hong-Yeoul; Hochstrasser, Mark (2021): Histone sumoylation and chromatin dynamics. In *Nucleic acids research* 49 (11), pp. 6043–6052. DOI: 10.1093/nar/gkab280.

Schmidt, Nicole; Gonzalez, Erik; Visekruna, Alexander; Kühl, Anja A.; Loddenkemper, Christoph; Mollenkopf, Hans et al. (2010): Targeting the proteasome: partial inhibition of the proteasome by bortezomib or deletion of the immunosubunit LMP7 attenuates experimental colitis. In *Gut* 59 (7), pp. 896–906. DOI: 10.1136/gut.2009.203554.

Schmitt, Edgar; Klein, Matthias; Bopp, Tobias (2014): Th9 cells, new players in adaptive immunity. In *Trends in immunology* 35 (2), pp. 61–68. DOI: 10.1016/j.it.2013.10.004.

Shang, Kun; Bai, Yu-Pan; Wang, Chen; Wang, Zhen; Gu, Hong-Yu; Du, Xiang et al. (2012): Crucial involvement of tumor-associated neutrophils in the regulation of chronic colitis-associated carcinogenesis in mice. In *PloS one* 7 (12), e51848. DOI: 10.1371/journal.pone.0051848.

Shimizu, Akira; Honjo, Tasuku (1984): Immunoglobulin class switching. In *Cell* 36 (4), pp. 801–803. DOI: 10.1016/0092-8674(84)90029-1.

Simone, V. de; Franzè, E.; Ronchetti, G.; Colantoni, A.; Fantini, M. C.; Di Fusco, D. et al. (2015): Th17-type cytokines, IL-6 and TNF-α synergistically activate STAT3 and NF-kB to promote colorectal cancer cell growth. In *Oncogene* 34 (27), pp. 3493–3503. DOI: 10.1038/onc.2014.286.

Singh, Nagendra; Gurav, Ashish; Sivaprakasam, Sathish; Brady, Evan; Padia, Ravi; Shi, Huidong et al. (2014): Activation of Gpr109a, receptor for niacin and the commensal metabolite butyrate, suppresses colonic inflammation and carcinogenesis. In *Immunity* 40 (1), pp. 128–139. DOI: 10.1016/j.immuni.2013.12.007.

Sivan, Ayelet; Corrales, Leticia; Hubert, Nathaniel; Williams, Jason B.; Aquino-Michaels, Keston; Earley, Zachary M. et al. (2015): Commensal Bifidobacterium promotes antitumor immunity and

facilitates anti-PD-L1 efficacy. In *Science (New York, N.Y.)* 350 (6264), pp. 1084–1089. DOI: 10.1126/science.aac4255.

Smith, Patrick M.; Howitt, Michael R.; Panikov, Nicolai; Michaud, Monia; Gallini, Carey Ann; Bohlooly-Y, Mohammad et al. (2013): The microbial metabolites, short-chain fatty acids, regulate colonic Treg cell homeostasis. In *Science (New York, N.Y.)* 341 (6145), pp. 569–573. DOI: 10.1126/science.1241165.

Srivastava, Shivani; Salter, Alexander I.; Liggitt, Denny; Yechan-Gunja, Sushma; Sarvothama, Megha; Cooper, Kirsten et al. (2019): Logic-Gated ROR1 Chimeric Antigen Receptor Expression Rescues T Cell-Mediated Toxicity to Normal Tissues and Enables Selective Tumor Targeting. In *Cancer cell* 35 (3), 489-503.e8. DOI: 10.1016/j.ccell.2019.02.003.

Sun, Shao-Cong; Ley, Steven C. (2008): New insights into NF-kappaB regulation and function. In *Trends in immunology* 29 (10), pp. 469–478. DOI: 10.1016/j.it.2008.07.003.

Takahama, Yousuke; Takada, Kensuke; Murata, Shigeo; Tanaka, Keiji (2012): β5t-containing thymoproteasome: specific expression in thymic cortical epithelial cells and role in positive selection of CD8+ T cells. In *Current opinion in immunology* 24 (1), pp. 92–98. DOI: 10.1016/j.coi.2012.01.006.

Tan, Jian; McKenzie, Craig; Vuillermin, Peter J.; Goverse, Gera; Vinuesa, Carola G.; Mebius, Reina E. et al. (2016): Dietary Fiber and Bacterial SCFA Enhance Oral Tolerance and Protect against Food Allergy through Diverse Cellular Pathways. In *Cell reports* 15 (12), pp. 2809–2824. DOI: 10.1016/j.celrep.2016.05.047.

Toes, R. E.; Nussbaum, A. K.; Degermann, S.; Schirle, M.; Emmerich, N. P.; Kraft, M. et al. (2001): Discrete cleavage motifs of constitutive and immunoproteasomes revealed by quantitative analysis of cleavage products. In *The Journal of experimental medicine* 194 (1), pp. 1–12. DOI: 10.1084/jem.194.1.1.

Trompette, Aurélien; Gollwitzer, Eva S.; Pattaroni, Céline; Lopez-Mejia, Isabel C.; Riva, Erika; Pernot, Julie et al. (2018): Dietary Fiber Confers Protection against Flu by Shaping Ly6c- Patrolling Monocyte Hematopoiesis and CD8+ T Cell Metabolism. In *Immunity* 48 (5), 992-1005.e8. DOI: 10.1016/j.immuni.2018.04.022.

Trompette, Aurélien; Gollwitzer, Eva S.; Yadava, Koshika; Sichelstiel, Anke K.; Sprenger, Norbert; Ngom-Bru, Catherine et al. (2014): Gut microbiota metabolism of dietary fiber influences allergic airway disease and hematopoiesis. In *Nature medicine* 20 (2), pp. 159–166. DOI: 10.1038/nm.3444.

Vachharajani, Niyati; Joeris, Thorsten; Luu, Maik; Hartmann, Sabrina; Pautz, Sabine; Jenike, Elena et al. (2017): Prevention of colitis-associated cancer by selective targeting of immunoproteasome subunit LMP7. In *Oncotarget* 8 (31), pp. 50447–50459. DOI: 10.18632/oncotarget.14579.

Vigneron, Nathalie; Abi Habib, Joanna; van den Eynde, Benoit J. (2017): Learning from the Proteasome How To Fine-Tune Cancer Immunotherapy. In *Trends in cancer* 3 (10), pp. 726–741. DOI: 10.1016/j.trecan.2017.07.007.

Visekruna, Alexander; Joeris, Thorsten; Seidel, Daniel; Kroesen, Anjo; Loddenkemper, Christoph; Zeitz, Martin et al. (2006): Proteasome-mediated degradation of IkappaBalpha and processing of p105 in Crohn disease and ulcerative colitis. In *The Journal of clinical investigation* 116 (12), pp. 3195–3203. DOI: 10.1172/JCI28804.

Wang, Y.; Wang, K.; Han, G-C; Wang, R-X; Xiao, H.; Hou, C-M et al. (2014): Neutrophil infiltration favors colitis-associated tumorigenesis by activating the interleukin-1 (IL-1)/IL-6 axis. In *Mucosal immunology* 7 (5), pp. 1106–1115. DOI: 10.1038/mi.2013.126.

Wang, Yiming; Ma, Rena; Liu, Fang; Lee, Seul A.; Zhang, Li (2018): Modulation of Gut Microbiota: A Novel Paradigm of Enhancing the Efficacy of Programmed Death-1 and Programmed Death Ligand-1 Blockade Therapy. In *Frontiers in immunology* 9, p. 374. DOI: 10.3389/fimmu.2018.00374.

West, Nathan R.; McCuaig, Sarah; Franchini, Fanny; Powrie, Fiona (2015): Emerging cytokine networks in colorectal cancer. In *Nature reviews. Immunology* 15 (10), pp. 615–629. DOI: 10.1038/nri3896.

Wolf, Dieter H.; Hilt, Wolfgang (2004): The proteasome: a proteolytic nanomachine of cell regulation and waste disposal. In *Biochimica et biophysica acta* 1695 (1-3), pp. 19–31. DOI: 10.1016/j.bbamcr.2004.10.007.

Yuille, Samantha; Reichardt, Nicole; Panda, Suchita; Dunbar, Hayley; Mulder, Imke E. (2018): Human gut bacteria as potent class I histone deacetylase inhibitors in vitro through production of butyric acid and valeric acid. In *PloS one* 13 (7), e0201073. DOI: 10.1371/journal.pone.0201073.

Zentner, Gabriel E.; Henikoff, Steven (2013): Regulation of nucleosome dynamics by histone modifications. In *Nature structural & molecular biology* 20 (3), pp. 259–266. DOI: 10.1038/nsmb.2470.

Zollner, Thomas M.; Podda, Maurizio; Pien, Christine; Elliott, Peter J.; Kaufmann, Roland; Boehncke, Wolf-Henning (2002): Proteasome inhibition reduces superantigen-mediated T cell activation and the severity of psoriasis in a SCID-hu model. In *The Journal of clinical investigation* 109 (5), pp. 671–679. DOI: 10.1172/JCI12736.

9 Apendix

9.1 Publications

- **"**Regulation of the effector function of CD8$^+$ T cells by gut microbiota-derived metabolite butyrate."
  by Luu M, Weigand K, Wedi F, Breidenbend C, **Leister H**, Pautz S, Adhikary T, Visekruna A.
  ***Scientific Reports 8*, Article number: 14430 (2018)**

- **"**The NF-κB transcription factor c-Rel controls host defense against Citrobacter rodentium."
  by Luu M, Romero R, Bazant J, Abass E, Hartmann S, **Leister H**, Fischer F, Mahdavi R, Plaza-Sirvent C, Schmitz I, Steinhoff U, Visekruna A.
  ***European Journal of Immunology 2'20,* Volume 50, Issue 2**

- "Microbial short-chain fatty acids modulate CD8$^+$ T cell responses and improve adoptive immunotherapy for cancer. "
  by Luu M, Riester Z, Baldrich A, Reichardt N, Yuille S, Busetti A, Klein M, Wempe A, **Leister H**, Raifer H, Picard F, Muhammad K, Ohl K, Romero R, Fischer F, Bauer CA, Huber M, Gress TM, Lauth M, Danhof S, Bopp T, Nerreter T, Mulder IE, Steinhoff U, Hudecek M, Visekruna A.
  Nat Commun. 2021 Jul 1;12(1):4077.

- "Pro- and Antitumorigenic Capacity of Immunoproteasomes in Shaping the Tumor Microenvironment."
  by **Leister H**, Luu M, Staudenraus D, Lopez Krol A, Mollenkopf HJ, Sharma A, Schmerer N, Schulte LN, Bertrams W, Schmeck B, Bosmann M, Steinhoff U, Visekruna A.
  Cancer Immunol Res. 2021 Jun;9(6):682-692.

- "Verteporfin protects against Th17 cell-mediated EAE independently of YAP inhibition."
  by Brosinsky P, **Leister H**, Cheng N, Varelas X, Visekruna A, Luu M.
  Eur J Immunol. 2022 Sep;52(9):1523-1526

- "The Role of Immunoproteasomes in Tumor-Immune Cell Interactions in Melanoma and Colon Cancer."
  by **Leister H**, Krause FF, Mahdavi R, Steinhoff U, Visekruna A.
  Arch Immunol Ther Exp (Warsz). 2022 Jan 22;70(1):5.

- "Point mutation L116R in interferon-regulatory factor 4 differentially impacts key cytokine production in Th2, Th9, and Th17 cells."
  by Staudenraus D, Porapu A, **Leister H**, Gupta DD, Lohoff M.
  Eur J Immunol. 2022 Sep 1.

- **"**Lactate induces metabolic and epigenetic reprogramming of pro-inflammatory Th17 cells."
  by Lopez Krol A, Nehring HP, Krause FF, Wempe A, Raifer H, Nist A, Stiewe T, Bertrams W, Schmeck B, Luu M, **Leister H**, Chung HR, Bauer UM, Adhikary T, Visekruna A.
  EMBO Rep. 2022 Oct 10:e54685

- **"**Selected commensals educate the intestinal vascular and immune system for immunocompetence."
  by Romero R, Zarzycka A, Preussner M, Fischer F, Hain T, Herrmann JP, Roth K, Keber CU, Suryamohan K, Raifer H, Luu M, **Leister H**, Bertrams W, Klein M, Shams-Eldin H, Jacob R, Mollenkopf HJ, Rajalingam K, Visekruna A, Steinhoff U.
  Microbiome. 2022 Sep 28;10(1):158

9.2 Academic teachers

Academic teachers at Johan Wolfgang Goethe-Universität Frankfurt am Main: PD Dr. Abele, Prof. Dr. Auner, Prof. Dr. Bratzke, Prof. Dr. Dötsch, Prof. Dr. Fendler, Prof. Dr. Glaubitz, Prof. Dr. Göbel, Prof. Dr. Grininger, Prof. Dr. Hildt, Prof. Dr. Klein, Prof. Dr. Pos, Prof. Dr. Schwalbe, Prof. Dr. Tampe, Prof. Dr. Verhoff

Academic teachers at Philipps-Universität Marburg: PD Dr. Adhikary, Prof. Dr. Bauer, Prof. Dr. Buchholz, Prof. Dr. Huber, Prof. Dr. Laut, Prof. Dr. Lohoff, Prof. Dr. Müller-Brüsselbach, Prof. Dr. Pogge von Strandmann, Prof. Dr. Schmeck, Prof. Dr. Schnarre, Prof. Dr. Steinhoff, Prof. Dr. Stiewe, Prof. Dr. Visekruna

9.3 Acknowledgement

An dieser Stelle möchte ich allen Menschen danken, die durch fachliche und persönliche Hilfestellung zu dieser Arbeit beigetragen haben. Meiner Auffassung nach lebt die Wissenschaft von fachlicher Diskussion und Austausch. Aus diesem Grund ein ganz herzliches Dankeschön an das Institut für Medizinische Mikrobiologie und Krankenhaushygiene in welchem ich in zahlreichen Seminaren die Möglichkeit hatte meine Arbeit zu diskutieren und neue Anreize zu bekommen.

Ein Labor kann nur funktionieren, wenn es organisiert ist. An dieser Stelle ein herzliches Dankeschön an die TAs Anne Hellhund, Claudia Trier, Nadine Buschmann, Anna Guralnik und Bärbel Camara. Ihr haltet das Labor am Laufen.

Ein großes Dankeschön an Prof. Michael Lohoff der sowohl für fachliche als auch persönliche Probleme immer ein offenes Ohr hatte. Michael ich wusste immer, dass ich mich im Zweifel an dich wenden kann und du mich, wenn es sein muss sogar aus der Notaufnahme abholst. Danke, dass du dir immer Zeit genommen hast.

Ein herzliches Dankeschön auch an Prof. Ulrich Steinhoff für seine Unterstützung und seinen Rat. Danke für die zahlreichen interessanten Gespräche. Dafür, dass du immer gut gelaunt und für einen Scherz zu haben warst.

Danke natürlich auch an Prof. Magdalena Huber. Danke Magda für zahlreiche hilfreiche Tipps und Ratschläge.

Ein ganz besonders großes Dankeschön geht an Prof. Alexander Visekruna! Alex du warst in den 5 Jahren, die wir uns mittlerweile kennen immer für mich da und hast mir gekonnt auch durch schwerere Zeiten geholfen. Wir haben zahlreiche Stunden über mein Projekt diskutiert und Einiges zusammen erlebt. Momente, die ich vermutlich niemals vergessen werde. Danke für deine Hilfe und deinen Einsatz!!! Ich bin mir sicher, dass wir uns auch in Zukunft nicht aus den Augen verlieren werden.

Danke auch an Dr. Maik Luu. Maik du warst mir während meiner Masterarbeit und auch zu Beginn meiner Doktorarbeit eine große Hilfe. Ich bin dankbar dafür was ich von dir lernen konnte.

Danke auch an Dr. Tobias Engel dafür, dass er das Epilepsie Projekt möglich gemacht hat. Außerdem Tobias danke ich dir für die Zeit in Dublin, für die Erfahrung die ich dadurch gewinnen konnte.

Danke auch an Felix Krause. Felix du bist eine echte Bereicherung für das Labor! Du bist stets gut gelaunt und ich habe die Zeit mit dir wirklich sehr genossen, egal ob an der Bench, beim Bouldern oder beim Bahamamama trinken. Ich bin stolz darauf wie gut du bereits geworden bist seit du da bist und

habe absolut keinen Zweifel daran, dass du die nächsten Studenten auch ohne mich super ausbilden wirst.

Danke auch an Anne Hellhund. Anne du bist eine fantastische TA und mir war deine Meinung immer wichtig. Abgesehen davon danke ich dir für deine Freundschaft. Auch du bereicherst das Labor!

Danke auch an Manuel Gerlach. Du bist ein echter Freund geworden. Egal ob beim Joggen oder gemeinsamen Kochen wir hatten immer eine gute Zeit zusammen.

Danke auch an Carina Breidenbend, Vanessa Kohl, Fatana Wedi, Paulin Brosinski, Heide Monning, Anne Wempe, Aleksandra Lopez-Krohl, Dennis Das Gupta, Johanna Böttcher, Rebecca Seitz, Lars Jager, Felix Picard, Florence Fischer, Rossana Romero, Hartmann Raifer, Melanie Wolf, Janis Patten, Rouzbeh Mahdavi und Jasmin Bazant. Ihr alle seid zu guten Freunden geworden und habt meine Doktorandenzeit zu etwas Besonderem gemacht.

Ganz besonders möchte ich Daniel Staudenraus danken. Dafür, dass du immer an mich geglaubt hast und mir in jeder Situation beistandst. Diese Zeit war für uns beide nicht immer einfach, aber wir haben sie gemeinsam durchgestanden und das verbindet nur umso mehr.

Außerdem möchte ich meiner Familie danken, die mich stets unterstützt hat und mir Mut zugesprochen hat. Ohne euren Glauben an mich hätte ich es niemals geschafft.

Zuletzt möchte ich mich herzlich bei unseren Förderern bedanken. Ein großes Dankeschön an die Fazit Stiftung ohne die diese Promotion niemals möglich gewesen wäre. Durch Ihre Hilfe konnte ich die ersten beiden Jahre meiner Promotion finanzieren und somit an dem Projekt in dem Institut meiner Wahl arbeiten. Desweiteren möchte ich mich bei der DfG bedanken, welche die Anschlussförderung dieser Arbeit ermöglichte. Und zuletzt möchte ich der Kempkes Stiftung danken, welche uns in einem weiteren Projekt unterstützte und somit die Publikation von drei Papern ermöglichte.

9.4 Ehrenwörtliche Erklärung

„Ich erkläre ehrenwörtlich, dass ich die dem Fachbereich Medizin Marburg zur Promotionsprüfung eingereichte Arbeit mit dem Titel „Die vielfältigen Auswirkungen des Immunoproteasoms und kurzkettiger Fettsäuren auf die Anti-Tumor-Immunität“ im Institut für medizinische Mikrobiologie und Krankenhaushygiene unter Leitung von Prof. Lohoff mit Unterstützung durch Prof. Visekruna ohne sonstige Hilfe selbst durchgeführt und bei der Abfassung der Arbeit keine anderen als die in der Dissertation aufgeführten Hilfsmittel benutzt habe. Ich habe bisher an keinem in- oder ausländischen Medizinischen Fachbereich ein Gesuch um Zulassung zur Promotion eingereicht, noch die vorliegende oder eine andere Arbeit als Dissertation vorgelegt.

Ich versichere, dass ich sämtliche wörtlichen oder sinngemäßen Übernahmen und Zitate kenntlich gemacht habe.

Mit dem Einsatz von Software zur Erkennung von Plagiaten bin ich einverstanden.

Vorliegende Arbeit wurde (oder wird) in folgenden Publikationsorganen:

- “Pro- and Antitumorigenic Capacity of Immunoproteasomes in Shaping the Tumor Microenvironment.”
  by **Leister H**, Luu M, Staudenraus D, Lopez Krol A, Mollenkopf HJ, Sharma A, Schmerer N, Schulte LN, Bertrams W, Schmeck B, Bosmann M, Steinhoff U, Visekruna A.
- **Cancer Immunol Res. 2021 Jun;9(6):682-692**
  “Regulation of the effector function of $CD8^+$ T cells by gut microbiota-derived metabolite butyrate.”
  by Luu M, Weigand K, Wedi F, Breidenbend C, **Leister H**, Pautz S, Adhikary T, Visekruna A.
  ***Scientific Reports 8*, Article number: 14430 (2018)**
- “Microbial short-chain fatty acids modulate $CD8^+$ T cell responses and improve adoptive immunotherapy for cancer. “
  by Luu M, Riester Z, Baldrich A, Reichardt N, Yuille S, Busetti A, Klein M, Wempe A, **Leister H**, Raifer H, Picard F, Muhammad K, Ohl K, Romero R, Fischer F, Bauer CA, Huber M, Gress TM, Lauth M, Danhof S, Bopp T, Nerreter T, Mulder IE, Steinhoff U, Hudecek M, Visekruna A.
  Nat Commun. 2021 Jul 1;12(1):4077

veröffentlicht.“ ***1**

Ort, Datum, Unterschrift Doktorandin/Doktorand

„Die Hinweise zur Erkennung von Plagiaten habe ich zur Kenntnis genommen.“***2**

Ort, Datum, Unterschrift Referentin/Referent

***1** Hier sind Publikationen/Abstracts aufzuführen, die aus der Dissertation entstanden sind bzw. eingereicht oder angenommen wurden. Für jedes DIN A4 Exemplar ist eine Kopie beizufügen.

***2** Die „Hinweise zur Erkennung von Plagiaten“ sind auf unserer Homepage hinterlegt.

Pro- and Antitumorigenic Capacity of Immunoproteasomes in Shaping the Tumor Microenvironment

Hanna Leister[1], Maik Luu[1], Daniel Staudenraus[1], Aleksandra Lopez Krol[1], Hans-Joachim Mollenkopf[2], Arjun Sharma[3,4], Nils Schmerer[5,6], Leon N. Schulte[5,6], Wilhelm Bertrams[5,6], Bernd Schmeck[5,6], Markus Bosmann[3,4], Ulrich Steinhoff[1], and Alexander Visekruna[1]

ABSTRACT

Apart from the constitutive proteasome, the immunoproteasome that comprises the three proteolytic subunits LMP2, MECL-1, and LMP7 is expressed in most immune cells. In this study, we describe opposing roles for immunoproteasomes in regulating the tumor microenvironment (TME). During chronic inflammation, immunoproteasomes modulated the expression of protumorigenic cytokines and chemokines and enhanced infiltration of innate immune cells, thus triggering the onset of colitis-associated carcinogenesis (CAC) in wild-type mice. Consequently, immunoproteasome-deficient animals (LMP2/MECL-1/LMP7–null mice) were almost completely resistant to CAC development. In patients with ulcerative colitis with high risk for CAC, immunoproteasome-induced protumorigenic mediators were upregulated. In melanoma tumors, the role of immunoproteasomes is relatively unknown. We found that high expression of immunoproteasomes in human melanoma was associated with better prognosis. Similarly, our data revealed that the immunoproteasome has antitumorigenic activity in a mouse model of melanoma. The antitumor immunity against melanoma was compromised in immunoproteasome-deficient mice because of the impaired activity of $CD8^+$ CTLs, $CD4^+$ Th1 cells, and antigen-presenting cells. These findings show that immunoproteasomes may exert opposing roles with either pro- or antitumoral properties in a context-dependent manner.

Introduction

The 20S proteasome, which is a part of the proteolytic enzyme called the 26S proteasome, is a barrel-shaped complex consisting of four heptameric rings that envelop the catalytic chamber, in which unneeded or damaged proteins are degraded by proteolysis (1). The two outer rings of the 20S proteasome are structurally related α subunits (α1–α7), and the two inner rings are made of seven β subunits (2). Three of the β proteasomal proteins, namely β1, β2, and β5, are catalytically active in vertebrate proteasomes. On the basis of their substrate specificity, catalytic subunits of the 20S proteasome (called the constitutive or standard proteasome) exhibit caspase-like (β1), trypsin-like (β2), or chymotrypsin-like (β5) activities (3). In mammals, IFN-inducible catalytic subunits low-molecular mass polypeptide (LMP) 2, LMP7, and multicatalytic endopeptidase complex-like (MECL)-1 can incorporate into the 20S proteasome instead of the constitutive subunits, leading to the assembly of immunoproteasomes (4, 5). The immunoproteasome was originally described as an enzymatic complex abundantly expressed in immune cells, with an enhanced capacity to cleave proteins after their basic and hydrophobic residues, thereby optimizing the antigen presentation of MHC class I–restricted epitopes to $CD8^+$ T cells (6, 7). Thus, the function of the immunoproteasome is to optimize $CD8^+$ T-cell responses to various epitopes during viral and intracellular bacterial infections (8). Immunoproteasomes may also be important for recognition of neoantigens, which are newly formed antigens created by mutations in tumor cells. Various antigenic peptides derived from human tumors have been described to be more efficiently produced by immunoproteasomes or intermediate proteasomes than constitutive proteasomes (9, 10). Overall, the composition of proteasomes in the cell dictates the peptide repertoire displayed by MHC class I molecules, which has important consequences for elimination of viral infection and recognition of tumor antigens by CTLs.

Interestingly, the depletion of immunoproteasomes has a crucial impact on the onset of autoimmune responses and course of inflammation in mouse models of rheumatoid arthritis and colitis, suggesting that this enzymatic complex is not only involved in antigen presentation, but also in the regulation of inflammatory reactions (11–13). Novel studies have revealed that selective immunoproteasome inhibitors, such as ONX 0914, might be promising therapeutic agents for treatment of autoimmune disorders, such as multiple sclerosis, but also for inhibiting chronic inflammation in the colon, which is associated with development of colorectal cancer (14–16). Thus, the immunoproteasome seems to have some protumorigenic propensities due to its role in the regulation of expression of proinflammatory mediators, which perpetuate the chronic inflammation and lead to tumorigenesis. In this study, we reveal opposing roles for immunoproteasomes in two nonrelated cancer models. Although immunoproteasome deficiency

[1]Institute for Medical Microbiology and Hygiene, Philipps-University Marburg, Marburg, Germany. [2]Max Planck Institute for Infection Biology, Core Facility Microarray/Genomics, Berlin, Germany. [3]Pulmonary Center, Department of Medicine, Boston University School of Medicine, Boston, Massachusetts. [4]Center for Thrombosis and Hemostasis, University Medical Center of the Johannes Gutenberg-University, Mainz, Germany. [5]Institute for Lung Research, UGMLC, Philipps-University Marburg, Marburg, Germany. [6]German Center for Lung Research (DZL), Philipps-University Marburg, Marburg, Germany.

Note: Supplementary data for this article are available at Cancer Immunology Research Online (http://cancerimmunolres.aacrjournals.org/).

H. Leister and M. Luu contributed equally to this article.

Corresponding Author: Alexander Visekruna, Institute for Medical Microbiology and Hygiene, Philipps-University, Marburg, Hans Meerwein-Strasse 2, Marburg 35032, Germany. Phone: 4964-2158-66455; Fax: 4964-2158-66420; E-mail: alexander.visekruna@staff.uni-marburg.de

Cancer Immunol Res 2021;9:682–92

doi: 10.1158/2326-6066.CIR-20-0492

©2021 American Association for Cancer Research.

Downloaded from http://aacrjournals.org/cancerimmunolres/article-pdf/9/6/682/3099404/682.pdf by University of Marburg user on 14 February 2023

resulted in almost complete inhibition of tumor growth in colitis-associated colonic cancer (CAC), the absence of the same enzymatic complex resulted in enhanced tumor load and insufficient anticancer immune responses in a murine melanoma model. These findings suggest that the involvement of immunoproteasomes in shaping the tumor microenvironment (TME) diverges between different cancer types. During development of chronic inflammation–associated cancer, the protumoral capacity of immunoproteasomes appeared to contribute to carcinogenesis by inducing various proinflammatory factors, such as CXCL1, CXCL2, CXCL3, IL17A, IL1β, and IL6. In contrast, in the TME of melanoma, the immunoproteasome acted as an antitumorigenic factor by supporting the effector function of T cells and by promoting CTL-mediated anticancer immunity.

Materials and Methods

Human samples

Human tissue was obtained from colonic specimens immediately after the surgery performed at the Charité University Hospital (Berlin, Germany). This study was approved by the Local Ethics Committee of the Charité - Universitätsmedizin (Berlin, Germany). Written informed consent was obtained from all patients. Following the surgery, colonic tissue was separated from the underlying submucosa, subsequently frozen in liquid nitrogen, and stored at –196°C until use. The degree of inflammation in the surgical specimens was evaluated using a standard scoring system. A total of 10 patients with active ulcerative colitis, 10 patients with active Crohn disease, and 10 control tissues were examined by microarray analysis, as described in the next section.

Gene array analysis

Samples from patients were used in microarrays. Total RNA from colonic tissues was extracted with TRizol (Invitrogen). RNA quality was routinely tested using 2100 Bioanalyzer (Agilent Technologies). Labeling of RNA for hybridization was performed using the Low RNA Input Linear Amp Kit from Agilent Technologies according to the manufacturer's instructions. Briefly, 500 ng total RNA was reverse transcribed with an oligo-dT-T7 promoter primer and MMLV-RT. Second, strand synthesis was carried out with random hexamers. Fluorescence antisense cRNA (aRNA) was synthesized with either cyanine 3-CTP or cyanine 5-CTP and T7 polymerase. Purified products were quantified, and 2 μg labeled aRNA for each sample was fragmented and mixed with control targets and hybridization buffer. Hybridizations were performed at 60°C for 17 hours. Slides were washed according to the manufacturer's protocol (SSC wash protocol), and scanning of the arrays was performed at a 5 μm resolution using a DNA Microarray Laser Scanner (Agilent Technologies). Features were extracted from raw image data using the Agilent Technologies image analysis software (G2567AA Feature Extraction Software, version A7.5.1) and default settings. The microarray gene expression markup language data analysis was performed with the Rosetta Resolver Software Package (licensed by Aventis Pharmaceuticals) comprising a preprocessing pipeline of the feature extraction. This includes error model adjustments to the raw scan data, background subtraction by "spatial detrend," and array normalization using rank consistency filtering of normalization feature selection with a combination of linear and LOWESS curve fitting methods. Ratios were calculated by the most conservative estimates between universal error model and propagated error. Ratio profiles were combined in an error-weighted fashion by resolver to create ratio experiments. To compensate for dye-specific effects, and to ensure statistically significant data, a color-swap analysis (fluorescence reversal) was performed. Expression patterns were identified using 1.5-fold expression cutoffs of the ratio experiments and anticorrelation of the dye reversal profiles with an error weighted $P < 0.05$, rendering the microarray analysis significant ($P < 0.01$), robust, and reproducible. Raw intensity data of the .txt files without preprocessing were analyzed using the R package limma (Bioconductor). Gene set enrichment analysis (GSEA; https://www.gsea-msigdb.org/gsea/index.jsp) was performed using the "on" genes preranked by gene expression–based t-score using standard settings with 1,000 permutations. The microarray data have been deposited in the NCBI Gene Expression Omnibus under accession code GSE150979.

Analysis of publicly available transcriptomes

For the association of melanoma patient survival with expression of *PSMB8* (ENSG00000204264), *PSMB9* (ENSG00000240065), and *PSMB10* (ENSG00000205220), we interrogated The Cancer Genome Atlas (TCGA) database, accessed on March 30, 2020, using the package TCGAbiolinks v. 2.15.3 in the R programming environment v. 3.5.1. We retrieved harmonized fragments per kilobase million (FPKM) values from RNA sequencing experiments for *PSMB8, PSMB9*, and *PSMB10* from the Skin Cancer Melanoma project. FPKM values were grouped into quartiles, and the upper and lower quartiles were used for correlation with patient survival over a course of 3,650 days.

For patients with ulcerative colitis, colon cancer–associated genes were extracted from the publicly available gene sets (TCGA, M14524, and GRADE_COLON_CANCER_UP). Heatmaps were constructed by plotting z-score–transformed array intensities with the R package gplots v. 3.0.1.1. GSEA (https://www.gsea-msigdb.org/gsea/index.jsp) was used to determine overrepresentation of selected genes in publicly available datasets. Genes were chosen on the basis of absolute fold change in patients with ulcerative colitis versus control.

Mice

Mice were maintained under specific pathogen–free conditions at the Biomedical Research Center, Philipps-University of Marburg (Marburg, Germany). Female, 8- to 12-week-old wild-type (WT) mice, *PBSM8*/*PSMB9*/*PSMB10*-null [triple-knockout (TKO)] mice, and *LMP7*$^{-/-}$ mice on a C57BL/6 background were used for animal experiments. WT mice were obtained from The Jackson Laboratory. *LMP7*$^{-/-}$ mice were provided by Antje Behling (Charité - Universitätsmedizin Berlin, Berlin, Germany). TKO mice were generated by Kenneth Rock (University of Massachusetts, Worcester, MA) as reported previously (17) and were bred in our own animal facility. The study was approved by Regierungspräsidium Gießen, Germany (Nr. 70/2014 and Nr. 24/2019) and conducted according to the German animal protection law.

Cell lines and cell line treatment

The human colorectal cancer cell line HT-29 was purchased from the ATCC (HTB-38). B16-F10 and B16-GFP melanoma cells were kindly provided by Tobias Bopp (Johannes Gutenberg-University Mainz, Mainz, Germany). X6310-GM-CSF cell line used for generation of conditioned media was provided by Markus Schnare (Philipps-University Marburg, Marburg, Germany). HT-29 and X6310-GM-CSF cells were cultured in DMEM (Sigma-Aldrich) supplemented with 10% FCS, 100 U/mL Penicillin/Streptomycin (AppliChem), and 2 mmol/L Glutamine (PAN-Biotech) at 37°C with 5% CO_2. Cell lines used in experiments were routinely checked for *Mycoplasma* contamination. A total of 1.5×10^6 HT-29 cells per well were seeded into a 12-well plate and pretreated with IFNγ (200 U/mL, PeproTech)

Downloaded from http://aacrjournals.org/cancerimmunolres/article-pdf/9/6/682/3099404/682.pdf by University of Marburg user on 14 February 2023

for 24 hours. Afterwards, the cells were treated with TNFα (10 ng/mL, PeproTech) and IL1β (10 ng/mL, PeproTech) in absence or presence of ONX 0914 (0.5 μmol/L; an immunoproteasome inhibitor, Onyx Pharmaceuticals) for additional 24 hours and subjected to qRT-PCR analysis as described in the next section. An equal volume of Captisol (Ligand Pharmaceuticals, solvent for ONX 0914) without ONX 0914 was used as control. For detection of immunoproteasome expression in melanoma cells, 2×10^6 B16-F10 cells were cultured in a 12-well plate and treated with IFNγ (500 U/mL) for 48 hours. Subsequently, qRT-PCR was performed.

Subcutaneous melanoma tumor model

B16-F10 melanoma cells were cultured in RPMI1640 Medium (Thermo Fisher Scientific) supplemented with 100 U/mL penicillin/streptomycin, 10% FCS, and 2 mmol/L glutamine for 1 week before inoculation into mice. WT, TKO, and *LMP7*$^{-/-}$ mice were subcutaneously injected with 1×10^6 B16-F10 cells. In some experiments, the B16-GFP cell line was used as well. Tumor growth was monitored daily for 15 days by caliper measurements. To analyze T cells in tumors and tumor draining lymph nodes, mice were sacrificed, and tumor tissues and draining lymph nodes were harvested. The single-cell suspensions from lymph nodes were obtained by mechanical disruption using 30-μm Preseparation Filters (Miltenyi Biotec). Tumor-infiltrating lymphocytes (TIL) were isolated using the Miltenyi TIL Isolation Kit (Miltenyi Biotec, 130-096-730) and the GentleMACS Octo Dissociator (Miltenyi Biotec) according to the manufacturer's instructions. Briefly, the melanoma tumors were cut into small pieces and the tissue was transferred into GentleMACS tubes containing the enzyme mix. The tumors were dissociated into single-cell suspensions by combining enzymatic digestion with mechanical dissociation. After termination of the program, the cell suspensions were centrifuged (300 × *g*, 7 minutes) and supernatant was completely aspirated.

Induction of colitis-associated carcinogenesis

Age- and sex-matched WT and TKO mice were injected with Azoxymethane (AOM; Sigma-Aldrich) intraperitoneally (8 mg/kg body weight). After 5 days, mice were treated with 3% dextran sodium sulfate (DSS; MP Biomedicals) administered in the drinking water for 5 days, followed by 14 days of normal drinking water. Two additional cycles of DSS treatment were performed as described previously (16). The body weight of mice was monitored three times per week. After 80 days, mice were sacrificed and tumor numbers were counted. For investigation of recruitment of inflammatory cells, mice were analyzed by flow cytometric analysis and qRT-PCR on day 30 after induction of CAC by AOM/DSS as described below.

Isolation of colonic lamina propria mononuclear cells

Colonic tissue from WT and TKO mice was isolated and cut into pieces. The colonic tissue was homogenized using the Miltenyi Lamina Propria Dissociation Kit (Miltenyi Biotec, 130-097-410) and Miltenyi GentleMACS Octo dissociator, according to the protocol. After digestion, the cell suspensions were washed and further separated by a discontinuous density gradient centrifugation. The cells were resuspended in 40% Percoll (Merck) and carefully layered on 70% Percoll. After centrifugation at 625 × *g* for 20 minutes, the lamina propria mononuclear cells (LPMC) were collected from the interphase, washed, and prepared for further analysis as described below.

Histology

Hematoxylin and eosin (H&E) staining was performed on 5-μm thick colon tissue cryosections derived from WT and TKO mice. The samples were stained for 10 minutes with Hematoxylin (Carl Roth). Subsequently, cryosections were washed with water and incubated for 15 seconds with Eosin (Carl Roth). Following eosin staining, incubation of samples with 70% (1 second), 80% (10 seconds), and 96% ethanol (20 seconds), isopropanol (5 minutes), and Roti-Histol (Carl Roth, 2 × 3 minutes) was performed. The slides were dried and examined by bright-field microscopy. Leica DFC480 camera was used to take digital images by Leica Application Suite V3.8 software.

Generation of bone marrow–derived dendritic cells

Bone marrow progenitor cells were harvested from bone marrow (tibia or femur) of 8- to 12-week-old WT and TKO mice and cultured for 1 week in petri dishes in RPMI1640 media supplemented with 10% X6310-derived culture supernatant containing GMCSF. On day 7 of cell culture, the purity of cultured cells was tested by flow cytometry as described below. Afterwards, the cells were stimulated with Lipopolysaccharide (LPS; 100 ng/mL, Sigma-Aldrich) for 24 hours and assessed for NF-κB and ERK signaling by Western blotting.

Western blots on bone marrow–derived dendritic cells and thymocytes

For generating whole-cell lysates from murine bone marrow–derived dendritic cells (BMDC) and thymocytes, RIPA Lysis Buffer (Sigma-Aldrich) supplemented with protease inhibitors (Protease Inhibitor Cocktail, Thermo Fisher Scientific) was used. The quantification of total protein within the cell lysates was performed with Pierce BCA Protein Assays (Thermo Fisher Scientific). All samples were loaded on 12% SDS-PAGE gels with 20 μg of total protein. Following separation by electrophoresis, the samples were transferred on a Polyvinylidene Difluoride (PVDF) Membrane (Bio-Rad Laboratories). Subsequently, PVDF membranes containing transferred proteins were blocked for 1 hour with 5% BSA, followed by incubating the membrane with primary antibodies overnight at 4°C. The following primary antibodies were used: anti-p105 (eBioscience, catalog no. 14-6732-81), anti-p-RelA (Cell Signaling Technology, catalog no. 3033), and anti-p-ERK 1/2 (Cell Signaling Technology, catalog no. 4370). Afterwards, the samples were incubated with secondary antibodies for 2 hours at room temperature. Horseradish peroxidase linked anti-rabbit IgG (Cell Signaling Technology, catalog no. 7074) and anti-mouse IgG (Cell Signaling Technology, catalog no. 7076) were used. As a loading control, anti-β-actin (Sigma-Aldrich, catalog no. A551-2ML) and anti-α-tubulin (Sigma-Aldrich, catalog no. T5168) were used. The analyzed proteins were detected by using Western Blotting Luminol Reagent (Santa Cruz Biotechnology, catalog no. sc-2048) at the MicroChemi High-performance Imager (DNR Bio-Imaging Systems).

Thymocyte and peripheral CD8$^+$ T-cell assessment

For *ex vivo* analysis of thymocytes and CD8$^+$ T cells derived from spleens and lymph nodes, female 8- to 12-week-old WT, *LMP7*-deficient, and TKO mice were used. The single-cell suspensions were generated by mechanical disruption of thymi, spleens, and lymph nodes using 30-μm Preseparation Filters (Miltenyi Biotec). Afterwards, single-cell suspensions were counted before proceeding with the flow cytometry.

Antibodies and flow cytometry

Single-cell suspensions derived from thymocytes, spleens, lymph nodes, and TILs from melanoma tumors and LPMCs were used for flow cytometry. In some experiments, cells were incubated with Fc Block (Miltenyi Biotec, catalog no. 130-092-575) for 15 minutes prior

Downloaded from http://aacrjournals.org/cancerimmunolres/article-pdf/9/6/682/3099404/682.pdf by University of Marburg user on 14 February 2023

to cell surface staining according to the manufacturer's protocol. After performing surface staining with various antibodies for 15 minutes at 4°C, TILs and LPMCs were restimulated for 4 hours with PMA (50 ng/mL) and ionomycin (750 ng/mL) in the presence of Brefeldin A (10 mg/mL; all reagents, Sigma-Aldrich). Following fixation with 2% formaldehyde and permeabilization with 0.3% saponin buffer, the intracellular cytokine staining was performed with antibodies at recommended dilutions for 15 minutes at 4°C. Flow cytometry was performed using ARIA III and FACSCalibur Flow Cytometers (both BD Biosciences), followed by analysis using FlowJ_V10 Software (Tree Star). The following antibodies were used for staining: anti-CD3 (145-2C11), anti-CD4 (RM4-5), anti-CD8 (53-6.7), anti-IFNγ (XMG1.2), anti-IL17A (eBio17B7), anti-CD11b (clone M1/70), anti-Ly6G (1A8-Ly6g), anti-MHCI (AF6-88.5), and anti-MHCII (TIB 120). All antibodies were purchased from eBioscience, BD Biosciences, or BioLegend. A sample gating strategy for murine T cells can be found in Supplementary Fig. S1.

qRT-PCR

Colon tissues were homogenized using TRI Reagent (Sigma-Aldrich). For HT-29 and B16-F10 cells, the RNA isolation was performed using EXTRACTME TOTAL RNA KIT (BLIRT, catalog no. EM09.1-250). Total RNA was extracted according to the manufacturer's instructions. RevertAid First Strand cDNASynthesis Kit (Thermo Fisher Scientific) was used to generate cDNA according to the manufacturer's instructions. qRT-PCR was conducted using 500 ng template on a StepOne Plus Device (Applied Biosystems). For qRT-PCR analysis, the Takyon ROX SYBR Master Mix Blue dTTP Kit (Eurogentec) was used. Quantification of cDNA was carried out by normalization to expression of the housekeeping gene *Hprt1* using the $2^{-\Delta\Delta C_t}$ method. The following murine primers were used: *Cxcl1* forward: GCT TGA AGG TGT CCT CAG, reverse: AAG CCT CGC GAC CAT TCT TG; *Cxcl2* forward: GCG GTC TCA ATG CCT GAA GA, reverse: TTT GAC CGC CCT TGA GAG TG; *Cxcl3* forward: CAT CCA GAG CTT GAC GGT GAC, reverse: CTT GCC GCT CTT CAG TAT CTT CTT; *Cox2* forward: ATT CTT TGC CCA GCA CTT CA, reverse: GGG ATA CAC CTC TCC ACC AA; *Il1b* forward: TGG GCC TCA AAG GAA AGA AT, reverse: CAG GCT TGT GCT CTG CTT GT; *Il6* forward: GGA TAC CAC TCC CAA CAG ACC, reverse: TTC TCA TTT CCA CGA TTT CCC A; *Il12p40* forward: ATG TGT CCT CAG AAG CTA ACC ATC, *Il12p40* reverse: CGT GTC ACA GGT GAG GTT CAC T; *Il12p35* forward: TAC TAG AGA GAC TTC TTC CAC AAC AAG AG, *Il12p40* reverse: TCT GGT ACA TCT TCA AGT CCT CAT AGA; *Tnfα* forward: AAA ATT CGA GTG ACA AGC CTG TAG, *Tnfα* reverse: CCC TTG AAG AGA ACC TGG GAG TAG; and *Hprt1* forward: CTG GTG AAA AGG ACC TCT CG, reverse: TGA AGT ACT CAT TAT AGT CAA GGG CA. The following human primers were used: *Cxcl1* forward: AGT GTG AAC GTG AAG TCC CC, reverse: GAT GCA GGA TTG AGG CAA GC; *Cxcl2* forward: TGC AGG GAA TTC ACC TCA AGA, reverse: TGA GAC AAG CTT TCT GCC CA; *Cxcl3* forward: GCG CCC AAA CCG AAG TCA, reverse: GGT GCT CCC CTT GTT CAG TAT C; *Psmb8* forward: TGC TCG AGA TGT GAT GAA GG, reverse: TGT AAT CCA GCA GGT CAG CA; and *Hprt1* forward: TGC TCG AGA TGT GAT GAA GG, reverse: TGT AAT CCA GCA GGT CAG CA.

Statistical analysis

For all experiments with two groups, mean values were compared by using an unpaired Student *t* test (GraphPad Prism 8). For the comparison of the multiple groups, the statistical significance was determined by the one-way ANOVA test (GraphPad Prism 8). *P* values of $P < 0.05$ were considered as significant. Following *P* values were used: *, $P = 0.01$–0.05; **, $P = 0.001$–0.01; ***, $P < 0.001$. Data are presented as mean ± SEM.

Results

The immunoproteasome is essential for effective antitumor immunity against melanoma

The immunoproteasome is involved in modulation of chronic inflammatory environments, as well as in optimal antigen presentation of tumor epitopes to tumor-infiltrating $CD8^+$ T cells (10, 18). This dichotomy emphasizes the importance of this enzymatic complex in the TME. The role of immunoproteasomes in the onset of melanoma tumorigenesis and in melanoma-specific antitumor immunity is largely unknown. To assess the impact of immunoproteasomes on the survival of patients with melanoma, we examined the expression of immunoproteasome subunits LMP2 (*PSMB9*), MECL-1 (PSMB10), and LMP7 (*PSMB8*) in TCGA datasets from 470 patients with skin cutaneous melanoma. We observed that high expression of all three immunosubunits significantly associated with better overall survival, suggesting that the immunoproteasome might be an important prognostic biomarker for patients with melanoma (**Fig. 1A**).

Much research has focused on the inhibition of proteasome activity in tumor cells to promote cell death (19, 20). However, the effect of immunoproteasomes and constitutive proteasomes on the TME is poorly characterized. To test our hypothesis that the immunoproteasome might play a crucial role in $CD8^+$ T-cell–mediated anticancer immunity, we analyzed WT mice and animals lacking all three immunoproteasome proteins (TKO mice) implanted with B16-F10 melanoma tumors. In TKO mice, we observed a significantly higher increase in tumor volume and tumor weight compared with WT counterparts, suggesting that the immunoproteasome exhibits antitumor effects in this model (**Fig. 1B–D**). TKO mice had significantly fewer $CD8^+$ T cells in tumor draining lymph nodes (Supplementary Fig. S2). Less CTLs were recruited into the tumors at day 15 after injection of tumor cells, which led to reduced cell numbers of IFNγ-producing $CD8^+$ T lymphocytes in the TME (**Fig. 1E–G**).

Absence of LMP7 in the TME results in impaired antitumor immunity against melanoma

A new catalytic subunit of the proteasome, β5t, which is expressed primarily in cortical thymic epithelial cells, has been described previously (21). Together with LMP2 and MECL-1, β5t forms the so-called thymoproteasomes that are crucial for positive selection of immature thymocytes (22). We observed that both the frequencies and cell numbers of CD8 single-positive thymocytes and $CD8^+$ T cells in the periphery were reduced in naïve TKO mice as compared with WT animals (Supplementary Fig. S3). These results confirm previous findings (17), and suggest that the lack of LMP2 and MECL-1, as a part of the thymoproteasome, is responsible for reduced numbers of $CD8^+$ T cells in TKO mice because the LMP7-deficient animals displayed normal $CD8^+$ T-cell numbers and frequencies at steady state (Supplementary Fig. S4).

To assess the impact of TME-derived LMP7 on melanoma growth, we subcutaneously injected B16-F10 cells into WT and LMP7-deficient animals and monitored the tumor growth for 2 weeks. We observed progressively increased growth of melanomas in mice lacking LMP7 compared with WT mice, as shown by accelerated tumor size growth and weight (**Fig. 2A** and **B**). Although the frequency

Downloaded from http://aacrjournals.org/cancerimmunolres/article-pdf/9/6/682/3099404/682.pdf by University of Marburg user on 14 February 2023

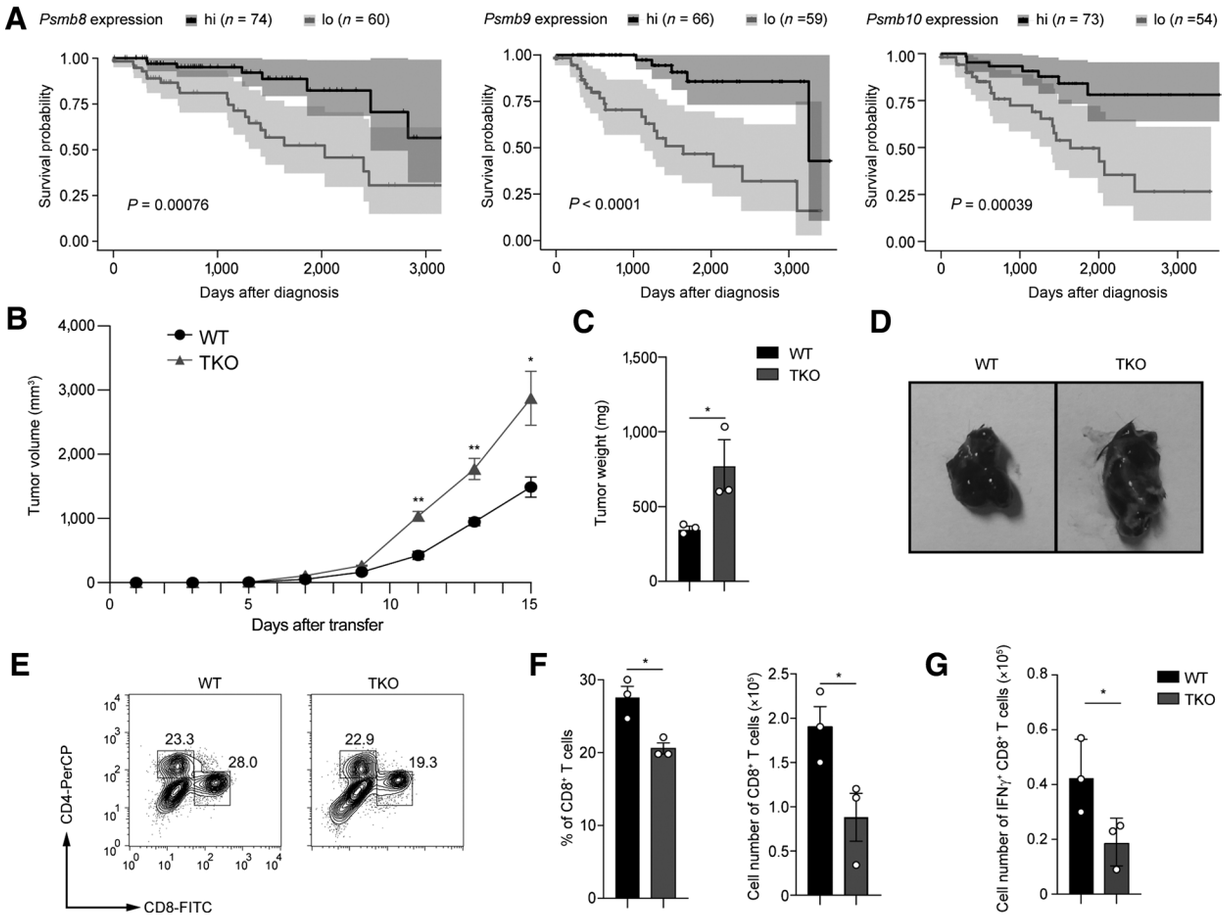

Figure 1.

Immunoproteasome expression in the TME is crucial for optimal CTL-mediated antitumor responses. **A,** Kaplan–Meier plots of melanoma patient survival depending on expression (FPKM, lower and upper quartile) of the respective immunoproteasome subunits (TCGA datasets). Number of patients per group is indicated in the panel. **B–G,** B16-F10 melanoma cells were transplanted subcutaneously into WT and immunoproteasome-deficient TKO mice ($n = 9$ mice/group) for 15 days. **B–D,** Tumor volume and tumor mass were analyzed. **E,** Representative contour plots of $CD4^+$ and $CD8^+$ T cells in mice. Bar graphs of frequencies (**F**) and cell numbers (**G**) of $CD8^+$ and $IFN\gamma^+CD8^+$ T cells in tumors. One of three independent experiments with $n = 3$ mice/condition. **B–G,** Data were analyzed by two-tailed unpaired Student *t* test (*, $P = 0.01$–0.05; **, $P = 0.001$–0.01; mean ± SEM).

of $CD4^+$ and $CD8^+$ T lymphocytes was not reduced in tumors and draining lymph nodes in mice lacking LMP7, the cell number of $IFN\gamma^+$ T lymphocytes was impaired in LMP7-deficient mice (**Fig. 2C** and **D**; Supplementary Fig. S5). Apart from $CD8^+$ CTLs, Th1 cells are also crucially involved in promoting anticancer immunity (23). In the absence of LMP7, reduced expression of IFNγ and IL17A was detected in $CD4^+$ T cells isolated from tumors (**Fig. 2E**). Similarly, compared with WT $CD8^+$ T cells, LMP7-deficient CTLs derived from tumors produced less IFNγ (**Fig. 2F**). The defective antitumor response in LMP7-deficient mice was also reflected in reduced TNFα and IL12 production in the TME (**Fig. 2G**), indicating that antigen-presenting cell (APC)–derived cytokines that induce T-cell IFNγ secretion are also affected by the absence of LMP7. In contrast to WT control cells, *in vitro*–generated BMDCs from TKO and LMP7-deficient mice were not able to upregulate IL12 expression following stimulation with LPS (Supplementary Fig. S6). Collectively, these results highlight the important role of immunoproteasomes in shaping the TME and promoting antitumor activity of CTLs and Th1 cells.

The TME induces immunoproteasome expression in melanoma cells

The cytokines and chemokines secreted by immune and stroma cells within the melanoma microenvironment play an important role in recruiting immune cells and in communication with tumor cells. To assess the effect of immunoproteasome absence in the TME on the proteasome composition in tumor cells, we inoculated B16-GFP cells into WT, LMP7-deficient, and TKO mice, respectively. On day 15 after tumor inoculation, we measured the expression of immunoproteasomes within the GFP^+ melanoma cells. The induction of the immunoproteasome subunit LMP7 was observed only in tumor cells derived from WT, but not from LMP7-deficient or TKO mice (Supplementary Fig. S7). This implies that immune cells with high expression of IFNγ in the TME of WT mice directly impact the proteasome activity of neighboring tumor cells. This observation was confirmed in *in vitro* experiments, as IFNγ increased the expression of all three immunoproteasome subunits in B16-F10 cells (Supplementary Fig. S7). Human melanoma cells overexpressing immunoproteasomes have been shown to have a clear tendency to increase their immunogenic

Downloaded from http://aacrjournals.org/cancerimmunolres/article-pdf/9/6/682/3099404/682.pdf by University of Marburg user on 14 February 2023

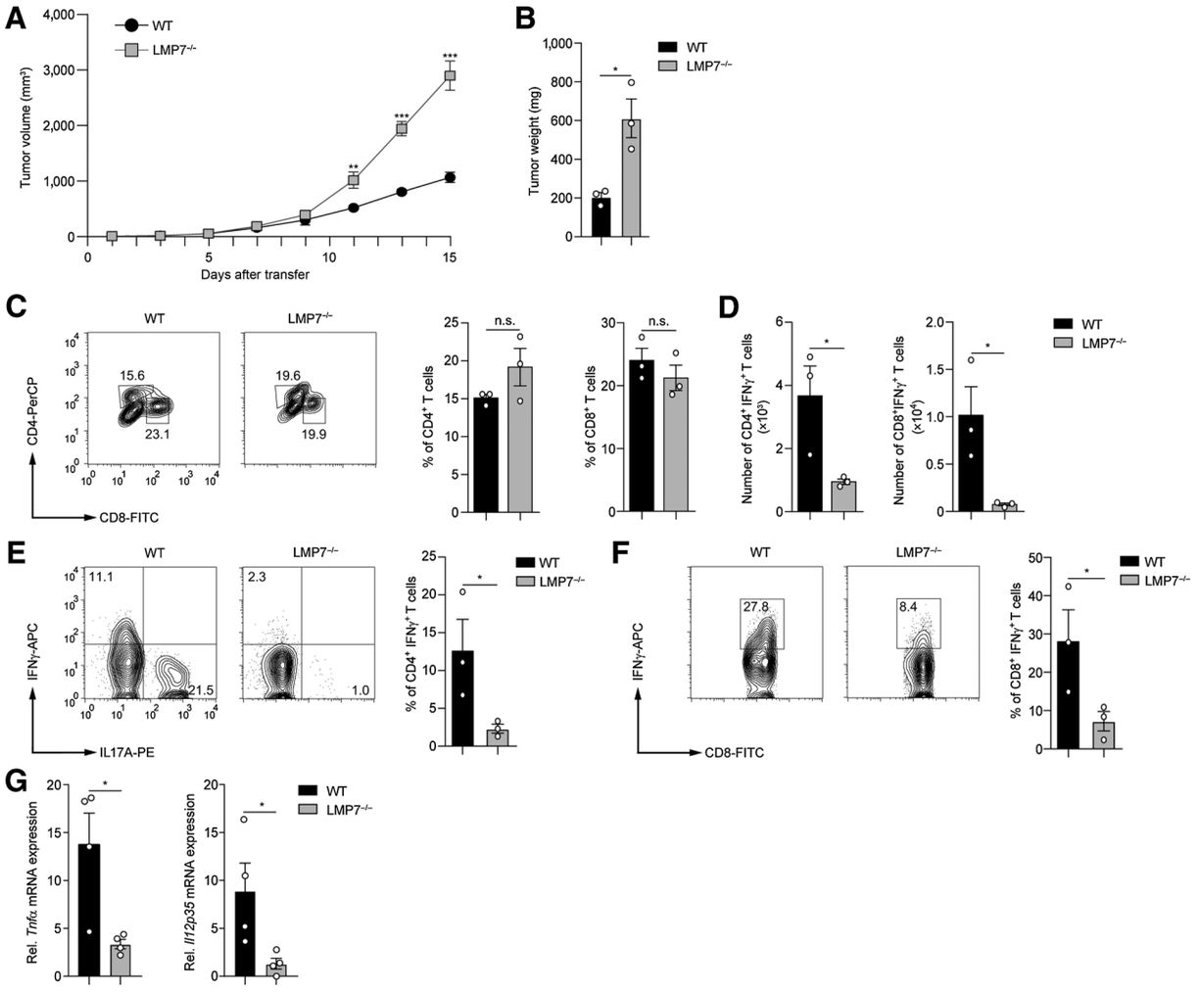

Figure 2.

LMP7-deficient mice display reduced antitumor immunity against melanoma. **A** and **B,** Tumor volume and tumor mass were analyzed after subcutaneous inoculation of B16-F10 melanoma cells into WT and *LMP7*-deficient mice ($n = 6$ mice/group). Tumor weight was analyzed at day 15 after inoculation. The percentage of $CD4^+$ and $CD8^+$ T cells (**C**) and total cell number of IFNγ-producing $CD4^+$ and $CD8^+$ T lymphocytes (**D**) in tumors were analyzed by flow cytometry at day 15 after tumor inoculation. Bar graphs and representative contour plots show percentages of $IFN\gamma^+CD4^+$ T cells and $IL17A^+CD4^+$ T cells (**E**) and $IFN\gamma^+CD8^+$ T cells (**F**) on day 15 after inoculation. **G,** Relative mRNA expression for *Tnfa* and *Il12p35* was measured in the TME by qRT-PCR on day 15 after B16 inoculation. Two-tailed unpaired Student *t* test was applied (n.s., not significant; *, $P = 0.01$–0.05; **, $P = 0.001$–0.01; ***, $P < 0.001$, results are shown as mean ± SEM). One of two independent experiments is shown ($n = 6$ mice/group).

antigen repertoire (24). Together, this may affect the magnitude and quality of CTL-mediated anticancer responses, as the immunoproteasome expressed in melanoma cells might be implicated in generation of neoantigens.

Protumoral function of immunoproteasomes during inflammation-driven carcinogenesis

Although the immunoproteasome was originally described as a multi-subunit catalytic complex required for optimizing the generation of peptides for MHC class I antigen processing, we and others have shown that the pharmacologic blockade of immunoproteasomes efficiently inhibits the development of colitis and colitis-associated cancer (CAC; refs. 13, 15, 16). Over the past few years, findings from several laboratories have demonstrated that immunoproteasomes orchestrate the onset of immunopathology in diseases such as Crohn disease and rheumatoid arthritis (11, 25). To better understand the role of immunoproteasomes in regulating the TME during chronic inflammation, we induced CAC in WT mice and mice lacking immunoproteasomes by treating them with the carcinogens azoxymethane and DSS. As expected, at day 80 after AOM/DSS treatment, we found enhanced development of cancer-associated neoplasia in WT mice, as indicated by the measurement of body weight, tumor numbers, colon length, and the H&E staining. In contrast, animals lacking immunoproteasomes did not show any signs of pathology. Although some minor alterations in the morphology of intestinal epithelial cells were observed, TKO mice exhibited less pronounced weight loss and shortening of the colon, as well as almost no detectable tumors (**Fig. 3A–D**).

To examine the role of the immunoproteasome in shaping the TME during chronic inflammation in more detail, we analyzed the immune

Downloaded from http://aacrjournals.org/cancerimmunolres/article-pdf/9/6/682/3099404/682.pdf by University of Marburg user on 14 February 2023

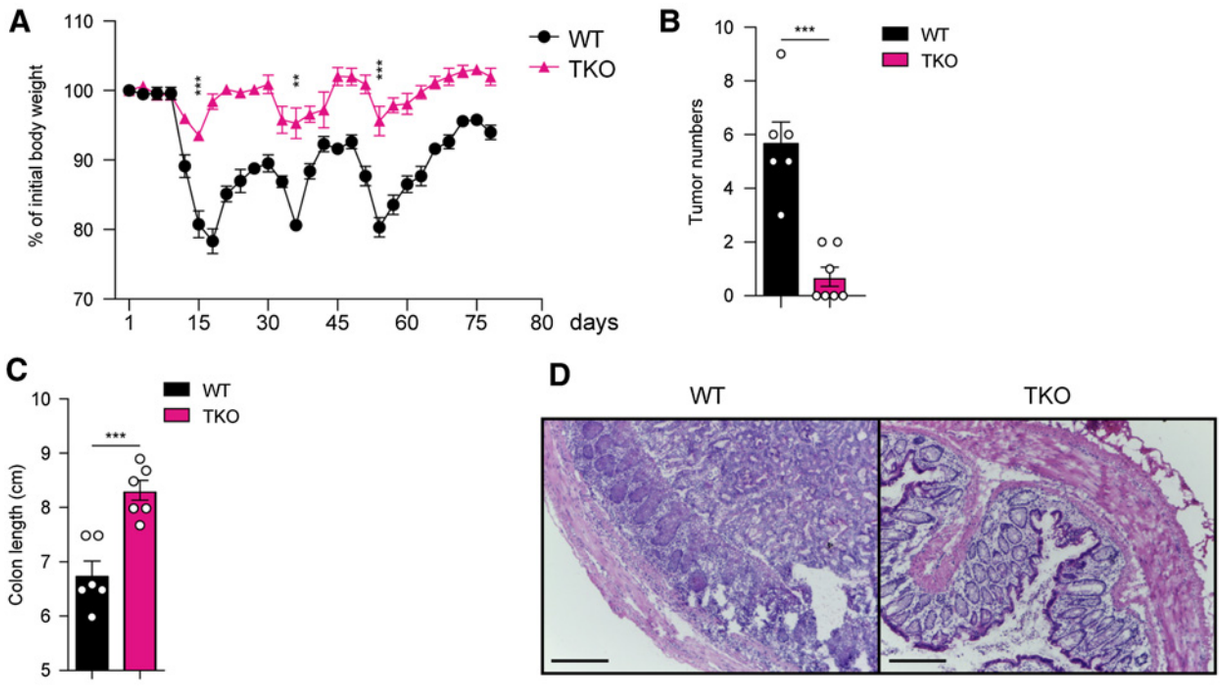

Figure 3.

Immunoproteasome-deficient mice are protected from CAC. **A–D,** WT and TKO mice ($n = 6$ mice/group) were treated with three rounds of DSS after intraperitoneal azoxymethane administration for CAC induction. On day 80, colonic tissue was isolated. **A,** Relative weight loss was monitored for 80 days. Bar graphs of numbers of colorectal tumors (**B**) and colon length (**C**). **D,** Histology of distal colon tissue (scale bars, 100 μm). Data were pooled from two independent experiments with $n = 3$ mice per experiment and were analyzed by two-tailed unpaired Student t test (**, $P = 0.001$–0.01; ***, $P < 0.001$; mean ± SEM).

cells in colonic lamina propria of WT and TKO mice at day 30 after induction of AOM/DSS-mediated carcinogenesis. Along with reduced tumor numbers, a lower percentage of IFNγ- and IL17A-producing $CD4^+$ T cells and a lower frequency of infiltrating neutrophils were found in TKO animals compared with WT mice (**Fig. 4A–C**). qRT-PCR analysis revealed that many protumorigenic factors are involved in the development of CAC, such as the enzyme COX-2 and the cytokines IL6 and IL1β, which directly enhance the proliferative capacity of epithelial cells, as well as protumorigenic chemokines CXCL1, CXCL2, and CXCL3, governing the recruitment of neutrophils, were downregulated in TKO mice at day 30 (**Fig. 4D**). It is known that activated neutrophils produce high IL1β and reactive oxygen species, directly contributing to the pathogenesis of CAC by inducing DNA damage in epithelial cells (26, 27). Neutrophil maturation in the bone marrow of TKO mice was normal (Supplementary Fig. S8), suggesting that impaired recruitment of neutrophilic granulocytes into the intestinal lamina propria, rather than formation of these cells in the absence of immunoproteasomes, is responsible for the observed phenotype. We observed partially defective NF-κB and ERK signaling pathways in LPS/IFNγ-treated APCs lacking immunoproteasomes (Supplementary Fig. S9). These signaling cascades are involved in the transcription control of proinflammatory mediators that are associated with CAC development, and their activation is known to be dependent on optimal function of the proteasome/ubiquitin system (28). The NF-κB pathway was intact in thymocytes derived from naïve immunoproteasome-deficient mice, indicating that only inflammation-driven, but not tonic activity of NF-κB is affected in the absence of immunoproteasomes (Supplementary Fig. S9). Together, these findings demonstrate protumoral activity of immunoproteasomes in the context of chronic inflammation.

Patients with ulcerative colitis exhibit increased immunoproteasome-regulated mediators

Ulcerative colitis is a chronic inflammatory disease associated with high risk to develop colorectal cancer (29). Because immunoproteasome-induced factors play a central role in both chronic colonic inflammation and colorectal cancer, we asked whether we could find a signature of genes that was regulated by immunoproteasomes in human patients with ulcerative colitis. We observed that patients with ulcerative colitis with a severe course of disease displayed different patterns of chemokines in the inflamed colon compared with control tissue and patients with Crohn disease. Microarray analysis revealed that in patients with ulcerative colitis, but not in patients with Crohn disease, the gene signature associated with recruitment of innate immune cells, including neutrophil-attracting chemokines CXCL1, CXCL2, and CXCL3 (which were downregulated in immunoproteasome-deficient mice), was pronounced (**Fig. 5A**). The genes characteristic for adenoma/adenocarcinoma were significantly enriched in patients with ulcerative colitis compared with control colonic tissue (**Fig. 5B**). We also found a significant upregulation of immunoproteasome subunits in the chronically inflamed intestines of patients with ulcerative colitis compared with control gut tissue (**Fig. 5C**).

To test whether malignant epithelial cells were able to upregulate the expression of immunoproteasomes, we treated HT-29 cells, a human colorectal adenocarcinoma cell line, with diverse stimuli. The assembly

Downloaded from http://aacrjournals.org/cancerimmunolres/article-pdf/9/6/682/3099404/682.pdf by University of Marburg user on 14 February 2023

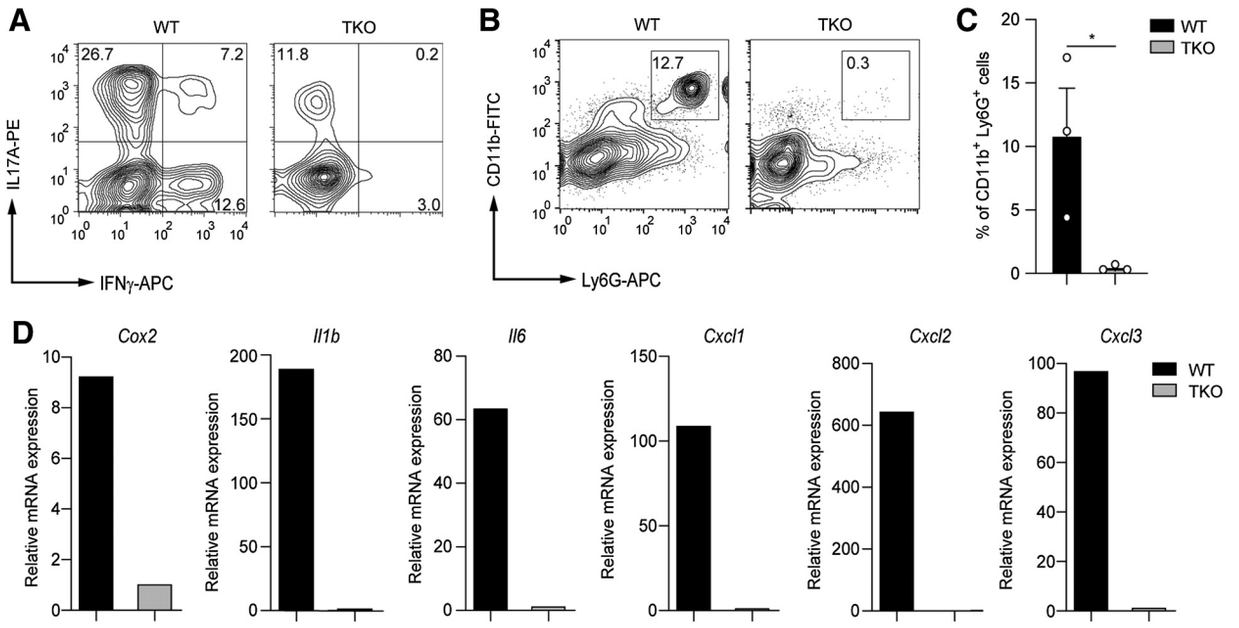

Figure 4.

Impaired recruitment of immune cells in the intestine of immunoproteasome-deficient mice during development of CAC. **A–C,** WT and immunoproteasome-deficient TKO mice were treated with two cycles of DSS after peritoneal azoxymethane injection. On day 30 after AOM/DSS administration, colonic tissue was isolated and analyzed by flow cytometry and qRT-PCR. **A,** Representative contour plots show the frequencies of $IL17A^+$ and $IFN\gamma^+CD4^+$ T cells. Representative contour plots (**B**) and bar graphs (**C**) show the frequency of infiltrating neutrophils. Cells were gated on SSC^{high} granulocyte gate (**B** and **C**). One of two similar experiments with $n = 3$ mice per group per experiment is shown. **D,** Representative bar graphs ($n = 6$ mice/group) show qRT-PCR analysis of colonic tissue analyzed on day 30 after AOM/DSS administration. One representative qRT-PCR analysis of three experiments is shown. Data were analyzed by two-tailed unpaired Student *t* test (*, $P = 0.01$–0.05; mean ± SEM).

of immunoproteasomes is known to be accomplished by IFNγ treatment, but it remains unclear whether colon cancer cells are capable of expressing immunoproteasomes. Only IFNγ, but not other stimuli tested, was able to induce the expression of the immunoproteasome subunit LMP7 in HT-29 cells (**Fig. 5D**). To assess the relative expression of protumorigenic chemokines in the presence of immunoproteasomes, we treated HT-29 cells with IFNγ, TNFα, and IL1β. TNFα and IL1β are known to synergistically induce the expression of CXCL1–3 (30). We found that upregulation of all three chemokines was completely abrogated when HT-29 cells were treated with the immunoproteasome inhibitor, ONX 0914 (**Fig. 5E**). Thus, immunoproteasomes are not only important regulators of TME, but they are also active in cancer cells to promote recruitment of innate immune cells and to support carcinogenesis. Our data provide insight into CAC pathogenesis and suggest that the treatment of patients with a severe course of ulcerative colitis with specific immunoproteasome inhibitors may reduce the high risk of developing colon cancer.

Discussion

The function of the immunoproteasome in cancer development is not as well understood as its role in regulating innate immunity and cytokine production. One report has demonstrated that deficiency of LMP7 in breast cancer cells suppresses tumor invasion and metastasis (31). Another study revealed that the high expression of immunoproteasomes in human melanoma is associated with a favorable response to treatment with immune checkpoint inhibitors (24). Although, the primary activity of immunoproteasomes has been attributed to optimal processing of viral and intercellular bacterial proteins for MHC class I antigen presentation, novel findings suggest that this enzymatic molecule is also an important regulator of the neoantigen repertoire that can be more efficiently presented when the expression of immunoproteasome is higher (10).

In this study, we describe opposing roles for immunoproteasomes in association with shaping the TME. The immunoproteasome, which contains three proteolytic subunits LMP2, MECL-1, and LMP7, appears to play a crucial role in modulating immune responses during infection and inflammation (32). We show here that during chronic colonic inflammation, the immunoproteasome supports the progression of colonic tumors by elevating production of protumorigenic factors in immune and cancer cells, as well as by recruiting innate immune cells into the inflamed gut. The capacity of immunoproteasomes to alter the gene expression of proinflammatory and protumorigenic mediators likely results from the posttranscriptional regulation of key transcription factors, such as NF-κB, STAT3, and IRF4, in immune cells (16, 33), but also by the upregulation of immunoproteasome activity in the gut epithelium. The experiments with colon cancer cells support the novel concept that immunoproteasomes are not only active in immune cells, but also in neoplastic epithelial cells during CAC development. IL6-, IL1β-, and NF-κB–controlled protumorigenic chemokines CXCL1–3 were downregulated in TKO compared with WT animals, providing evidence that immunoproteasomes act as a functional link between chronic inflammation and cancer development in the large intestine. In contrast to inflammation-driven carcinogenesis, we observed that, in the absence of immunoproteasomes, the lack of efficient CTL-mediated antitumor immunity and reduced expression of APC-derived cytokines, such as

Downloaded from http://aacrjournals.org/cancerimmunolres/article-pdf/9/6/682/3099404/682.pdf by University of Marburg user on 14 February 2023

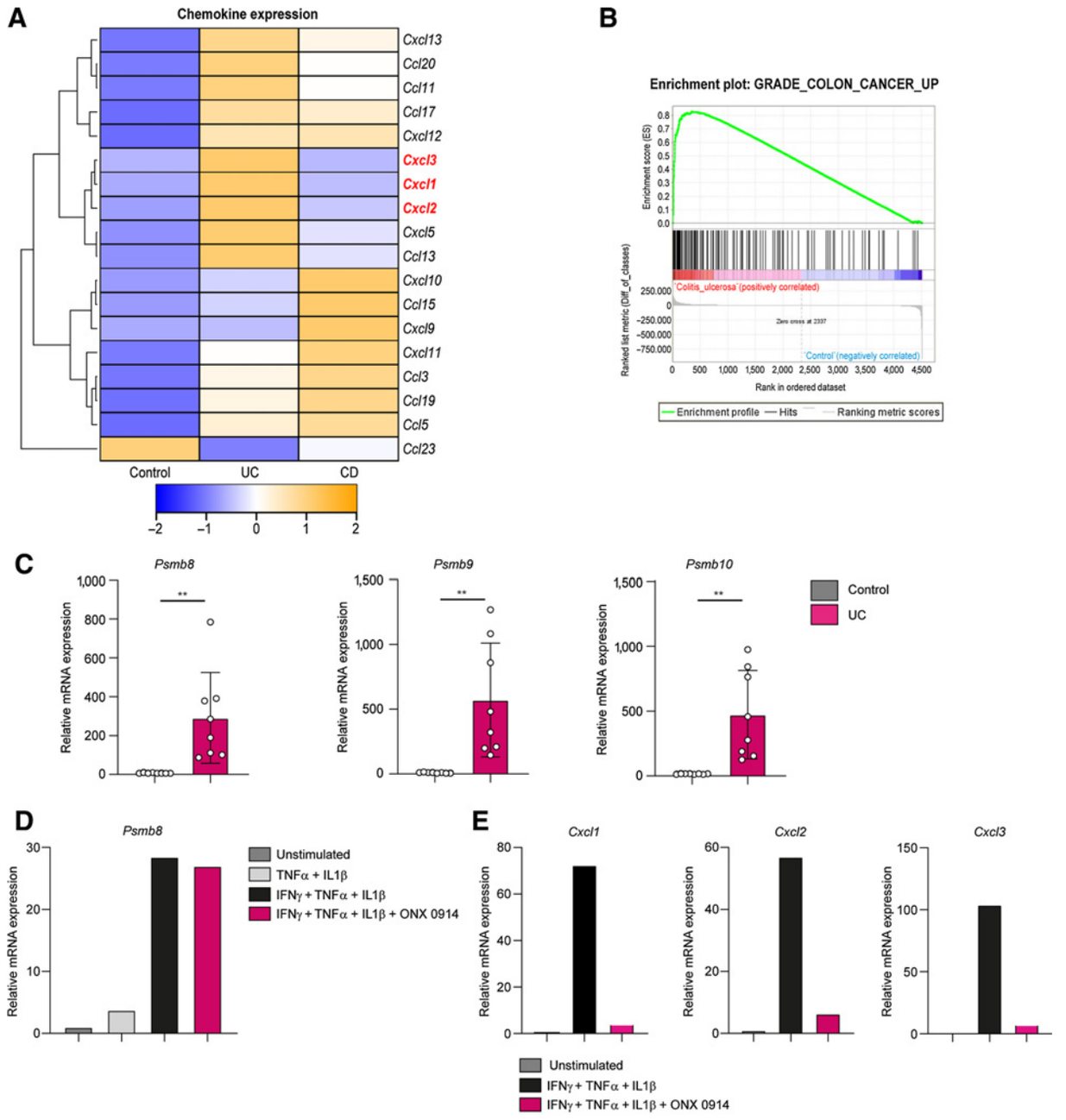

Figure 5.

Patients with ulcerative colitis show an enrichment of adenocarcinoma and innate immune genes. **A** and **B,** Transcriptional analysis of colonic tissue derived from patients with ulcerative colitis (UC) and Crohn disease (CD) compared with healthy controls ($n = 10$ patients/group). **A,** Heatmap showing the chemokine expression signature. Array intensity values were z-transformed and plotted. **B,** Genes with an absolute fold change of at least 2 in ulcerative colitis versus control samples were probed by GSEA. Enrichment of adenocarcinoma genes enhanced in patients with ulcerative colitis was compared with control group. Adenocarcinoma-associated genes for colon cancer were extracted from the publicly available gene set (see Materials and Methods). **C,** Relative mRNA expression for immunoproteasome genes *Psmb8, Psmb9*, and *Psmb10* in the large intestine of patients with ulcerative colitis compared with control tissue, assessed by qRT-PCR analysis (same cohort as in **A** and **B**). Data were analyzed by two-tailed unpaired Student *t* test (**, $P = 0.001$–0.01; mean ± SEM). **D** and **E,** HT-29 colon cancer cells were stimulated with the indicated cytokines for 2 days in absence or presence of ONX 0914. Representative bar graphs indicating gene expression of immunoproteasome gene *Psmb8* (**D**) and chemokines *Cxcl1*, *Cxcl2*, and *Cxcl3* (**E**), obtained by qRT-PCR analysis. Three independent experiments were performed.

Downloaded from http://aacrjournals.org/cancerimmunolres/article-pdf/9/6/682/3099404/682.pdf by University of Marburg user on 14 February 2023

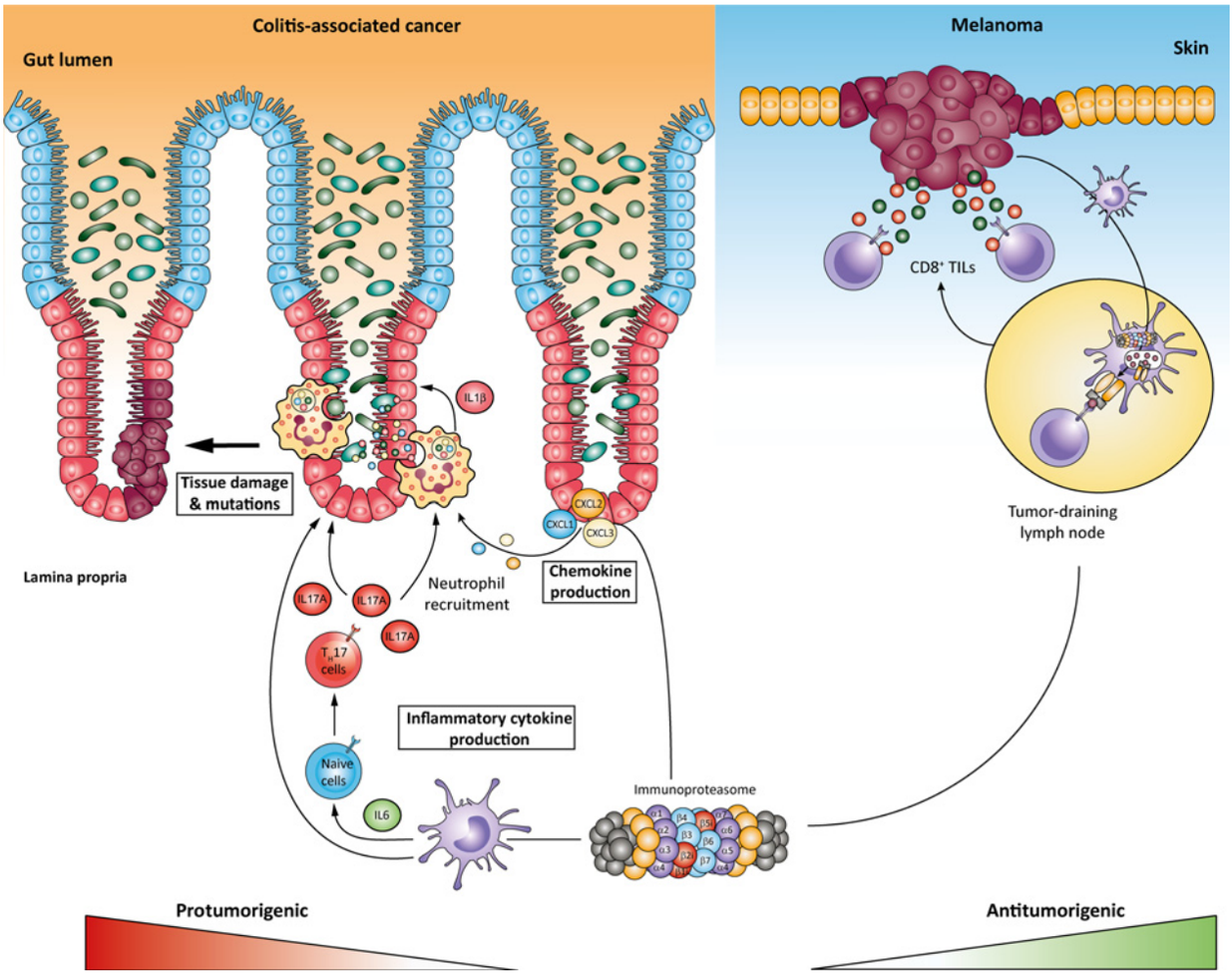

Figure 6.
Schematic overview showing opposing activities of immunoproteasomes in two different cancer types. Immunoproteasomes promote development of colon cancer associated with chronic inflammation by recruiting immune cells and by regulating the expression of protumorigenic cytokines and chemokines in inflamed tissues. In contrast, in melanoma, immunoproteasomes are crucial antitumorigenic molecules supporting the function of APCs and T lymphocytes, leading to optimal CTL-mediated antitumor immunity.

IL12, led to the enhanced growth of melanoma tumors. We also observed an upregulation of immunoproteasomes in melanoma cells, a phenomenon which was dependent on the presence of IFNγ in the TME. The immunogenicity and presence of neoantigens are shown to be increased in human melanoma cells with high immunoproteasome expression (24). Collectively, the role of immunoproteasomes during development of carcinogenesis depends on the tumor-specific environment. By promoting recruitment and activation of immune cells, immunoproteasomes upregulate cytokine and chemokine networks that perpetuate inflammatory reactions leading to development of CAC. In contrast to the intestinal inflammatory milieu, the immunoproteasome has an antitumorigenic potential in melanoma tumors by supporting APC function and T-cell–mediated antitumor immunity (**Fig. 6**). Our findings demonstrate that the role of immunoproteasomes in TME interactions should be considered in a more differentiated way. Future studies will be needed to elucidate the function of the immunoproteasome in different cancer types to develop adequate therapeutic strategies.

Authors' Disclosures

M. Luu reports grants from Von Behring-Röntgen-Stiftung and Studienstiftung des Deutschen Volkes during the conduct of the study. M. Bosmann reports grants from NIH, German Research Foundation, and German Ministry for Education and Research (BMBF) during the conduct of the study. No disclosures were reported by the other authors.

Disclaimer

The authors are responsible for the content of this article.

Authors' Contributions

H. Leister: Validation, visualization, methodology. **M. Luu:** Supervision, validation, investigation, methodology. **D. Staudenraus:** Investigation, methodology. **A. Lopez Krol:** Investigation, methodology. **H.-J. Mollenkopf:** Conceptualization, software, formal analysis. **A. Sharma:** Investigation, methodology. **N. Schmerer:** Validation, methodology. **L.N. Schulte:** Supervision, validation, visualization, methodology. **W. Bertrams:** Investigation, visualization, methodology. **B. Schmeck:** Supervision, investigation. **M. Bosmann:** Software, supervision,

Downloaded from http://aacrjournals.org/cancerimmunolres/article-pdf/9/6/682/3099404/682.pdf by University of Marburg user on 14 February 2023

validation, investigation. **U. Steinhoff:** Supervision, funding acquisition. **A. Visekruna:** Supervision, funding acquisition, validation.

Acknowledgments

The authors thank Anne Hellhund for excellent technical support. The technical expertise in breeding and maintaining specific pathogen–free animals by staff of the animal facility, Biomedical Research Center, Philipps-University of Marburg, is gratefully acknowledged. This project was supported by the Von Behring-Röntgen-Stiftung (to M. Luu, U. Steinhoff, and B. Schmeck), FAZIT-Stiftung (to H. Leister and A. Visekruna), Bundesministerium für Bildung und Forschung (JPI-AMR – FKZ 01Kl1702 and ERACoSysMed2 – SysMed-COPD – FKZ 031L0140 to B. Schmeck and 01EO1003 and 01EO1503 to M. Bosmann), German Research Foundation (SFB/TR-84 TP C01 to B. Schmeck and VI 562/10-1 to A. Visekruna), LOEWE Center DRUID (Project C4 to U. Steinhoff), Stiftung Kempkes PE (to M. Luu), and the NIH (1R01HL141513 and 1R01HL139641 to M. Bosmann).

The costs of publication of this article were defrayed in part by the payment of page charges. This article must therefore be hereby marked *advertisement* in accordance with 18 U.S.C. Section 1734 solely to indicate this fact.

Received June 10, 2020; revised December 14, 2020; accepted March 9, 2021; published first March 11, 2021.

References

1. Ciechanover A. The ubiquitin-proteasome pathway: on protein death and cell life. EMBO J 1998;17:7151–60.
2. Wolf DH, Hilt W. The proteasome: a proteolytic nanomachine of cell regulation and waste disposal. Biochim Biophys Acta 2004;1695:19–31.
3. Groll M, Huber R. Substrate access and processing by the 20S proteasome core particle. Int J Biochem Cell Biol 2003;35:606–16.
4. Kloetzel PM. Antigen processing by the proteasome. Nat Rev Mol Cell Biol 2001; 2:179–87.
5. Kruger E, Kuckelkorn U, Sijts A, Kloetzel PM. The components of the proteasome system and their role in MHC class I antigen processing. Rev Physiol Biochem Pharmacol 2003;148:81–104.
6. Stohwasser R, Kuckelkorn U, Kraft R, Kostka S, Kloetzel PM. 20S proteasome from LMP7 knock out mice reveals altered proteolytic activities and cleavage site preferences. FEBS Lett 1996;383:109–13.
7. Groettrup M, Kraft R, Kostka S, Standera S, Stohwasser R, Kloetzel PM. A third interferon-gamma-induced subunit exchange in the 20S proteasome. Eur J Immunol 1996;26:863–9.
8. Stoltze L, Nussbaum AK, Sijts A, Emmerich NP, Kloetzel PM, Schild H. The function of the proteasome system in MHC class I antigen processing. Immunol Today 2000;21:317–9.
9. Guillaume B, Chapiro J, Stroobant V, Colau D, Van Holle B, Parvizi G, et al. Two abundant proteasome subtypes that uniquely process some antigens presented by HLA class I molecules. Proc Natl Acad Sci U S A 2010;107: 18599–604.
10. Vigneron N, Abi Habib J, Van den Eynde BJ. Learning from the proteasome how to fine-tune cancer immunotherapy. Trends Cancer 2017;3:726–41.
11. Muchamuel T, Basler M, Aujay MA, Suzuki E, Kalim KW, Lauer C, et al. A selective inhibitor of the immunoproteasome subunit LMP7 blocks cytokine production and attenuates progression of experimental arthritis. Nat Med 2009; 15:781–7.
12. Basler M, Dajee M, Moll C, Groettrup M, Kirk CJ. Prevention of experimental colitis by a selective inhibitor of the immunoproteasome. J Immunol 2010;185: 634–41.
13. Schmidt N, Gonzalez E, Visekruna A, Kuhl AA, Loddenkemper C, Mollenkopf H, et al. Targeting the proteasome: partial inhibition of the proteasome by bortezomib or deletion of the immunosubunit LMP7 attenuates experimental colitis. Gut 2010;59:896–906.
14. Basler M, Mundt S, Muchamuel T, Moll C, Jiang J, Groettrup M, et al. Inhibition of the immunoproteasome ameliorates experimental autoimmune encephalomyelitis. EMBO Mol Med 2014;6:226–38.
15. Koerner J, Brunner T, Groettrup M. Inhibition and deficiency of the immunoproteasome subunit LMP7 suppress the development and progression of colorectal carcinoma in mice. Oncotarget 2017;8:50873–88.
16. Vachharajani N, Joeris T, Luu M, Hartmann S, Pautz S, Jenike E, et al. Prevention of colitis-associated cancer by selective targeting of immunoproteasome subunit LMP7. Oncotarget 2017;8:50447–59.
17. Kincaid EZ, Che JW, York I, Escobar H, Reyes-Vargas E, Delgado JC, et al. Mice completely lacking immunoproteasomes show major changes in antigen presentation. Nat Immunol 2012;13:129–35.
18. Groettrup M, Kirk CJ, Basler M. Proteasomes in immune cells: more than peptide producers? Nat Rev Immunol 2010;10:73–8.
19. Adams J. The development of proteasome inhibitors as anticancer drugs. Cancer Cell 2004;5:417–21.
20. Adams J. The proteasome: a suitable antineoplastic target. Nat Rev Cancer 2004; 4:349–60.
21. Murata S, Sasaki K, Kishimoto T, Niwa S, Hayashi H, Takahama Y, et al. Regulation of CD8+ T cell development by thymus-specific proteasomes. Science 2007;316:1349–53.
22. Nitta T, Murata S, Sasaki K, Fujii H, Ripen AM, Ishimaru N, et al. Thymoproteasome shapes immunocompetent repertoire of CD8+ T cells. Immunity 2010;32: 29–40.
23. Hung K, Hayashi R, Lafond-Walker A, Lowenstein C, Pardoll D, Levitsky H. The central role of CD4(+) T cells in the antitumor immune response. J Exp Med 1998;188:2357–68.
24. Kalaora S, Lee JS, Barnea E, Levy R, Greenberg P, Alon M, et al. Immunoproteasome expression is associated with better prognosis and response to checkpoint therapies in melanoma. Nat Commun 2020;11:896.
25. Visekruna A, Joeris T, Seidel D, Kroesen A, Loddenkemper C, Zeitz M, et al. Proteasome-mediated degradation of IkappaBalpha and processing of p105 in Crohn disease and ulcerative colitis. J Clin Invest 2006;116: 3195–203.
26. Shang K, Bai YP, Wang C, Wang Z, Gu HY, Du X, et al. Crucial involvement of tumor-associated neutrophils in the regulation of chronic colitis-associated carcinogenesis in mice. PLoS One 2012;7:e51848.
27. Wang Y, Wang K, Han GC, Wang RX, Xiao H, Hou CM, et al. Neutrophil infiltration favors colitis-associated tumorigenesis by activating the interleukin-1 (IL-1)/IL-6 axis. Mucosal Immunol 2014;7:1106–15.
28. Sun SC, Ley SC. New insights into NF-kappaB regulation and function. Trends Immunol 2008;29:469–78.
29. Neurath MF. Cytokines in inflammatory bowel disease. Nat Rev Immunol 2014; 14:329–42.
30. Puleston J, Cooper M, Murch S, Bid K, Makh S, Ashwood P, et al. A distinct subset of chemokines dominates the mucosal chemokine response in inflammatory bowel disease. Aliment Pharmacol Ther 2005;21:109–20.
31. Li S, Dai X, Gong K, Song K, Tai F, Shi J. PA28alpha/beta promote breast cancer cell invasion and metastasis via down-regulation of CDK15. Front Oncol 2019;9:1283.
32. Rock KL, Reits E, Neefjes J. Present yourself! by MHC class I and MHC class II molecules. Trends Immunol 2016;37:724–37.
33. Kalim KW, Basler M, Kirk CJ, Groettrup M. Immunoproteasome subunit LMP7 deficiency and inhibition suppresses Th1 and Th17 but enhances regulatory T cell differentiation. J Immunol 2012;189:4182–93.

Downloaded from http://aacrjournals.org/cancerimmunolres/article-pdf/9/6/682/3099404/682.pdf by University of Marburg user on 14 February 2023

SCIENTIFIC REPORTS

OPEN

Regulation of the effector function of CD8$^+$ T cells by gut microbiota-derived metabolite butyrate

Received: 15 June 2018
Accepted: 17 September 2018
Published online: 26 September 2018

Maik Luu[1], Katharina Weigand[1], Fatana Wedi[1], Carina Breidenbend[1], Hanna Leister[1], Sabine Pautz[1,2], Till Adhikary[3] & Alexander Visekruna[1]

The gut microbiota produces metabolites such as short-chain fatty acids (SCFAs) that regulate the energy homeostasis and impact on immune cell function of the host. Recently, innovative approaches based on the oral administration of SCFAs have been discussed for therapeutic modification of inflammatory immune responses in autoimmune diseases. So far, most studies have investigated the SCFA-mediated effects on CD4$^+$ T cells and antigen presenting cells. Here we show that butyrate and, to a lesser degree, propionate directly modulate the gene expression of CD8$^+$ cytotoxic T lymphocytes (CTLs) and Tc17 cells. Increased IFN-γ and granzyme B expression by CTLs as well as the molecular switch of Tc17 cells towards the CTL phenotype was mediated by butyrate independently of its interaction with specific SCFA-receptors GPR41 and GPR43. Our results indicate that butyrate strongly inhibited histone-deacetylases (HDACs) in CD8$^+$ T cells thereby affecting the gene expression of effector molecules. Accordingly, the pan-HDAC inhibitors trichostatin A (TSA) and sodium valproate exerted similar influence on CD8$^+$ T cells. Furthermore, higher acetate concentrations were also able to increase IFN-γ production in CD8$^+$ T lymphocytes by modulating cellular metabolism and mTOR activity. These findings might have significant implications in adoptive immunotherapy of cancers and in anti-viral immunity.

The short-chain fatty acids (SCFAs) acetate, propionate and butyrate are synthesized in the intestinal lumen of caecum and large intestine by bacterial fermentation of non-digestible, complex carbohydrates such as dietary fiber[1]. SCFAs are capable of crossing the intestinal epithelium and of reaching the lamina propria, where they can directly shape mucosal immune responses. A high intake of dietary fiber or oral administration of SCFAs have been shown to mediate protective effects in experimental models of colitis, multiple sclerosis, type 1 diabetes, allergic airway inflammation and food allergy[2–6]. Acetate, which is the most abundant SCFA in the intestinal lumen, has been shown to be an important substrate for hepatic lipogenesis. Propionate can also be metabolized in the liver acting as substrate for the hepatic gluconeogenesis. Butyrate, which is mainly produced by strictly anaerobic spore-forming bacteria such as *Clostridium butyricum*, is used locally as energy source for colonocytes[7]. Novel reports have found that butyrate and other SCFAs are able to interact with their specific receptor GPR43, which is selectively expressed on colonic regulatory T cells (Tregs)[8]. Alternatively, SCFAs taken up by mucosal T cells act directly in the nucleus as histone deacetylase (HDAC) inhibitors, thereby promoting differentiation of peripheral Tregs. This effect of butyrate on Tregs can be explained by increasing the acetylation of histones H3 and H4 at the *Foxp3* gene locus[9,10]. Taken together, SCFAs that are absorbed first into colonocytes and then into mucosal immune cells profoundly impact on intestinal homeostasis by inducing generation of Tregs, by enhancing the gut barrier function and by influencing signaling pathways that govern dendritic cells (DCs) to a tolerogenic state[7].

While the anti-inflammatory capacity of butyrate and other SCFAs has been extensively investigated, novel studies have revealed that CD4$^+$ effector T cells might also be a cellular target for SCFAs[11–14]. Therefore, it will be particularly interesting to better understand the molecular mechanisms underlying cell- and tissue-specific responsive immune cell subsets in order to develop and provide a safe SCFA-based therapy for patients with autoimmune diseases. Due to their HDAC-inhibitory activity and strong interaction with cell surface receptors

[1]Institute for Medical Microbiology and Hygiene, Philipps University of Marburg, Marburg, Germany. [2]Department of Biochemistry, University of Kassel, Kassel, Germany. [3]Institute of Molecular Biology and Tumor Research (IMT), Center for Tumor- and Immunobiology, Philipps- University Marburg, Marburg, Germany. Correspondence and requests for materials should be addressed to A.V. (email: alexander.visekruna@staff.uni-marburg.de)

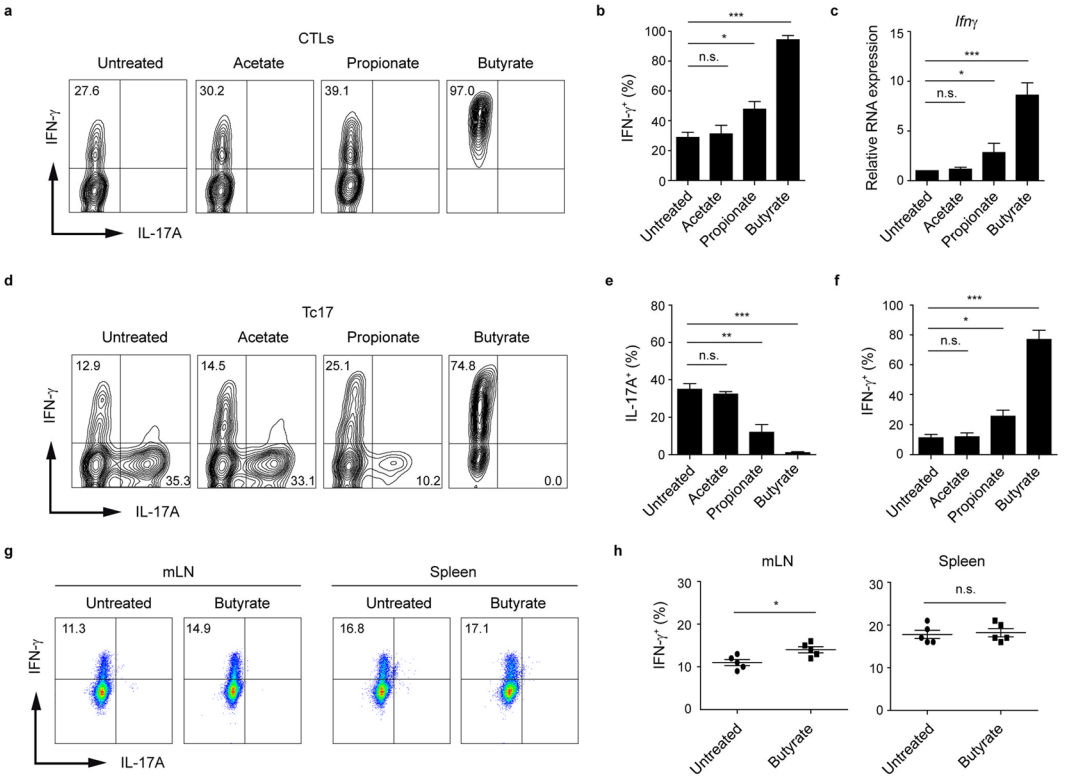

Figure 1. Treatment of CD8$^+$ T cells with butyrate results in preferential increase of IFN-γ production. (**a**,**b**) Frequency of IFN-γ$^+$ cells cultured under sub-optimal CTL-inducing conditions and treated with SCFAs (1 mM). (**c**) Relative mRNA expression of *Ifn*γ in CTLs treated with 1 mM of various SCFAs. (**d**–**f**) Frequencies of IFN-γ$^+$ and IL-17A$^+$ Tc17 lymphocytes upon treatment with SCFAs (1 mM). (**g**,**h**) Frequency of IFN-γ$^+$ CTLs in mLNs and spleen four weeks after oral treatment of WT mice with 150 mM sodium butyrate. Two experiments with five mice per group were performed. (**b**,**c**,**e**,**f**) Data are pooled from three independent experiments. Results are expressed as mean ± SEM. n. s. = not significant, $^*p < 0.05$, $^{**}p < 0.01$, $^{***}p < 0.001$.

such as GPR41, GPR43 and GPR109A, SCFAs have a strong potential to regulate the function of immune cells in extra-intestinal organs as well (particularly if administered intravenously or intraperitoneally). So far it has clearly been demonstrated that SCFAs are able to modulate the phenotype and function of numerous immunologically relevant cells such as colonic epithelial cells, macrophages, neutrophils and DCs[15–18].

The unanswered question is if microbial metabolites are capable of regulating the gene expression and function of CD8$^+$ T lymphocytes. Our current findings suggests a strong effect of butyrate on two CD8$^+$ T cell subsets, cytotoxic T lymphocytes (CTLs) and Tc17 cells. Several lines of evidence point to epigenetic regulatory mechanisms causing effects of butyrate on CD8$^+$ T cell function. Thus, our study supports the concept that SCFAs not only optimize the function of Tregs and conventional CD4$^+$ T cells, but also modulate the expression of effector molecules in CD8$^+$ T lymphocytes in a context-specific manner.

Results

Butyrate promotes the increased expression of IFN-γ and granzyme B in CTLs and Tc17 cells. To investigate if SCFAs are able to influence the phenotype of CD8$^+$ T cells, we treated CTLs and Tc17 cells with acetate, propionate and butyrate for three days and measured the expression of IL-17A and IFN-γ in both CD8$^+$ T cell subsets by flow cytometry. As compared to acetate-treated or untreated T cells, the frequency of IFN-γ$^+$ cells increased significantly following butyrate treatment of both, CTLs and Tc17 cells (Fig. 1a–f). Moreover, the reduction of IL-17A was detected in Tc17 cells treated with butyrate but not with acetate. Propionate treatment also led to increased percentages of IFN-γ$^+$ cells, however this effect was less pronounced as compared to the treatment with butyrate. We next investigated whether *in vivo* treatment with butyrate could specifically alter IFN-γ production by CD8$^+$ T cells. To test if IFN-γ production in CD8$^+$ T cells might be upregulated by butyrate, WT mice were orally treated with this SCFA for three weeks (according to the published protocol[8]) and afterwards the frequency of IFN-γ-expressing CD8$^+$ and CD4$^+$ T cells in the spleen and mLNs was examined by FACS analysis. Intracellular staining revealed a slight, but reproducible increase in percentage of IFN-γ$^+$ CD8$^+$ T lymphocytes in mLNs but not in spleen (Fig. 1g,h). In contrast, CD4$^+$ effector T cells derived from both organs were not able to increase their IFN-γ production after treatment with butyrate (Supplementary Fig. 1a,b). Negligible percentages of Th17 and Tc17 cells were measured in both tissues independently of butyrate treatment. Previously, it was demonstrated that early, autocrine IFN-γ signaling promotes the CTL cell differentiation and

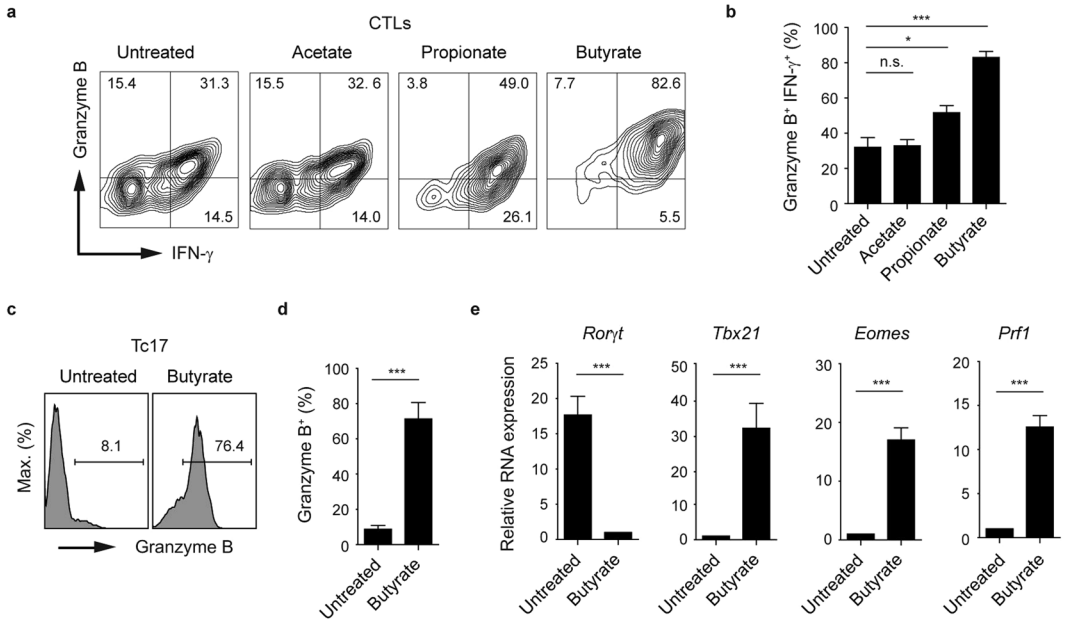

Figure 2. Effects of butyrate on the expression of CTL-related effector molecules. (**a**,**b**) Percentages of granzyme B$^+$ IFN-γ$^+$ CTLs in the presence of various SCFAs (1 mM). (**c**,**d**) Expression of granzyme B in Tc17 cells treated with 1 mM sodium butyrate for three days. (**e**) Quantitative RT-PCR analysis of *Rorγt* and CTL-associated genes *Tbx21*, *Eomes* and *Prf1* in Tc17 cells treated with 1 mM sodium butyrate for two days. (**b**,**d**,**e**) Three independent experiments were performed. Results are shown as mean ± SEM. n. s. = not significant, $^*p < 0.05$, $^{***}p < 0.001$.

upregulates T-bet and granzyme B expression in CD8$^+$ T cells[19]. It is tempting to speculate that butyrate could locally enhance already high production of IFN-γ in mLNs by supporting the autocrine IFN-γ signals.

To test whether CTLs are able to upregulate their granzyme B expression upon SCFA treatment, we treated CD8$^+$ T lymphocytes with acetate, propionate and butyrate for three days, and measured the concurrent production of the CTL-associated effector molecules IFN-γ and granzyme B. While butyrate was capable of strongly upregulating the frequency of granzyme B$^+$ IFN-γ$^+$ CD8$^+$ T cell population, no effect of acetate on CTLs was observed. Furthermore, a slight increase in percentages of double-positive population was detected after propionate treatment (Fig. 2a,b). To examine the stability of butyrate-mediated phenotype, we treated CTLs with butyrate for two days. Subsequently, butyrate was removed from cell culture supernatants and three days later the expression of IFN-γ was measured by flow cytometry. After 5 days, we observed an increase in the frequency of IFN-γ$^+$ cells in butyrate-pretreated cell cultures as compared to control CTLs suggesting stable phenotypic changes mediated by butyrate (Supplementary Fig. 2a). Similarly, Ly5.1$^+$ CTLs pretreated with butyrate and adoptively transferred into Ly5.2$^+$ host mice, maintained high levels of T-bet and IFN-γ as compared to untreated Ly5.1$^+$CD8$^+$ T lymphocytes (Supplementary Fig. 2b).

For CD4$^+$ T cells, it is known that very early transcription programs govern development of specific lineages. Recently, we described an increasing heterogeneity within CD8$^+$ T cells by identifying two new CD8$^+$ T cell subsets, Tc17 and Tc9 cells, that might be implicated in the pathogenesis of multiple sclerosis and airway inflammation, respectively[20,21]. Interestingly, the treatment of Tc17 cells with butyrate completely altered the specific expression pattern of these lymphocytes, which is normally associated with very low amounts of granzyme B, perforin, T-bet and Eomes and high levels of IL-17A and RORγt. Upon butyrate treatment, Tc17 cells increased the levels of granzyme B, down-regulated the gene expression of Tc17-related transcription factor *Rorγt* and significantly induced expression levels of CTL-associated genes *Tbx21*, *Eomes* and *Prf1* (Fig. 2c–e). To understand the molecular basis for this phenotypical switch, we treated Tc17 cells and CTLs derived from spleen and LNs of WT and T-bet deficient mice with butyrate and analyzed the expression of IFN-γ and IL-17A. In *Tbx21*$^{-/-}$ cells, only partially defective IFN-γ production in CTLs and an incomplete switch of Tc17 cells towards the CTL phenotype was observed after three day of butyrate treatment (Fig. 3a,b). It is known that the transcription factor Eomes is essential for optimal expression of IFN-γ, granzyme B and perforin in CD8$^+$ T cells[22,23]. It is conceivable that not only T-bet but also butyrate-mediated induction of Eomes might be needed for phenotypical alterations within CD8$^+$ T cell subsets.

SCFA-receptors GPR41 and GPR43 are not involved in the butyrate-mediated regulation of CD8$^+$ T lymphocytes. SCFA-promoted effects on cells include both, the interaction with their specific cell surface receptors and intracellular inhibition of HDAC enzymes, thereby impacting significantly on the gene expression. SCFAs are able to directly activate their receptors GPR41 and GPR43 on intestinal epithelial cells and lymphocytes, which leads to activation of mitogen-activated protein kinase signaling, inhibition of NF-κB signaling cascades, rapid production of cytokines and chemokines and increased cell death[15,24,25]. Therefore, it is of great interest to examine the cellular pathways that are regulated by SCFAs and are involved in mediating immune

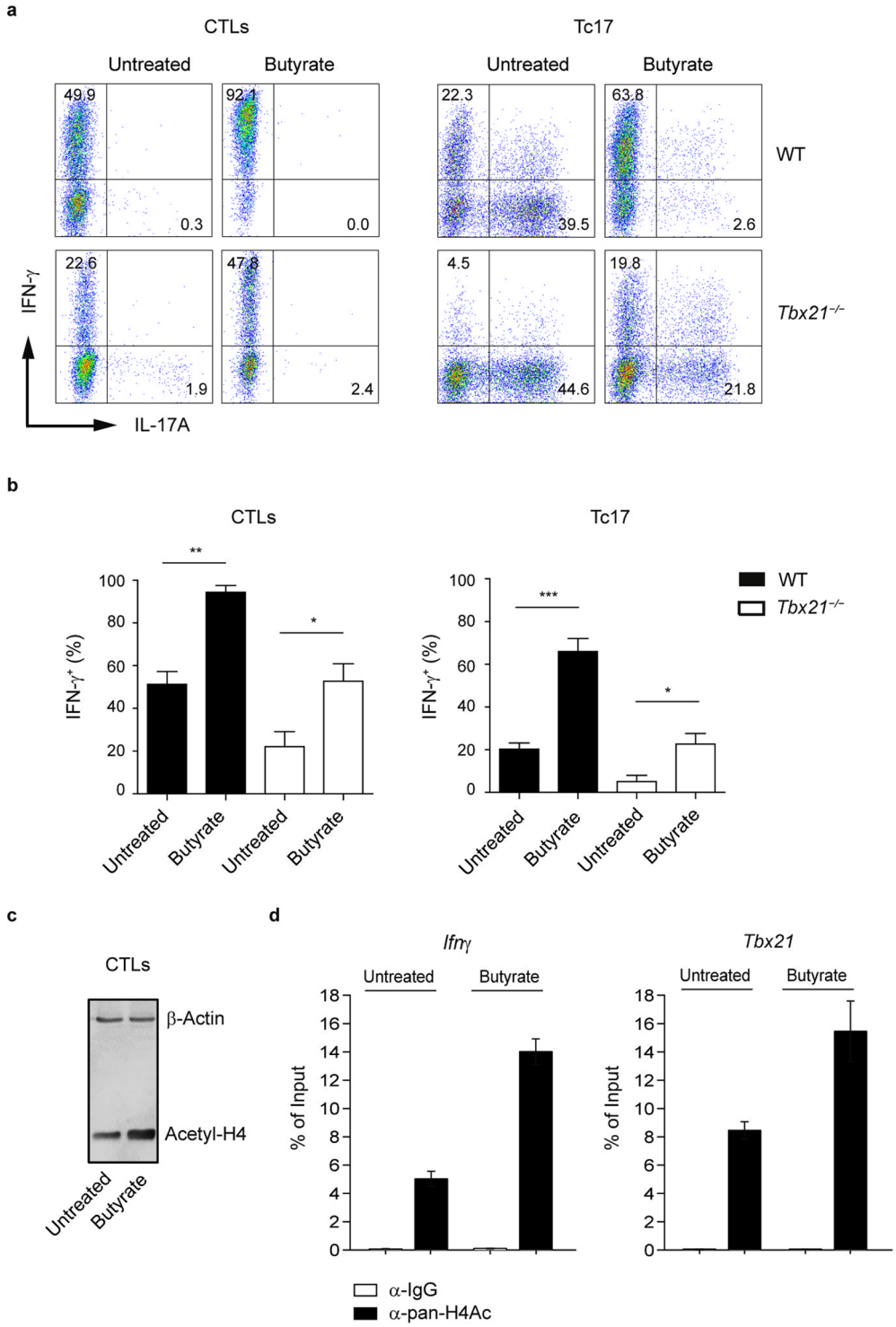

Figure 3. Impact of butyrate on T-bet-deficient CTLs and Tc17 cells. (**a**,**b**) Percentages of IFN-γ$^+$ and IL-17A$^+$ cells within CTLs and Tc17 cells derived from WT and *Tbx21*$^{-/-}$ mice. Cells were treated with 1 mM sodium butyrate or left untreated for three days. Results (**b**) are displayed as mean ± SEM. $^*p < 0.05$, $^{**}p < 0.01$, $^{***}p < 0.001$. (**c**) CTLs were cultured for two days in the presence or absence of 1 mM butyrate. Immunoblot analysis was performed by using the antibody specific for acetylated histone H4. Three independent experiments were performed. (**d**) ChIP analysis for acetylation of histone H4 at the promoter region of *Ifn*γ and *Tbx21* genes after 24 hours of treatment of CTLs with 1 mM butyrate.

responses. To investigate whether observed effects of butyrate on CD8$^+$ T cells are mediated by activating the signaling pathways downstream of SCFA-receptors GPR41 and GPR43, we next tested if CD8$^+$ T cells deficient for both receptors, GPR41 and GPR43, are able to upregulate their IFN-γ production upon butyrate treatment. No

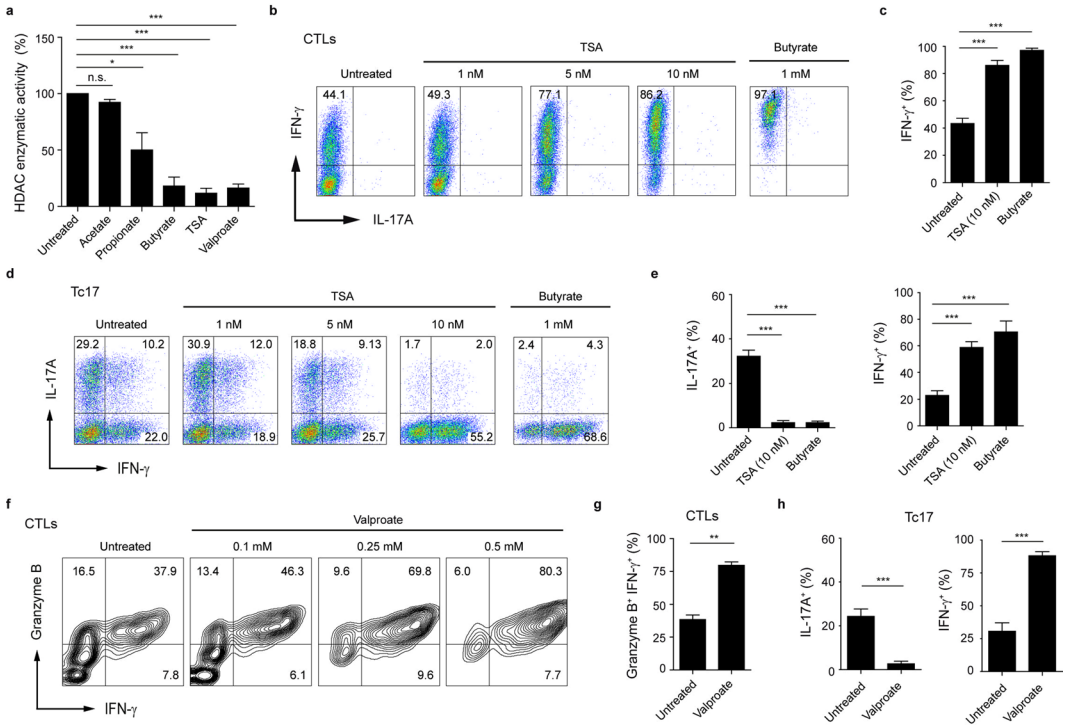

Figure 4. HDAC-inhibitory activity of butyrate promotes IFN-γ production in CTLs and Tc17 cells. (**a**) Impact of SCFAs on HDAC enzymatic activity in CTLs. 5 mM SCFAs or 500 nM TSA were added to CTL-derived cell lysates for 15 minutes. Fluorometric HDAC activity assay was performed as described in the section Methods. (**b**,**c**) Frequency of IFN-γ$^+$ CTLs treated with indicated concentrations of TSA or sodium butyrate (1 mM). (**d**,**e**) CD8$^+$ T cells were cultured under Tc17-inducing conditions and treated with increasing concentrations of TSA. Tc17 cells treated with 1 mM butyrate served as a control. (**f**,**g**) CTLs were treated with increased valproate concentrations (in **g**, 0.5 mM valproate is shown) for three days and the percentage of granzyme B$^+$ IFN-γ$^+$ cells was determined by flow cytometry. (**h**) Tc17 cells treated with 1 mM valproate for three days were analyzed for IL-17A and IFN-γ expression. The percentage of IFN-γ$^+$ and IL-17A$^+$ cells was measured by FACS analysis. (**a**,**c**,**e**,**g**,**h**) Results are pooled from three experiments. Data are expressed as mean ± SEM. n. s. = not significant, $^*p < 0.05$, $^{**}p < 0.01$, $^{***}p < 0.001$.

difference in frequencies of IFN-γ$^+$ cells were found after three days of incubation of GPR41 and GPR43 deficient CTLs or Tc17 cells with butyrate as compared to butyrate-treated WT cells (Supplementary Fig. 3a–c). Similarly to WT mice, *in vivo* treatment of *Ffar2*$^{-/-}$*Ffar3*$^{-/-}$ mice (deficient for GPR41 and GPR43) revealed an increase in percentage of IFN-γ$^+$CD8$^+$ T cells in mLNs (Supplementary Fig. 3d). Together, these data show that surface receptors GPR41 and GPR43 are dispensable for butyrate-mediated effects on CD8$^+$ T cells.

HDAC-inhibitory activity of butyrate enhances the expression of CTL-associated effector molecules. Butyrate is known to induce histone hyperacetylation through HDAC inhibition[26]. Western blot analysis of acetylated histone H4 revealed that butyrate induced a significant increase in H4 acetylation in CTLs (Fig. 3c). We next investigated histone H4 acetylation directly at the *Tbx21* and *Ifn*γ loci in murine CD8$^+$ T cells after butyrate treatment by the quantitative ChIP analysis. Our results demonstrate that butyrate increases the histone H4 acetylation of *Tbx21* and *Ifn*γ promoters in CTLs (Fig. 3d). To further test the impact of butyrate on HDAC activity of CD8$^+$ T cells, we used the fluorometric HDAC activity assay for SCFA-treated cell lysates. Butyrate as well as the pan-HDAC inhibitors trichostatin A (TSA) and valproate exerted strong HDAC inhibitory activity, while acetate was not capable of blocking the enzymatic activity of CD8$^+$ T cell-derived HDACs (Fig. 4a). Furthermore, butyrate was also able to strongly inhibit HDACs in cell lysates derived from *Ffar2*$^{-/-}$*Ffar3*$^{-/-}$ CTLs (Supplementary Fig. 3e). Importantly, when we compared the impact of TSA and valproate on IFN-γ and IL-17A expression in CTLs and Tc17 cells, we found similar expression pattern as for butyrate-treated cells. TSA- and valproate-treated Tc17 cells were capable of increasing their IFN-γ production and of switching towards CTL phenotype. Similarly, the frequency of IFN-γ$^+$ or granzyme B$^+$ IFN-γ$^+$ cells was increased in TSA- and valproate-treated CTLs in comparison to untreated cells (Fig. 4b–h). These results suggest that increased histone acetylation mediated by physiological HDAC inhibitor butyrate might play an important role in rapid and selective induction of CTL-associated genes in CD8$^+$ T cells. Recently, an increase in Foxp3$^+$CD4$^+$ Treg differentiation was observed upon butyrate treatment[8–10]. In the immunosuppressive microenvironment of ovarian and colorectal cancer, a high prevalence of unusual Foxp3$^+$CD8$^+$ regulatory T cell has been described[27,28]. Further, the expansion of Foxp3$^+$CD8$^+$ T cells with suppressive potential has been detected in HIV-1-infected humans[29]. Interestingly, CD8$^+$ T cells cultured under Treg-inducing conditions and incubated with butyrate or TSA induced

a phenotypical switch towards CTLs, associated with increased expression of T-bet and IFN-γ. This molecular shift was partially dependent on T-bet as *Tbx21*$^{-/-}$ cells were not able to downregulate their Foxp3 expression in contrast to WT lymphocytes (Supplementary Fig. 4a–d). Previously, a molecular switch from Th2 to Th1 cell phenotype by restoring the histone acetylation at the *Ifn*γ and *Tbx21* loci was observed for human T cells treated with HDAC inhibitors[26]. Together, our novel findings indicate that in CD8$^+$ T cells, the butyrate-triggered increase in IFN-γ expression is mediated through HDAC-inhibitory activity and not by engaging GPR41 and GPR43 receptors.

Butyrate increases IFN-γ expression in CD8$^+$ T cells in a dose-dependent manner. Various cells were shown to be susceptible to apoptosis induced by butyrate and pentanoate[30,31]. We found that butyrate, and, to a lesser extent, propionate induced apoptosis in CTLs at the concentration of 5 mM. In contrast, CD8$^+$ T cells treated with acetate were resistant to apoptosis even at a concentration of 10 mM (Supplementary Fig. 5a,b), indicating that acetate is less toxic when compared to other SCFAs. Based on the results related to the susceptibility to apoptosis, we assessed if SCFAs exhibit a broad concentration-dependent effect on CTLs. Cells were exposed to a wide range of SCFA concentrations, and subsequently the expression of IFN-γ and IL-17A was measured by flow cytometry. Lower butyrate concentrations (starting at 0.25 mM) were able to increase the production of IFN-γ in CTLs while, at the concentration of 10 mM, acetate did not exhibit any effect on effector cytokines (Fig. 5a,b). Intestinal lumen concentrations as well as blood levels of acetate in the body are much higher than that of butyrate[1]. As acetate-treated CTLs were not capable of undergoing apoptosis, we included higher acetate concentrations (>10 mM) in the flow cytometry analysis. Notably, we found that at the concentration of 25 mM, acetate-mediated effects on CTLs were similar to that of 1 mM butyrate (Fig. 5c,d). As previously described for CD4$^+$ T cells and B lymphocytes[11,32], the treatment of CTLs with acetate was associated with heightened activity of AKT/mTOR pathway (data not shown). Rapamycin, the inhibitor of mTOR complex, was able to down-regulate the expression of IFN-γ in acetate-treated CTLs to the levels detected in control lymphocytes. In contrast, the treatment of butyrate-treated CTLs with rapamycin did not strongly affect the increased production of IFN-γ (Fig. 5c,d). By comparing the HDAC inhibition mediated by 25 mM acetate and 1 mM butyrate, we observed that butyrate (at a 25-fold lower concentration as compared to acetate) had much higher HDAC-inhibitory activity (Fig. 5e). Together, there seem to exist two mechanisms through which SCFAs are capable of modulating the functional properties of CD8$^+$ T cells. Our data demonstrate that butyrate, and less strongly propionate, inhibit activity of HDACs, thereby increasing the expression of IFN-γ in CD8$^+$ T lymphocytes. Additionally, acetate enhances IFN-γ production likely by acting as a metabolic substrate for CTLs. This observation is in line with a recent paper that has shown that in CD8$^+$ T cells, acetate was able to enhance glycolysis and cytosolic acetyl-CoA levels, which resulted in increased functional activity of memory T cells[33].

Discussion

The SCFAs acetate, propionate and butyrate are generated in human intestine by bacterial fermentation of undigested dietary fiber. Supplementation of diet rich in dietary fiber increases the intestinal levels of SCFAs and protects mice from allergic or autoimmune diseases[4–6]. SCFAs appear to impact on immune cells by manipulating their metabolic status, by activating or suppressing diverse signaling pathways and by inducing epigenetic changes. Hence, the scientific interest in better understanding the underlying mechanism on how SCFAs modulate immune responses has recently increased in order to develop novel therapeutic applications. Previously, it was shown that aerobic glycolysis was required for optimal INF-γ production by T cells. Interestingly, T lymphocytes prevented from engaging glycolysis were markedly compromised with regard to IFN-γ production[34]. Accordingly, we observed that the treatment of T cells with 2-deoxy-D-glucose (2-DG), an inhibitor of glycolysis, resulted in reduced IFN-γ production (data not shown). Additionally, our novel data suggest a strong involvement of epigenetic mechanisms in the modulation of IFN-γ expression since HDAC inhibition, mediated by butyrate or pan-HDAC inhibitors TSA and valproate, led to increased production of this cytokine in CD8$^+$ T cells. It is well accepted that optimizing the reactivity of CTLs might be a useful strategy for improving the efficacy of T cell-mediated anti-tumor therapy. In the presence of butyrate, CTLs upregulated expression of key effector molecules, which is needed for combating the tumors. Also, Tc17 cells, which are phenotypically distinct from CTLs, increased the expression of CTL-associated molecules upon butyrate treatment. Recently, it was shown that SCFAs could enhance IL-17A expression under Th17-inducing conditions[11]. For Tc17 cells, we observed an opposite effect of butyrate, which strongly suppressed IL-17A production and enhanced IFN-γ levels. One potential reason of this discrepancy might be the usage of different differentiation protocols. Secondly, the discrepancy might result from the specific phenotype of Tc17 cells. These lymphocytes have much higher basic levels of IFN-γ than Th17 cell. A sufficient availability of IFN-γ likely augments the butyrate-mediated phenotypic switch from Tc17 cells towards CTLs. Further, we found a significant difference among SCFAs with regard to their ability to regulate the gene expression of CTLs and Tc17 cells. The profound effect of butyrate on CD8$^+$ T cells was predominantly mediated by its HDAC-inhibitory activity since butyrate induced an increase in H4 acetylation at *Tbx21* and *Ifn*γ genes. For CD4$^+$ T cells, a previous study found that butyrate was able to enhance acetylation of histone H3 of *Tbx21* and *Ifn*γ promoter regions under Th1- and Th2-polarizing conditions[26]. Interestingly, acetate is not capable of acting as a strong HDAC inhibitor, but it can be efficiently metabolized by various cells. CD8$^+$ T cells have been shown to functionally integrate high systemic acetate concentrations to metabolically boost memory T cell responses[33]. We observed that higher acetate concentrations increased IFN-γ production in CTLs and that this effect was dependent on activity of mTOR complex.

High-fiber diet in association with enhanced intestinal butyrate synthesis has been shown to attenuate the development of colorectal cancer associated by chronic colitis[16]. Further, butyrate can directly promote cancer cell apoptosis[35]. Here, we suggest a novel mechanism of how butyrate can exert anti-cancer effects by stimulating CD8$^+$ T cells and increasing their effector functionality. While physiologically active, low butyrate amounts in

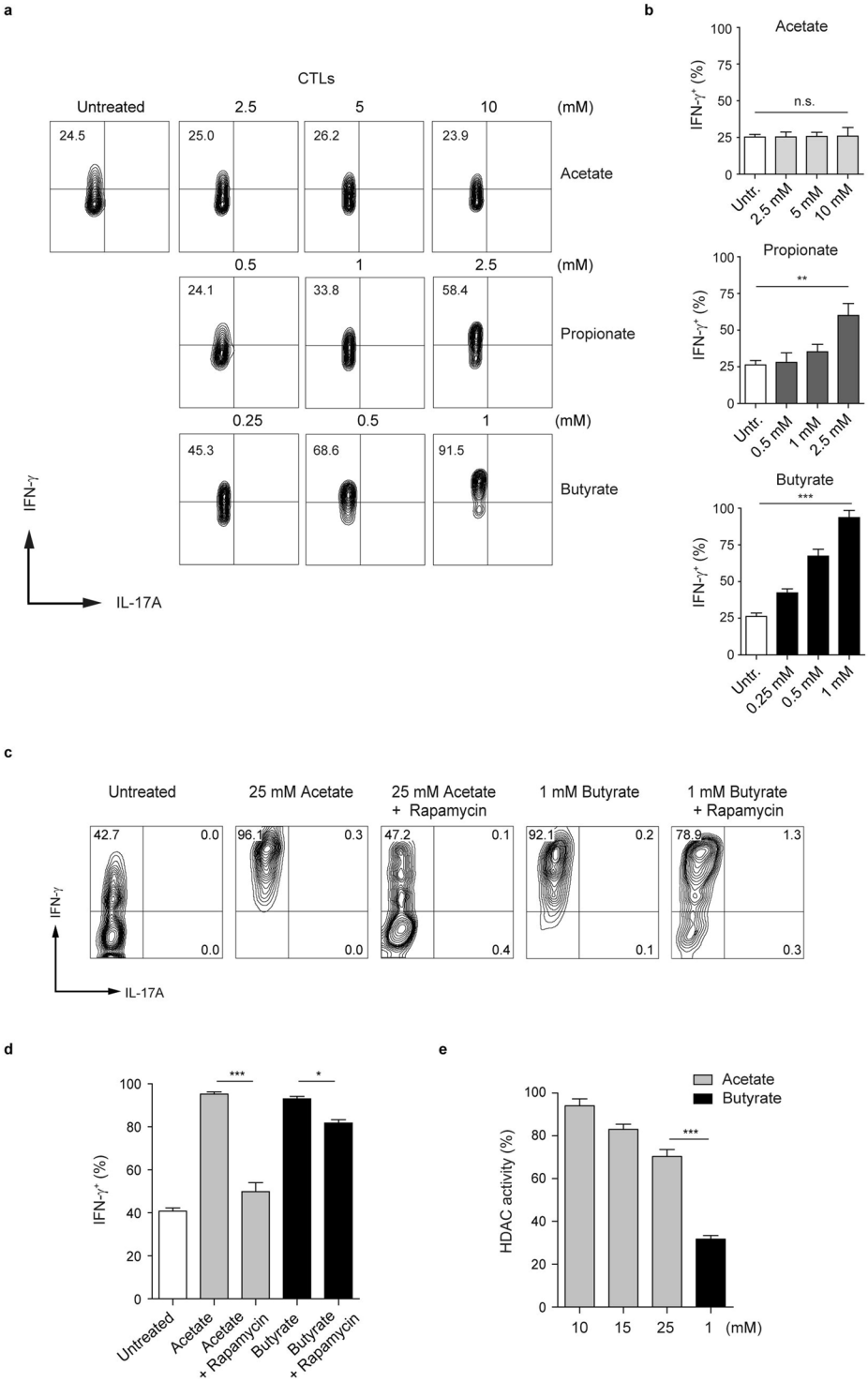

Figure 5. Dose-dependent impact of SCFAs on IFN-γ expression in CTLs. (**a**,**b**) CTLs were treated with increasing concentrations of SCFAs for three days. Flow cytometry analysis was used to determine percentages of IFN-γ^+ and IL-17A$^+$ cells within CTLs. Three experiments were performed. (**c**,**d**) CTLs were treated with 25 mM acetate or 1 mM butyrate in the presence or absence of rapamycin (25 nM). The production of IFN-γ is analyzed by flow cytometry. Three experiments were performed. (**e**) CTL-derived cell lysates were assayed for HDAC activity in the presence of acetate (10, 15 and 25 mM) or butyrate (1 mM). The data were compared to the HDAC activity of untreated CD8$^+$ T cells, which was arbitrary set at 100 percent. Three experiments were performed. Data (**b**,**d**,**e**) are expressed as mean ± SEM. n. s. = not significant, *$p < 0.05$, **$p < 0.01$, ***$p < 0.001$.

the intestine induce the differentiation of Foxp3$^+$ Tregs, higher concentration of this SCFA might rather promote anti-tumor effects by optimizing the effector function of CD8$^+$ T cells. Of note, a very recent study has revealed that the treatment of mice with butyrate was capable of enhancing the generation of influenza-specific CD8$^+$ T cells, which considerably contributed to the resolution of influenza infection[36]. In summary, natural HDAC inhibitors such as butyrate might be considered as novel therapeutic tools to modulate the function of CD8$^+$ T cells and to potentiate their anti-tumor and anti-viral capacity.

Methods

Mice and oral administration of butyrate. WT animals as well as *Tbx21*$^{-/-}$ and *Ffar2*$^{-/-}$*Ffar3*$^{-/-}$mice (all mouse strains were on C57BL/6 background) were housed in specific pathogen free (SPF) conditions at the animal facility of the Philipps-University of Marburg, Germany. WT mice were obtained from Charles River Laboratories. *Ffar2*$^{-/-}$*Ffar3*$^{-/-}$ mice were generously provided by Dr. Stefan Offermanns (Max Planck Institute for Heart and Lung Research, Bad Nauheim, Germany). All animal procedures were carried out according to the German animal protection law. Experiments were done after approval by Regierungspräsidium Gießen, Germany (animal experimentation application EX7-2015). In some experiments, WT mice were orally treated with 150 mM sodium butyrate for four weeks as described previously[8]. Water solutions containing butyrate were pH-matched and changed weekly.

Isolation and *in vitro* differentiation of CD8$^+$ T cells. CD8$^+$ T lymphocytes were purified from spleens and LNs using the kit for negative isolation (the purity of cells was between 90–95%). In brief, spleens and LNs were harvested and disrupted to obtain single-cell suspensions. Splenic cell suspensions were treated with RBC lysis buffer before lymphocyte isolation. To generate CTLs, purified CD8$^+$ cells were stimulated with 5 µg/ml plate-bound anti-CD3 (clone 145–2C11) and 1 µg/ml soluble anti-CD28 (clone 37.51) Abs in the presence of 50 U/ml rhIL-2 (Novartis) for three days. In some experiments, cells were treated with 10 µg/ml of anti-IFN-γ (clone XMG1.2) to obtain sub-optimal CTL conditions. For Tc17 cell differentiation, 1 ng/ml rhTGF-β1 (PeproTech) and 40 ng/ml IL-6 (PeproTech) together with 5 µg/ml anti-IFN-γ were added into RPMI medium during the cell stimulation. For Treg-inducing conditions, cell suspensions were treated with 2 ng/ml TGF-β1 and 100 U/ml rhIL-2 in the presence of anti-IFN-γ (5 µg/ml). Cells were treated with SCFAs and cultured at 37 °C for three days. For this purpose, 1 mM of sodium butyrate, sodium propionate or sodium acetate (all SCFAs, Sigma-Aldrich) were used.

Adoptive cell transfer. CD8$^+$ T cells were purified from spleens and LNs of Ly5.1$^+$ C57BL/6 mice and were cultured under CTL-inducing conditions for three days in the presence or absence of 1 mM butyrate. 2×10^6 CTLs were used for T cell adoptive transfer into Ly5.2$^+$ mice. Ten days after the transfer of cells, the expression of IFN-γ and T-bet within Ly5.1$^+$CD8$^+$ T lymphocytes was anylazed.

Flow cytometry and antibodies. After three days of the cell culture, CD8$^+$ T cell were restimulated for 4–5 h with PMA (50 ng/mL) and ionomycin (750 ng/mL) in the presence of 5 mg/mL brefeldin A (all three chemicals, Sigma-Aldrich). Afterwards, cells were treated with fluorochrome-labeled Abs. For the cytokine staining, cells were fixed with 2% formaldehyde and permeabilized by using saponin buffer. For intracellular staining of transcription factors, the Foxp3 staining kit (eBioscience) was used. The analysis of FACS data was performed using FlowJ_V10 software (TreeStar). The following anti-mouse Abs were used: anti-IFN-γ (XMG1.2), anti-CD3 (145-2C11), anti-CD8 (53-6.7), anti-CD45.1 (A20), anti-granzyme B (16G6), anti-IL-17A (eBio17B7), anti-Foxp3 (FJK-16s) and anti-T-bet (eBio4B10). All Abs were purchased from eBioscience.

Chromatin immunoprecipitation (ChIP) analysis. CTLs were cultured for 24 hours in the presence or absence of 1 mM butyrate. After 24 hours of the cell culture, ChIP-qPCR was essentially performed as described previously[37]. Briefly, after fixation, lysis, sonication, and preclearing, chromatin equivalent to 2.5×10^6 nuclei per sample was precipitated with rabbit control IgG (Sigma-Aldrich I5006) or α-acetylated histone H4 (Millipore, Upstate, 06-866). After purification, DNA was amplified using the following primers: *Ifn*γ promoter fw CATACCCTTTCCTTGCTTTTC, rv TTGTGGGATTCTCTGAAAGCA; *Tbx21* (T-bet) promoter fw TGGGGCGACAAGAGACTTAC, rv GAATTCGCTTTTGGTGAGGA.

HDAC activity assay. Fluorometric HDAC activity was measured according to the manufacturer's protocol (Bachem). Briefly, CD8$^+$ T cells were cultured under CTL-inducing conditions for three days. Subsequently, CTL-derived cell lysates were incubated with various SCFAs (5 mM) or with TSA (500 nM) for 15 minutes. In some experiments, 25 mM acetate and 1 mM butyrate were used for HDAC assay. To measure the inhibitory activity of SCFAs on HDACs, the cell lysates were treated with fluorogenic substrate Ac-Arg-Gly-Lys-AMC (Bachem) for next 30 minutes. HDAC-inhibitory activity of SCFAs was calculated relative to the enzymatic activity of untreated CTLs (this value was arbitrarily set to 100%). The measurement of fluorescence (free AMC) was carried out at the FLUOstar Omega device (BMG Labtech).

Western blotting. Immunoblotting was performed as described previously[14]. In brief, cell lysates were generated from 2×10^6 CTLs on day 2 of the cell culture. Protein samples were loaded on 10% gel for SDS-PAGE and were subsequently transferred to a PVDF membrane. Acetylated Histone H4 was detected using an anti-acetyl-histone H4 Ab (Millipore, 06-866). For detection of β-actin, a monoclonal anti-β-actin Ab (Sigma-Aldrich, AC-74) was used.

Quantitative RT-PCR. To isolate the total RNA from cultured CTLs or Tc17 cells, the High Pure RNA Isolation Kit was used according to the manufacturer's instruction (Roche). Following the cDNA synthesis, the relative expression of *Ifn*γ, *Ror*γ*t*, *Tbx21, Eomes* and *Prf1* was performed with specific primers using a StepOnePlus

device (Applied Biosystems). The expression of all genes was normalized to the expression of the housekeeping gene *Hypoxanthine-guanine phosphoribosyl transferase (Hprt1)*. Quantitative RT-PCR was performed by using the following primers: *Ifnγ* fw GCAACAGCAAGGCGAAAAAG, *Ifnγ* rv TTCCTGAGGCTGGATTCGG; *Tbx21* fw CAACAACCCCTTTGCCAAAG, *Tbx21* rv TCCCCCAAGCAGTTGACAGT; *Eomes* fw CCTTCACCTTCTCAGAGACACAGTT, *Eomes* rv TCGATCTTTAGCTGGGTGATATCC; *Prf1* fw GCAGATGAGAAGAGCATACAGGAC, *Prf1* rv TCTGAGCGCCTTTTTGAAGTC; *Rorγt* fw TCCTGCCACCTTGAGTATAGTCC, *Rorγt* rv GGACTATACTCAAGGTGGCAGGA.

Statistical analysis. Mean values of two groups were compared by using the unpaired Student's *t*-test. To compare multiple groups, results were analyzed using the one-way analysis of variance (ANOVA). Values of $p < 0.05$ were considered statistically significant. Data are typically presented as means ± SEM. For statistical analysis, the GraphPad Prism 5 software was used.

References

1. Koh, A., De Vadder, F., Kovatcheva-Datchary, P. & Backhed, F. From Dietary Fiber to Host Physiology: Short-Chain Fatty Acids as Key Bacterial Metabolites. *Cell* **165**, 1332–1345, https://doi.org/10.1016/j.cell.2016.05.041 (2016).
2. Berndt, B. E. *et al*. Butyrate increases IL-23 production by stimulated dendritic cells. *American journal of physiology. Gastrointestinal and liver physiology* **303**, G1384–1392, https://doi.org/10.1152/ajpgi.00540.2011 (2012).
3. Haghikia, A. *et al*. Dietary Fatty Acids Directly Impact Central Nervous System Autoimmunity via the Small Intestine. *Immunity* **44**, 951–953, https://doi.org/10.1016/j.immuni.2016.04.006 (2016).
4. Trompette, A. *et al*. Gut microbiota metabolism of dietary fiber influences allergic airway disease and hematopoiesis. *Nature medicine* **20**, 159–166, https://doi.org/10.1038/nm.3444 (2014).
5. Tan, J. *et al*. Dietary Fiber and Bacterial SCFA Enhance Oral Tolerance and Protect against Food Allergy through Diverse CellularPathways. *Cell reports* **15**, 2809–2824, https://doi.org/10.1016/j.celrep.2016.05.047 (2016).
6. Marino, E. *et al*. Gut microbial metabolites limit the frequency of autoimmune T cells and protect against type 1 diabetes. *Nature immunology* **18**, 552–562, https://doi.org/10.1038/ni.3713 (2017).
7. Tanoue, T., Atarashi, K. & Honda, K. Development and maintenance of intestinal regulatory T cells. *Nature reviews. Immunology* **16**, 295–309, https://doi.org/10.1038/nri.2016.36 (2016).
8. Smith, P. M. *et al*. The microbial metabolites, short-chain fatty acids, regulate colonic Treg cell homeostasis. *Science* **341**, 569–573, https://doi.org/10.1126/science.1241165 (2013).
9. Furusawa, Y. *et al*. Commensal microbe-derived butyrate induces the differentiation of colonic regulatory T cells. *Nature* **504**, 446–450, https://doi.org/10.1038/nature12721 (2013).
10. Arpaia, N. *et al*. Metabolites produced by commensal bacteria promote peripheral regulatory T-cell generation. *Nature* **504**, 451–455, https://doi.org/10.1038/nature12726 (2013).
11. Park, J. *et al*. Short-chain fatty acids induce both effector and regulatory T cells by suppression of histone deacetylases and regulation of the mTOR-S6K pathway. *Mucosal immunology* **8**, 80–93, https://doi.org/10.1038/mi.2014.44 (2015).
12. Park, J., Goergen, C. J., HogenEsch, H. & Kim, C. H. Chronically Elevated Levels of Short-Chain Fatty Acids Induce T Cell-Mediated Ureteritis and Hydronephrosis. *Journal of immunology* **196**, 2388–2400, https://doi.org/10.4049/jimmunol.1502046 (2016).
13. Luu, M., Steinhoff, U. & Visekruna, A. Functional heterogeneity of gut-resident regulatory Tcells. *Clinical & translational immunology* **6**, e156, https://doi.org/10.1038/cti.2017.39 (2017).
14. Kespohl, M. *et al*. The Microbial Metabolite Butyrate Induces Expression of Th1-Associated Factors in CD4+ T Cells. *Frontiers in immunology* **8**, 1036, https://doi.org/10.3389/fimmu.2017.01036 (2017).
15. Kim, M. H., Kang, S. G., Park, J. H., Yanagisawa, M. & Kim, C. H. Short-chain fatty acids activate GPR41 and GPR43 on intestinal epithelial cells to promote inflammatory responses in mice. *Gastroenterology* **145**(396–406), e391–310, https://doi.org/10.1053/j.gastro.2013.04.056 (2013).
16. Singh, N. *et al*. Activation of Gpr109a, receptor for niacin and the commensal metabolite butyrate, suppresses colonic inflammation and carcinogenesis. *Immunity* **40**, 128–139, https://doi.org/10.1016/j.immuni.2013.12.007 (2014).
17. Meijer, K., de Vos, P. & Priebe, M. G. Butyrate and other short-chain fatty acids as modulators of immunity: what relevance for health? *Current opinion in clinical nutrition and metabolic care* **13**, 715–721, https://doi.org/10.1097/MCO.0b013e32833eebe5 (2010).
18. Kaisar, M. M. M., Pelgrom, L. R., van der Ham, A. J., Yazdanbakhsh, M. & Everts, B. Butyrate Conditions Human Dendritic Cells to Prime Type 1 Regulatory T Cells via both Histone Deacetylase Inhibition and G Protein-CoupledReceptor 109A Signaling. *Frontiers in immunology* **8**, 1429, https://doi.org/10.3389/fimmu.2017.01429 (2017).
19. Curtsinger, J. M., Agarwal, P., Lins, D. C. & Mescher, M. F. Autocrine IFN-gamma promotes naive CD8 T cell differentiation and synergizes with IFN-alpha to stimulate strong function. *Journal of immunology* **189**, 659–668, https://doi.org/10.4049/jimmunol.1102727 (2012).
20. Huber, M. *et al*. IL-17A secretion by CD8+ T cells supports Th17-mediated autoimmune encephalomyelitis. *The Journal of clinical investigation* **123**, 247–260, https://doi.org/10.1172/JCI63681 (2013).
21. Visekruna, A. *et al*. Tc9 cells, a new subset of CD8(+) T cells, support Th2-mediated airway inflammation. *European journal of immunology* **43**, 606–618, https://doi.org/10.1002/eji.201242825 (2013).
22. Intlekofer, A. M. *et al*. Effector and memory CD8+ T cell fate coupled by T-bet and eomesodermin. *Nature immunology* **6**, 1236–1244, https://doi.org/10.1038/ni1268 (2005).
23. Araki, Y., Fann, M., Wersto, R. & Weng, N. P. Histone acetylation facilitates rapid and robust memory CD8 T cell response through differential expression of effector molecules (eomesodermin and its targets: perforin and granzyme B). *Journal of immunology* **180**, 8102–8108 (2008).
24. Yin, L., Laevsky, G. & Giardina, C. Butyrate suppression of colonocyte NF-kappa B activation and cellular proteasome activity. *The Journal of biological chemistry* **276**, 44641–44646, https://doi.org/10.1074/jbc.M105170200 (2001).
25. Zimmerman, M. A. *et al*. Butyrate suppresses colonic inflammation through HDAC1-dependent Fas upregulation and Fas-mediated apoptosis of T cells. *American journal of physiology. Gastrointestinal and liver physiology* **302**, G1405–1415, https://doi.org/10.1152/ajpgi.00543.2011 (2012).
26. Morinobu, A., Kanno, Y. & O'Shea, J. J. Discrete roles for histone acetylation in human T helper 1 cell-specific gene expression. *The Journal of biological chemistry* **279**, 40640–40646, https://doi.org/10.1074/jbc.M407576200 (2004).
27. Chaput, N. *et al*. Identification of CD8+ CD25+ Foxp3+ suppressive T cells in colorectal cancer tissue. *Gut* **58**, 520–529, https://doi.org/10.1136/gut.2008.158824 (2009).
28. Zhang, S. *et al*. Analysis of CD8+ Treg cells in patients with ovarian cancer: a possible mechanism for immune impairment. *Cellular & molecular immunology* **12**, 580–591, https://doi.org/10.1038/cmi.2015.57 (2015).

29. Nigam, P. *et al*. Expansion of FOXP3+ CD8 T cells with suppressive potential in colorectal mucosa following a pathogenic simian immunodeficiency virus infection correlates with diminished antiviral T cell response and viral control. *Journal of immunology* **184**, 1690–1701, https://doi.org/10.4049/jimmunol.0902955 (2010).
30. Hague, A., Elder, D. J., Hicks, D. J. & Paraskeva, C. Apoptosis in colorectal tumour cells: induction by the short chain fatty acids butyrate, propionate and acetate and by the bile salt deoxycholate. *International journal of cancer* **60**, 400–406 (1995).
31. Tang, Y., Chen, Y., Jiang, H. & Nie, D. The role of short-chain fatty acids in orchestrating two types of programmed cell death in colon cancer. *Autophagy* **7**, 235–237 (2011).
32. Kim, M., Qie, Y., Park, J. & Kim, C. H. Gut Microbial Metabolites Fuel Host Antibody Responses. *Cell host & microbe* **20**, 202–214, https://doi.org/10.1016/j.chom.2016.07.001 (2016).
33. Balmer, M. L. *et al*. Memory CD8(+) T Cells Require Increased Concentrations of Acetate Induced by Stress for Optimal Function. *Immunity* **44**, 1312–1324, https://doi.org/10.1016/j.immuni.2016.03.016 (2016).
34. Chang, C. H. *et al*. Posttranscriptional control of T cell effector function by aerobic glycolysis. *Cell* **153**, 1239–1251, https://doi.org/10.1016/j.cell.2013.05.016 (2013).
35. Domokos, M. *et al*. Butyrate-induced cell death and differentiation are associated with distinct patterns of ROS in HT29-derived human colon cancer cells. *Digestive diseases and sciences* **55**, 920–930, https://doi.org/10.1007/s10620-009-0820-6 (2010).
36. Trompette, A. *et al*. Dietary Fiber Confers Protection against Flu by Shaping Ly6c(−) Patrolling Monocyte Hematopoiesis and CD8(+) T Cell Metabolism. *Immunity* **48**, 992–1005 e1008, https://doi.org/10.1016/j.immuni.2018.04.022 (2018).
37. Unger, A. *et al*. Chromatin Binding of c-REL and p65 Is Not Limiting for Macrophage IL12B Transcription During Immediate Suppression by Ovarian Carcinoma Ascites. *Frontiers in immunology* **9**, 1425, https://doi.org/10.3389/fimmu.2018.01425 (2018).

Acknowledgements

The authors thank Dr. Stefan Offermanns for providing us with *Ffar2*$^{-/-}$*Ffar3*$^{-/-}$ mice. We thank members of animal facility of the Biomedical Research Center, Philipps-University of Marburg. We also thank Elena Jenike for excellent technical assistance. This work was supported by Studienstiftung des deutschen Volkes (Maik Luu) and by a research grant from the Fritz Thyssen Foundation (Alexander Visekruna).

Author Contributions

M.L. and A.V. conceived the study, designed the experiments and A.V. wrote the manuscript. M.L., K.W., C.B, H.L. and S.P. performed the flow cytometry experiments and analyzed the data. F.W. and C.B. performed the HDAC activity assay. Western blot analysis was carried out by M.L. T.A. performed all ChIP analyses. All authors of the manuscript discussed the results and carefully read the paper.

Additional Information

Supplementary information accompanies this paper at https://doi.org/10.1038/s41598-018-32860-x.

Competing Interests: The authors declare no competing interests.

Publisher's note: Springer Nature remains neutral with regard to jurisdictional claims in published maps and institutional affiliations.

Open Access This article is licensed under a Creative Commons Attribution 4.0 International License, which permits use, sharing, adaptation, distribution and reproduction in any medium or format, as long as you give appropriate credit to the original author(s) and the source, provide a link to the Creative Commons license, and indicate if changes were made. The images or other third party material in this article are included in the article's Creative Commons license, unless indicated otherwise in a credit line to the material. If material is not included in the article's Creative Commons license and your intended use is not permitted by statutory regulation or exceeds the permitted use, you will need to obtain permission directly from the copyright holder. To view a copy of this license, visit http://creativecommons.org/licenses/by/4.0/.

© The Author(s) 2018

nature COMMUNICATIONS

ARTICLE

https://doi.org/10.1038/s41467-021-24331-1 OPEN

Microbial short-chain fatty acids modulate CD8$^+$ T cell responses and improve adoptive immunotherapy for cancer

Maik Luu[1,2], Zeno Riester[2], Adrian Baldrich[2], Nicole Reichardt[3], Samantha Yuille[3], Alessandro Busetti[3], Matthias Klein[4], Anne Wempe[1], Hanna Leister[1], Hartmann Raifer[5], Felix Picard[1], Khalid Muhammad[6], Kim Ohl[7], Rossana Romero[1], Florence Fischer[1], Christian A. Bauer[8], Magdalena Huber[1], Thomas M. Gress[8], Matthias Lauth[9], Sophia Danhof[2], Tobias Bopp[4], Thomas Nerreter[2], Imke E. Mulder[3], Ulrich Steinhoff[1], Michael Hudecek[2,10]✉ & Alexander Visekruna[1,10]✉

Emerging data demonstrate that the activity of immune cells can be modulated by microbial molecules. Here, we show that the short-chain fatty acids (SCFAs) pentanoate and butyrate enhance the anti-tumor activity of cytotoxic T lymphocytes (CTLs) and chimeric antigen receptor (CAR) T cells through metabolic and epigenetic reprograming. We show that in vitro treatment of CTLs and CAR T cells with pentanoate and butyrate increases the function of mTOR as a central cellular metabolic sensor, and inhibits class I histone deacetylase activity. This reprogramming results in elevated production of effector molecules such as CD25, IFN-γ and TNF-α, and significantly enhances the anti-tumor activity of antigen-specific CTLs and ROR1-targeting CAR T cells in syngeneic murine melanoma and pancreatic cancer models. Our data shed light onto microbial molecules that may be used for enhancing cellular anti-tumor immunity. Collectively, we identify pentanoate and butyrate as two SCFAs with therapeutic utility in the context of cellular cancer immunotherapy.

[1] Institute for Medical Microbiology and Hygiene, Philipps-University Marburg, Marburg, Germany. [2] Medizinische Klinik und Poliklinik II, Universitätsklinikum Würzburg, Würzburg, Germany. [3] 4DPharma Research Ltd., Aberdeen, United Kingdom. [4] Institute for Immunology, University Medical Center, Johannes Gutenberg University Mainz, Mainz, Germany. [5] Flow Cytometry Core Facility, Philipps University Marburg, Marburg, Germany. [6] Department of Biology, United Arab Emirates University, Al Ain, United Arab Emirates. [7] Department of Pediatrics, RWTH Aachen University, Aachen, Germany. [8] Department of Gastroenterology, Endocrinology, Metabolism and Infectiology, University Hospital Marburg, UKGM, Philipps University Marburg, Marburg, Germany. [9] Institute of Molecular Biology and Tumor Research, Center for Tumor- and Immunobiology, Philipps-University Marburg, Marburg, Germany. [10] These authors jointly supervised this work: Michael Hudecek, Alexander Visekruna. ✉email: Hudecek_M@ukw.de; alexander.visekruna@staff.uni-marburg.de

The intestinal microbiota has been shown to directly impact on the efficacy of specific cancer immune therapies[1–3]. Particularly, immune checkpoint inhibitory (ICI) therapy and adoptive cell therapy using tumor-specific CD8$^+$ cytotoxic T lymphocytes (CTLs) can be influenced by the composition of the intestinal microbiota[4,5]. Recently, several studies have demonstrated that members of the gut microbiota are able to enhance the anti-tumor efficacy of PD-1 and CTLA4 blockade therapy[6,7]. *Akkermansia muciniphila* and some *Bifidobacterium* strains have been shown to modulate anti-tumor immune responses and improve ICI treatment[1,3]. Furthermore, a defined commensal consortium consisting of 11 human bacterial strains elicited strong CD8$^+$ T cell-mediated anti-tumor immunity in an experimental subcutaneous tumor model[7]. This study has demonstrated that a mixture of human low-abundant commensals was able to substantially enhance the efficacy of ICI therapy in mice[7,8].

Relatively little is known about the therapeutic potential of soluble microbial molecules and metabolites to modulate the outcome of cellular cancer immunotherapy. Specific commensal bacteria have been shown to synthesize the metabolite inosine that is able to enhance the efficacy of ICI therapy[9]. Previous studies have identified acetate, propionate, and butyrate as major microbial metabolites, belonging to the class of short-chain fatty acids (SCFAs). These were shown to promote the expansion of Tregs, but they also seem to improve the function of effector T cells[10–15]. Butyrate is associated with protection from autoimmune processes and graft-versus-host disease[16,17]. Furthermore, two reports have highlighted the role of butyrate in promoting the memory potential and antiviral cytotoxic effector functions of CD8$^+$ T cells[18,19]. We have recently demonstrated that the SCFA pentanoate (valerate) is also a bacterial metabolite present in the gut of conventional but not of germ-free (GF) mice[20]. Interestingly, dominant commensal bacteria are not able to produce pentanoate. This SCFA is rather a rare bacterial metabolite generated by low-abundant commensals such as *Megasphaera massiliensis*, which we have classified as a pentanoate-producing bacterial species[21]. It has thus far been unknown if the ex vivo culture of cytotoxic T lymphocytes (CTLs)—either derived from the endogenous repertoire or through genetic engineering with a T cell receptor (TCR) or chimeric antigen receptor (CAR)—with bacterial metabolites is capable of augmenting their anti-tumor reactivity.

In this study, the influence of bacterial SCFAs on adoptive T cell therapy using antigen-specific CD8$^+$ CTLs and CAR T cells has been investigated. We demonstrate that the treatment with pentanoate and butyrate induces strong production of effector molecules in CTLs and CAR T cells, resulting in increased anti-tumor reactivity and improved therapeutic outcome. These data show that specific gut microbiota-derived metabolites such as butyrate and pentanoate have the potential to optimize adoptive T cell therapy for cancer in humans.

Results

***Megasphaera massiliensis*-derived pentanoate enhances the production of effector cytokines in CD8$^+$ T cells**. Commensal bacteria harboring a broad spectrum of enzymes have the ability to produce a large variety of small molecules that may be exploited for therapeutic interventions. Recently, we found that a human gut-isolated bacterial strain *Megasphaera massiliensis* was able to produce high levels of the SCFA pentanoate[21]. Previously, we showed that pentanoate substantially influenced the function of CD4$^+$ T lymphocytes by altering their epigenetic status via inhibition of histone deacetylases (HDACs)[20]. When compared to 14 abundant bacterial species, which represent proportional distribution of the most common phyla in the human intestine (Firmicutes: *Enterococcus faecalis*, *Faecalibacterium prausnitzii*, *Anaerostipes hadrus*, *Blautia coccoides*, *Dorea longicatena*, *Faecalicatena contorta* and *Ruminococcus gnavus*; Bacteroidetes: *Bacteroides fragilis*, *Parabacteroides distasonis*, *Bacteroides vulgatus*, and *Bacteroides ovatus*; Actinobacteria: *Bifidobacterium longum* and *Bifidobacterium breve*; and Proteobacteria: *Escherichia coli*), we observed that the low-abundant human commensal *M. massiliensis* was the only bacterium synthesizing high amounts of pentanoate (Fig. 1a). Interestingly, gas chromatography-mass spectrometry (GC-MS) analysis revealed that, in addition to two different *M. massiliensis* strains (DSM 26228 and NCIMB 42787), *Megasphaera elsdenii*, which is the closest phylogenetic neighbor of *M. massiliensis*[22], also produced pentanoate, although not at such high levels as *M. massiliensis*. Of note, two *M. massiliensis* strains were the only strong producers of the SCFAs pentanoate and butyrate. While most commensals generated high amounts of acetate and formate, *Faecalibacterium prausnitzii* and *Anaerostipes hadrus* synthesized high levels of butyrate (Fig. 1a).

We next investigated if the pentanoate- and butyrate-containing supernatant from *M. massiliensis* has any impact on the function of CD8$^+$ T cells. Indeed, the frequency of IFN-γ$^+$TNF-α$^+$CD8$^+$ T cells within CTLs was markedly increased after treatment with the *M. massiliensis*-derived supernatants (Fig. 1b). For comparison, we included supernatants from several highly abundant gut commensal bacteria (e.g,. *E. coli*, *E. faecalis*, and *B. fragilis*) and did not observe an effect on TNF-α secretion (Supplementary Fig. 1a), consistent with their lacking ability to produce pentanoate and butyrate (Fig. 1a). Because commensal bacteria produce various soluble molecules, we cannot exclude the involvement of other microbial metabolites apart from SCFAs in observed phenomenon. To elucidate the direct SCFA-mediated effects on CD8$^+$ T cells, we cultivated CTLs in the presence of acetate, propionate, butyrate or pentanoate. We found that among the investigated SCFAs, especially pentanoate and butyrate triggered a substantial increase in frequencies of TNF-α$^+$ IFN-γ$^+$ cells and secretion of TNF-α by CTLs (Fig. 1c, d). We exposed CTLs to a wide range of SCFA concentrations to select optimal concentrations promoting strong immunostimulatory effects with the least toxicity (Supplementary Fig. 2a–c). As pentanoate and butyrate promoted the most pronounced effects on CTLs, we decided to perform further functional analysis with these two SCFAs.

Butyrate and pentanoate inhibit HDAC class I enzymes and increase mTOR activity in CD8$^+$ T cells. SCFAs are known inhibitors of histone deacetylases (HDACs) enzymes, that are able to epigenetically modulate the fate of eukaryotic cells[23]. Our broad screening approach revealed that among the commensal strains tested, only a few bacterial species exhibited a strong pan-HDAC inhibitory capacity[21]. When we compared the HDAC inhibitory activity of supernatants derived from 16 human commensals, we observed that particularly the HDAC class I inhibitory effect was mediated by pentanoate- and butyrate-generating *M. massiliensis* and *M. elsdenii*, as well as by the butyrate producers *F. prausnitzii* and *A. hadrus* (Supplementary Fig. 1b), but not by other bacteria. Moreover, the activity of HDAC class I isoforms was strongly inhibited by propionate, butyrate and pentanoate. This effect was specific, since class II HDACs (HDAC4, HDAC5, HDAC6, and HDAC9) were not affected following treatment with SCFAs. As expected, the pan-HDAC inhibitor TSA inhibited both, class I and class II HDACs (Fig. 2a). Similarly, CTL-derived cell lysates exposed to propionate, butyrate, and pentanoate, but not to acetate and hexanoate, displayed a strong reduction of pan-HDAC activity (Fig. 2b). We

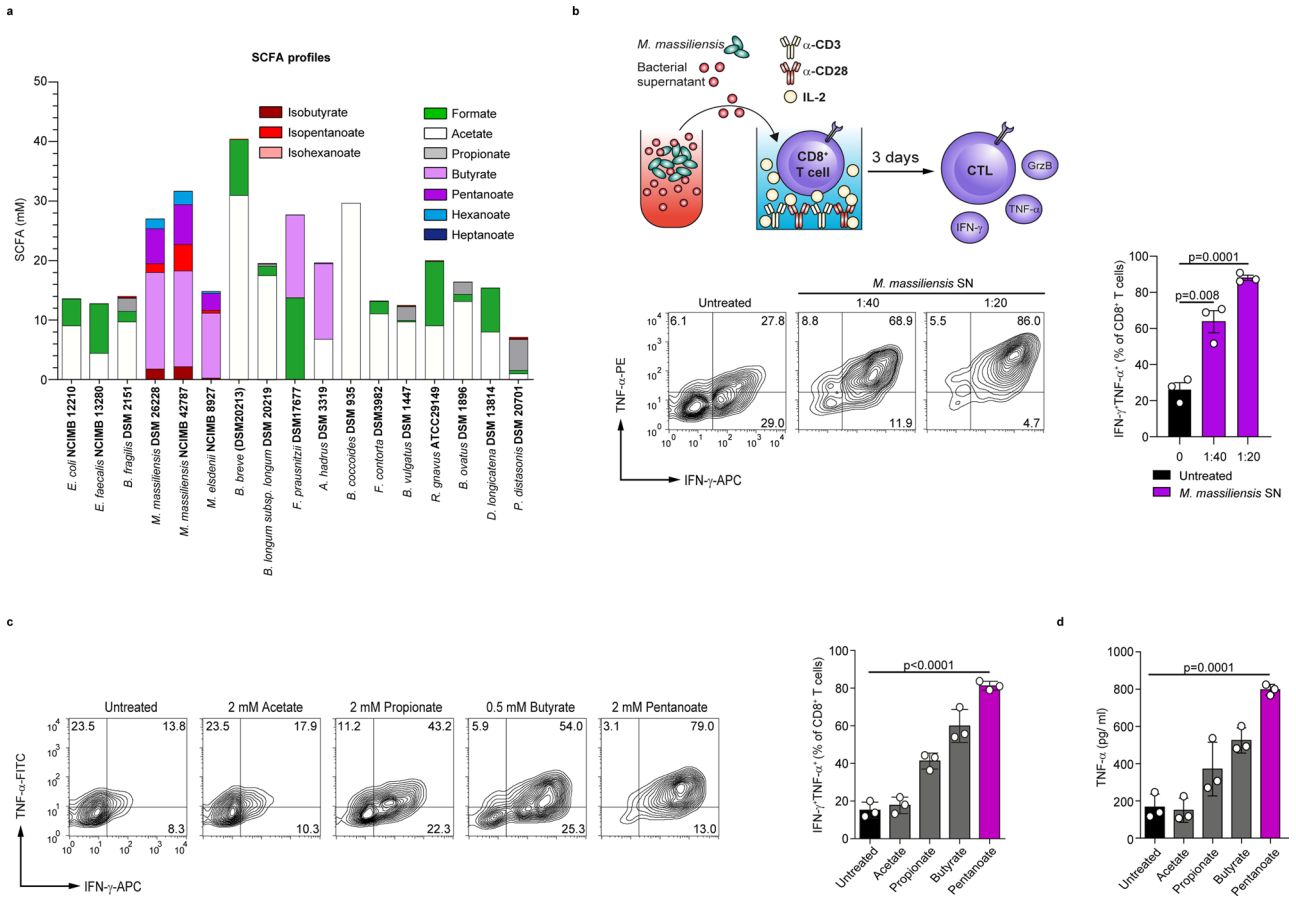

Fig. 1 Microbiota-derived SCFAs promote the production of effector cytokines in CTLs. a The production of SCFAs, branched-chain fatty acids (BCFAs) and medium-chain fatty acids (MCFAs) by 16 human commensals was measured by GC-MS. All bacteria were grown in vitro until the stationary growth phase before the measurement of fatty acids in supernatants ($n = 3$ independent experiments). **b** The frequency of IFN-γ- and TNF-α-expressing CD8$^+$ T cells cultured under suboptimal CTL conditions and stimulated with supernatant derived from *M. massiliensis* (1:40 or 1:20 supernatant-to-cell media ratios; $n = 3$ mice). **c** The percentage of IFN-γ$^+$TNF-α$^+$ CTLs, derived from SPF mice and treated with the indicated SCFAs for three days ($n = 3$ mice). **d** The secretion of TNF-α from CTLs treated with SCFAs was determined by ELISA ($n = 3$ mice). Statistical analysis was performed by two-tailed unpaired Student's *t*-test; mean ± s.e.m. values are presented. Source data are provided as a Source data file.

further observed that the pan-HDAC inhibitor trichostatin A (TSA) increased the percentages of IFN-γ$^+$ CD8$^+$ T cells as compared to control CTLs (Supplementary Fig. 3a). Also valproate, which is a synthetic branched SCFA derived from pentanoate with a strong HDAC inhibitory activity, potently enhanced the production of TNF-α and IFN-γ in CTLs (Supplementary Fig. 3b, c). Both pentanoate and valproate induced the expression of CTL-related transcription factors T-bet and Eomes in CD8$^+$ T cells (Supplementary Fig. 3d, e). Mocetinostat, a specific inhibitor of class I HDACs, also increased the percentage of IFN-γ$^+$TNF-α$^+$ cells and secretion of TNF-α by CTLs. In contrast, the class II HDAC inhibitor TMP-195 showed no significant effect (Fig. 2c–e). Together, these results show that the HDAC class I inhibitory activity of SCFAs pentanoate and butyrate modulates the expression of several effector molecules in CTLs.

It is known that the glycolytic metabolic pathway promotes IFN-γ expression and T cell effector function[20,24–27]. In line with these findings, inhibition of glycolysis by the glucose analog 2-deoxyglucose (2-DG) or the mTOR complex (which promotes glycolytic metabolism in effector T cells) by rapamycin led to a reduction in IFN-γ production in CTLs (Supplementary Fig. 4a). Since microbial metabolites can be utilized by T cells for their metabolic demand to enhance glycolysis and oxidative phosphorylation[28,29], we tested if pentanoate is capable of increasing the activity of the mTOR complex, a key regulator of cell growth and immunometabolism. Indeed, pentanoate elevated the phosphorylation levels of both mTOR and its downstream target S6 ribosomal protein in CTLs. Interestingly, neither mocetinostat nor TMP-195 had a significant effect on the phosphorylation of mTOR and S6, suggesting a HDAC-independent impact of pentanoate and butyrate on metabolic status of CD8$^+$ T cells (Fig. 2f). Moreover, the extracellular acidification rate (ECAR), as an indicator of glycolytic metabolism, increased upon pentanoate treatment of CTLs (Supplementary Fig. 4b). Notably, the co-treatment of CTLs with rapamycin led to partial reduction of pentanoate-triggered IFN-γ production (Supplementary Fig. 4c). SCFAs are not only HDAC inhibitors and metabolically active substance, but also ligands for G-protein-coupled receptors GPR41 (FFAR3) and GPR43 (FFAR2). Therefore, we tested the IFN-γ expression in CTLs lacking these two SCFA-receptors (*Ffar2*$^{-/-}$*Ffar3*$^{-/-}$ CTLs) following pentanoate treatment. We did not observe any effect of GPR41 and GPR43 on the frequency of IFN-γ$^+$CD8$^+$ T cells (Supplementary Fig. 5a, b). Finally, the pentanoate-mediated inhibition of HDAC activity in CTL-derived cell lysates was not affected in the absence of GPR41 and GPR43 (Supplementary Fig. 5c). In summary, our data show that pentanoate modulates the effector molecule expression in CTLs through HDAC-inhibition and metabolic modulation in a GPR41/GPR43-independent manner.

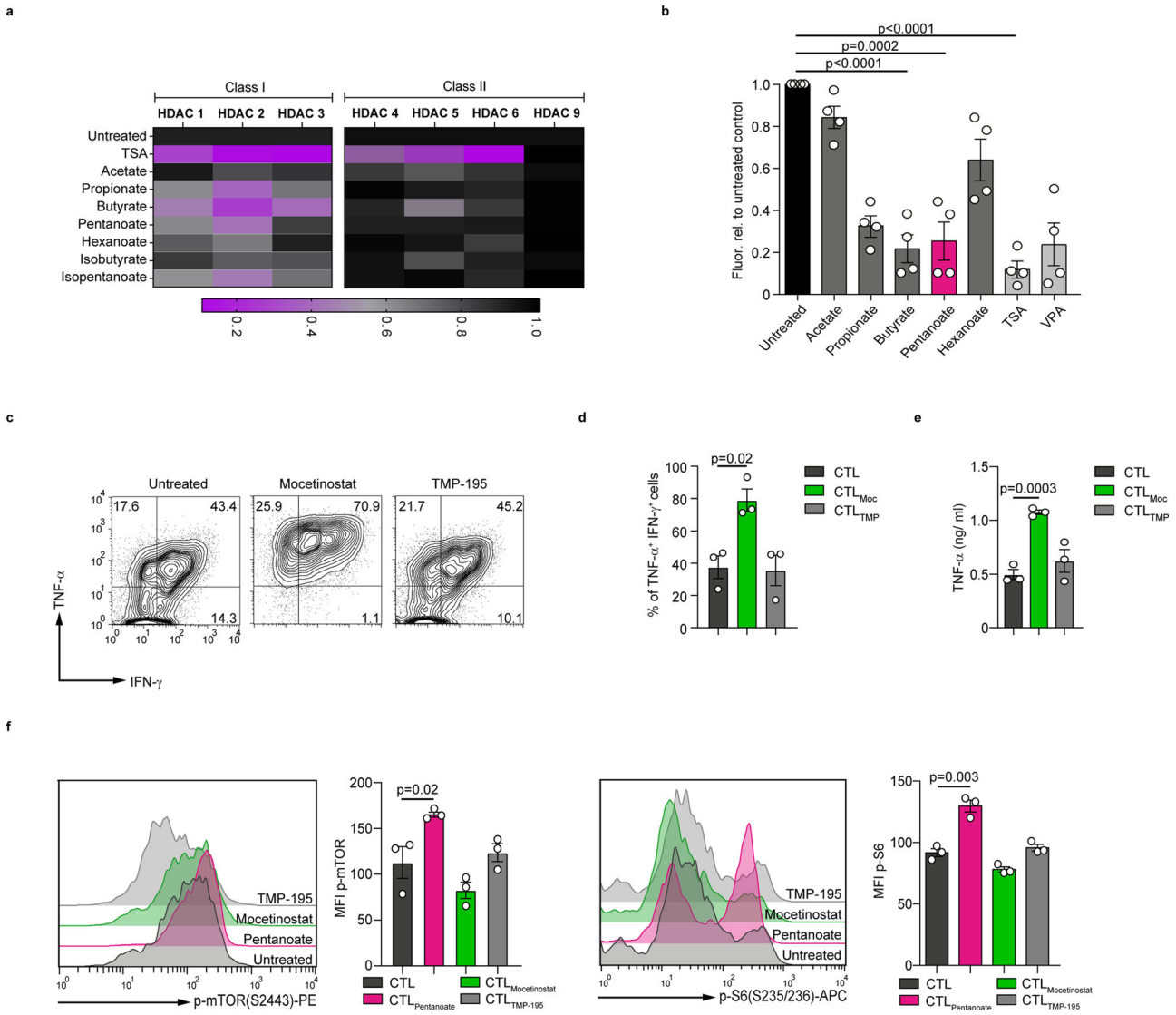

Fig. 2 Pentanoate inhibits the class I HDAC enzymes and enhances the activity of mTOR in CD8$^+$ T cells. a Impact of bacterial SCFAs, BCFAs, and MCFAs on the activity of recombinant class I and II HDAC enzymes. TSA was used as a control pan-HDAC inhibitor. One of three independent experiments is shown. **b** The fluorogenic HDAC assay was applied to measure the HDAC inhibitory activity of SCFAs on CTLs. The value for unstimulated CTLs was arbitrarily set to 1.0. Four independent experiments were performed (analyzed by two-tailed unpaired Student's *t*-test; data are shown as mean ± s.e.m). **c–e** Murine CD8$^+$ T cells were polarized under suboptimal CTL-inducing conditions for three days. Representative contour plots (**c**) and bar graphs (**d**) indicate the frequency of IFN-γ$^+$TNF-α$^+$ cells and TNF-α secretion (**e**) after treatment with 300 nM mocetinostat (class I HDAC inhibitor) or 2.5 μM TMP-195 (class II HDAC inhibitor), respectively ($n = 3$ mice, analyzed by two-tailed unpaired Student's *t*-test; data are shown as mean ± s.e.m). **f** Murine CTLs were cultured in medium containing 1.0% serum and treated with indicated HDACi for three days. Representative histogram plots and bar graphs indicate the phoshorylated levels of mTOR and S6 ribosomal protein, respectively ($n = 3$ mice, analyzed by two-tailed unpaired Student's *t*-test; data are shown as mean ± s.e.m). Source data are provided as a Source data file.

Pentanoate and butyrate treatment enhances the anti-tumor reactivity of antigen-specific CD8$^+$ T cells. We next sought to assess the effect of pentanoate and butyrate treatment on the anti-tumor reactivity of antigen-specific CD8$^+$ T cells in vivo. In a first set of experiments, we injected s.c. B16OVA melanoma cells into CD45.2$^+$ mice and transferred either pentanoate- or butyrate or non-treated CD45.1$^+$ OT-I CTLs into recipient animals on day 5 after tumor injection. Overall, the anti-tumor immunity mediated by antigen-specific CTLs was significantly improved after ex vivo culture with pentanoate or butyrate as shown by decreased tumor volume and weight (Fig. 3a–c). On day 10 after adoptive transfer of CTLs, we detected a higher percentage as well as absolute number of pentanoate- and butyrate-pretreated CD8$^+$ T cells, expressing more TNF-α and IFN-γ in comparison to non-treated OT-I CTLs in draining LNs (Fig. 3d–g). Similarly, pretreatment of CD45.1$^+$ OT-I CTLs with the supernatant of *M. massiliensis* also led to superior anti-tumor reactivity after adoptive transfer (Fig. 3b–g). Therefore, we examined if the specific HDAC class I inhibitor mocetinostat was capable of enhancing CTL-mediated anti-cancer immunity. Indeed, mocetinostat elicited a similar effect on adoptively transferred CTLs, but not to the same extent as butyrate and pentanoate, while the class II HDAC inhibitor TMP-195 did not enhance CTL-mediated anti-tumor immune responses (Fig. 3b–g). In a second set of experiments, we assessed the outcome of pentanoate pretreatment of antigen-specific CTLs in an aggressive pancreatic tumor model expressing OVA protein (OVA-expressing Panc02 cells, PancOVA). To this end, 1.5 ×10^6 PancOVA cells were injected s.c. into CD45.2$^+$ mice. The transfer

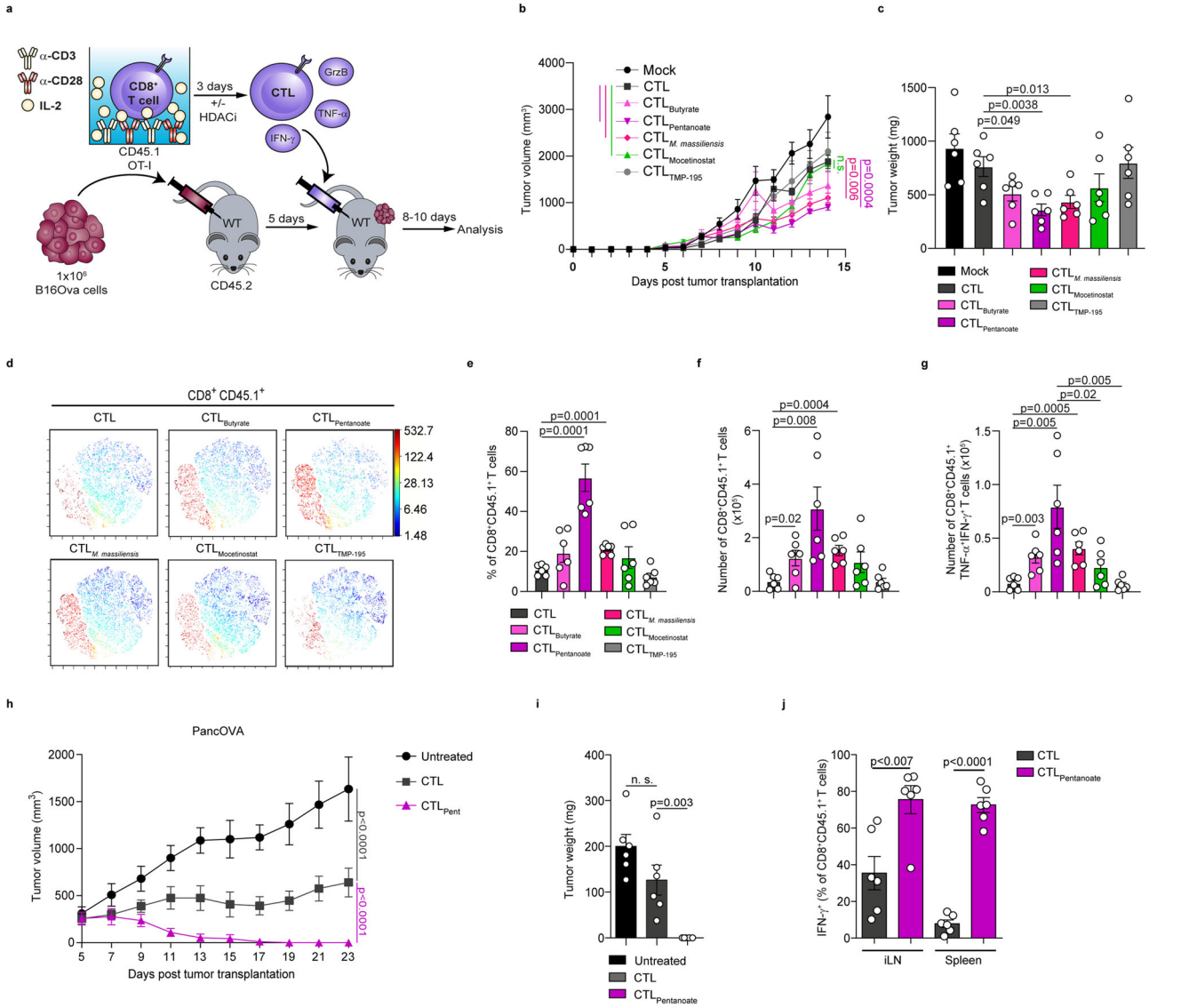

Fig. 3 Pentanoate enhances anti-tumor activity of antigen-specific CTLs. a Experimental design for the role of SCFAs in promoting anti-tumor immunity. **b**–**g** After three days of pretreatment with indicated HDAC inhibitors, CD8$^+$CD45.1$^+$ OVA-specific CTLs were transferred intraperitoneally (i.p.) into CD45.2$^+$ mice bearing 5-days old B16OVA tumors. Tumor volume (**b**) and tumor mass (**c**) were analyzed on day 14 after inoculation of tumor cells ($n = 6$ mice/group combined from two independent experiments). The t-SNE plots in (**d**) show CD8$^+$CD45.1$^+$ cells among lymphocytes from the tumor-draining LNs. The percentage (**e**) and total cell number (**f**) of transferred CD8$^+$CD45.1$^+$ OT-I CTLs in the tumor-draining LNs at day 14 after tumor inoculation are shown. In **g** the total cell numbers of transferred antigen-specific IFN-γ$^+$TNF-α$^+$ CTLs were examined on day 14 after inoculation of B16OVA tumors in tumor-draining LNs (in **e**–**g**, $n = 6$ mice/group combined from two independent experiments). **h**–**j** OVA-specific CD45.1$^+$ CTLs pretreated with pentanoate were adoptively transferred into CD45.2$^+$ mice bearing 5-days old PancOVA tumors. Tumor volume (**h**) and tumor weight (**i**) were determined on day 23 post tumor inoculation. In **j** frequencies of transferred IFN-γ-producing CD8$^+$ T cells in draining LNs and spleens were analyzed on day 23 post tumor inoculation ($n = 6$ mice/group combined from two independent experiments). Multiple group comparison (**b**, **h**) was performed by a linear-mixed effects model with Tukey correction. The two-tailed unpaired Student's *t*-test was applied to compare two groups (n.s. = not significant; results are shown as mean ± s.e.m). Source data are provided as a Source data file.

of low numbers (7.5 ×10^5) of pentanoate-treated CD45.1$^+$ OT-I CD8$^+$ T lymphocytes, but not of untreated ones, was able to abrogate the growth of PancOVA tumor cells in recipient animals (Fig. 3h–j). While the control CTLs were hardly found on day 23 after tumor inoculation, we observed a persistence of pentanoate-treated CTLs with high IFN-γ production within draining LNs and spleen of recipient mice even 10 days after first achievement of remission (Fig. 3j and Supplementary Fig. 6a, b). These data suggest that SCFAs pentanoate and butyrate may used to augment adoptive cell therapy to target tumors. However, it should be noticed that in vivo administration of pentanoate did not enhance anti-tumor immunity. Similarly, there was no beneficial effect of pentanoate on anti-PD-1 therapy (Supplementary Fig. 7a, b). In accordance with this observation, a recent study has revealed that the systemic administration of butyrate did not promote beneficial effects. Interestingly, butyrate even limited the effect of CTLA-4 blockade by inhibiting upregulation of CD80 and CD86 on dendritic cells[30].

Pentanoate promotes the expression of CD25 and IL-2 in CD8$^+$ T cells. To investigate the capacity of SCFAs on survival and persistence of CD8$^+$ T cells, we mixed pentanoate-treated CTLs (CD45.2$^+$) with control CTLs (CD45.1$^+$) at 1:1 ratio and co-

transferred them into Rag1-deficient mice. To better mimic the in vivo tumor microenvironment, we also adoptively co-transferred Tregs (CD45.2$^+$ from FIR × tiger reporter mice) that are frequently found in solid tumors. In addition, Foxp3$^-$CD4$^+$ T cells were co-transferred as the cellular source of IL-2 (Supplementary Fig. 8a, b). Surprisingly, in contrast to control CTLs, pentanoate-treated CTLs were found at a high cell number and frequency on day 15 after transfer, even without encounter of the cognate antigen (Supplementary Fig. 8c, d). The capacity of CFSE to label proliferative cells was used for in vivo monitoring of CD8$^+$ T cell proliferation in Rag1-deficient mice after pretreatment with pentanoate. We found that pentanoate-treated and CFSE-labeled CD8$^+$ T cells had a stronger proliferation as compared to control CTLs (Supplementary Fig. 8e). Furthermore, we detected higher frequencies and cell numbers of CD25$^+$ CTLs pretreated with pentanoate in Rag1-deficient mice (Supplementary Fig. 8f, g). Given the importance of the CD25 and IL-2 signaling in supporting proliferation and survival of lymphocytes[31], we next asked whether pentanoate is capable of modulating CD25 expression and IL-2 signaling in CTLs. By analyzing effects of pentanoate on CD25 upregulation and dynamics of IL-2-induced phosphorylation of STAT5, we found a higher expression of CD25 as well as a stronger STAT5 activity in response to IL-2 in pentanoate-treated CTLs in comparison to control cells (Supplementary Fig. 8h, i). Notably, the pharmacological inhibition of glycolysis with 2-DG completely abrogated pentanoate-mediated upregulation of CD25 (Supplementary Fig. 8h). Finally, pentanoate-treated CTLs robustly produced IL-2 in a prolonged manner as compared to control CTLs (Supplementary Fig. 8j), thus being able to sustain this autocrine loop for a longer period of time. Taken together, the pentanoate-induced upregulation of CD25, as well as continuous IL-2 production by CTLs, might contribute to their persistence in vivo.

Pentanoate treatment augments the anti-tumor potency of CAR T cells in a pancreatic cancer model. To gain further insight into potential therapeutic strategies, we examined the impact of SCFAs on genetically engineered chimeric antigen receptor (CAR) T cells. For this purpose, we used murine CD8$^+$ CAR T cells that recognize receptor tyrosine kinase-like orphan receptor 1 (ROR1) (Fig. 4a), a molecule frequently expressed in a variety of epithelial tumors and in some B cell malignancies[32]. Similar to our previous observations with CTLs, ROR1-CAR T cells that were treated with butyrate or pentanoate also enhanced the expression of CD25 upon stimulation (Fig. 4b). Moreover, ROR1-CAR T cells treated with butyrate or pentanoate enhanced their TNF-α and IFN-γ production as compared to non-treated ROR1-CAR T cells (Fig. 4c, d). We further sought to determine, whether pentanoate pretreatment of ROR1-CAR T cells had a supportive effect on their anti-tumor reactivity in a pancreatic cancer model. Therefore, we generated ROR1-expressing Panc02 pancreatic tumor cells (Panc02/ROR1) and injected them s.c. into WT mice (Fig. 4a). On day 5 after tumor cell injection, we adoptively transferred pentanoate-treated or untreated ROR1-CAR T cells and monitored T cell engraftment as well as tumor response. By day 10 following CAR T cell administration, tumor volume and weight were significantly diminished in mice that received pentanoate-treated CAR T cells as compared to animals with untreated CAR T cells (Fig. 4e, f). Furthermore, we found an elevated frequency and absolute number of IFN-γ$^+$TNF-α$^+$ pentanoate-pretreated CAR T cells in tumors, as compared to control CAR T cells (Fig. 4g).

Previously, we could demonstrate that human CD8$^+$ T lymphocytes equipped with a ROR1-CAR exert specific anti-tumor reactivity in vitro and xenograft models in immunodeficient mice[33,34]. Hence, we investigated the impact of SCFAs on human CD8$^+$ T lymphocytes and CAR T cells. Our data show that both pentanoate and butyrate as well as the class I HDAC inhibitor mocetinostat enhanced expression of TNF-α and IFN-γ in human CD8$^+$ T cells in non-toxic concentration range (Fig. 5a and Supplementary Fig. 9a). Moreover, both SCFAs increased the phosphorylation of mTOR and S6 ribosomal protein in CTLs. In contrast to SCFAs, mocetinostat and TMP-195 were not capable of significantly activating mTOR pathway in human CTLs (Supplementary Fig. 9b, c). Based on findings collected from murine CAR T cells, in a complementary approach, we pretreated human ROR1-CAR T cells with pentanoate for 4 days and subsequently investigated the cytokine production, proliferation, expression of activation markers and the cytotoxic capacity of untreated and pentanoate-treated CAR T cells as indicated in the Fig. 5b. In accordance with results generated with murine CTLs and CAR T cells, human CAR T cells also upregulated the expression of CD25 and secretion of IL-2 after pentanoate pretreatment as compared to untreated cells (Fig. 5c, d). When we co-cultured ROR1-specific CAR T cells with ROR1-expressing K562 human cancer cells, we found that pentanoate-pretreated cells elevated the production of CTL-related cytokines IFN-γ and TNF-α (Fig. 5e). Moreover, CAR T cells pretreated with pentanoate proliferated stronger than control CAR T cells and exerted a superior cytolytic activity after encounter of ROR1 (Fig. 5f, g). Together, these results show that pentanoate and butyrate treatment of murine and human ROR1-specific CAR T cells augments their anti-tumor function in vitro and in vivo. Collectively, the data demonstrate the potential to use pentanoate and butyrate treatment during CAR T cell manufacturing to exploit the beneficial effects of these bacterial metabolites on CTL function in order to increase the therapeutic potential and the outcome after adoptive transfer of CAR T cells.

Discussion

Gut microbiota and microbial metabolites influence many aspects of host physiology[35]. Previously, the commensal *Bifidobacterium* was shown to enhance anti-tumor immunity in mice. The eradication of established tumors was abrogated in CD8$^+$ T cell-depleted animals, indicating that the underlying mechanism was mediated through host anti-cancer CTL responses[1]. Similarly, *Akkermansia muciniphila* increased the recruitment of CD4$^+$ T cells into tumors[3]. SCFAs such as acetate, propionate, and butyrate are water-soluble and diffusible gut-microbiota-derived metabolites reaching their peak concentrations in the caecum and decrease from the proximal to the distal colon[36]. In this study, we demonstrate that the SCFAs pentanoate and butyrate are promising microbial metabolites augmenting adoptive cell therapy for cancer. Moreover, pentanoate was able to enhance the efficacy of ROR1-specific CAR T cells. SCFAs have been shown to impact on T cell immune responses[37]. Particularly, butyrate and propionate seem to be potent regulators of the suppressive activity of Tregs in diverse experimental settings of autoimmune and inflammatory disorders[16,38]. Commensal-derived butyrate was shown to induce epigenetic reprogramming of Tregs by enhancing the acetylation of histone H3 in the promoter and conserved non-coding sequence regions of the *Foxp3* locus[12]. On the other side, some reports suggest that SCFAs are also capable of promoting the activity of CD4$^+$ effector T cells, indicating that the influence of microbial metabolites on the immune system may be more complex than previously thought[13,15]. Two recent studies have demonstrated that SCFAs were able to affect the effector function of CD8$^+$ T cells and their transition into memory cells during viral infection[18,19].

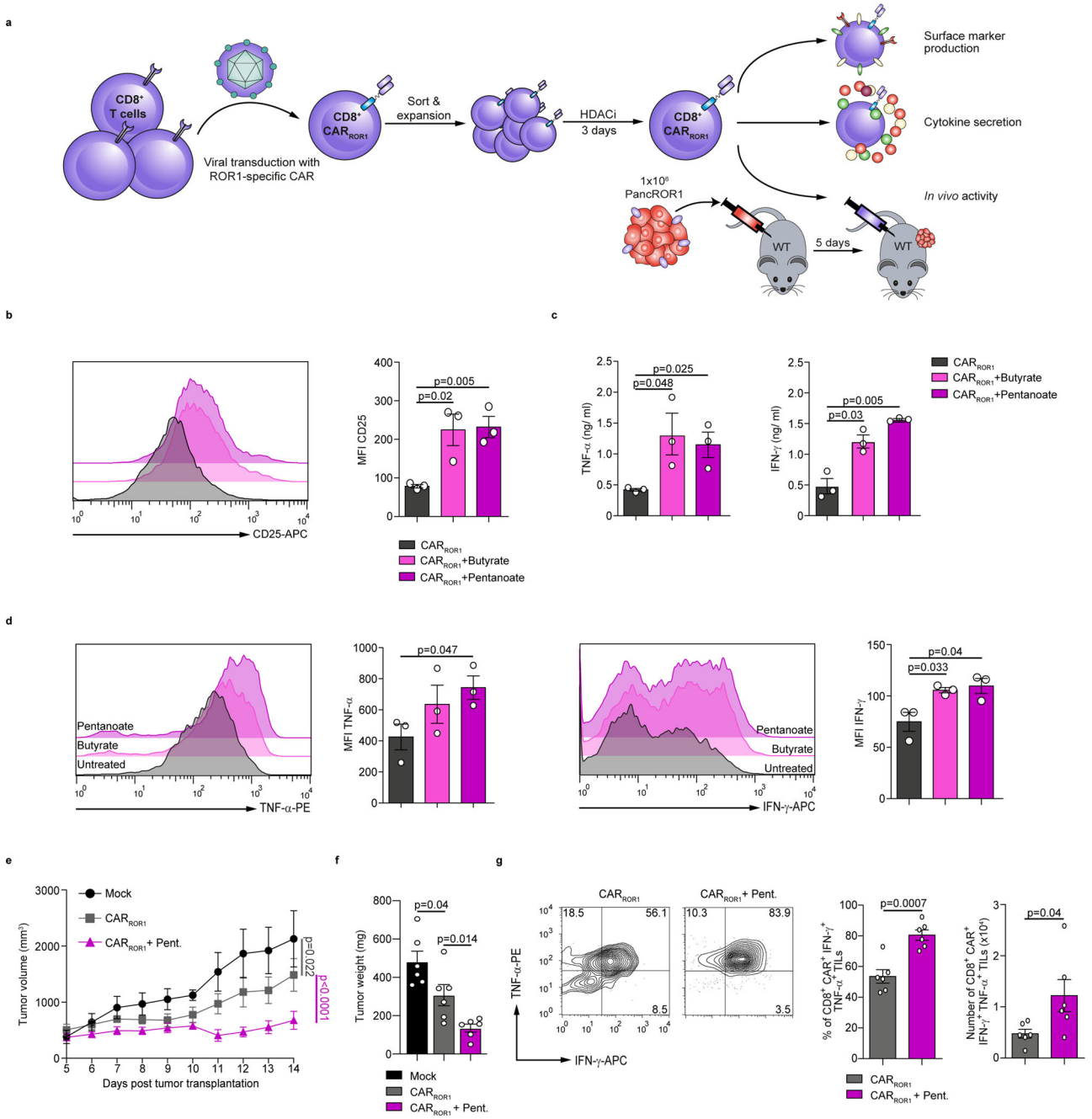

Fig. 4 Pentanoate-treatment enhances the anti-tumor activity of murine CAR T cells. a Experimental design for the analysis of SCFA-treated ROR1-specific murine CD8$^+$ CAR T cells (CAR_{ROR1}). **b** The surface expression of CD25 on CAR T cells was measured by flow cytometry analysis after three days of stimulation with butyrate or pentanoate ($n = 3$ independent experiments). **c**, **d** The production of TNF-α and IFN-γ from CAR T cells was measured by ELISA (**c**) and flow cytometry analysis (**d**) after three days of stimulation with butyrate or pentanoate. Three similar experiments were performed. **e**–**g** Following the pretreatment with pentanoate for three days, ROR1-specific CAR T cells were transferred i.p. into mice bearing 5-days old PancROR1 tumors. Tumor volume (**e**) and tumor mass (**f**) were analyzed on day 14 post tumor inoculation ($n = 6$ mice/group combined from two independent experiments). The percentage and total cell number of transferred TNF-α$^+$ and IFN-γ$^+$ CAR T cells in the tumor tissue at day 14 after tumor inoculation are shown in (**g**). For all experiments, 0.75 mM butyrate and 2.5 mM pentanoate were used, respectively. Multiple group comparison in (**e**) was performed by a linear-mixed effects model with Tukey correction. In **b**–**d** and **f**, **g**, the two-tailed unpaired Student's *t*-test was applied. Source data are provided as a Source data file.

Another potentially therapeutically useful SCFA, pentanoate, has not been investigated yet in the context of cancer immunotherapy. We recently found that pentanoate was able to impact on the function of CD4$^+$ effector T cells by modulating both cellular metabolism through the activation of mTOR pathway and epigenetic status of cells by inhibiting HDAC enzymes[20]. Our current findings have revealed that pentanoate and butyrate promoted their effects on CD8$^+$ T cells primarily by inhibiting class I HDAC enzymes and by inducing metabolic alterations, which resulted in enhancement of the expression of CTL-associated genes. Our recent report demonstrated that the T cell-specific deletion of class I HDACs HDAC1 and HDAC2 (a deletion of two *Hdac1* alleles and one *Hdac2* allele) triggered the expression of genes associated with cytolytic activity even in CD4$^+$ T cells[39]. Furthermore, pentanoate

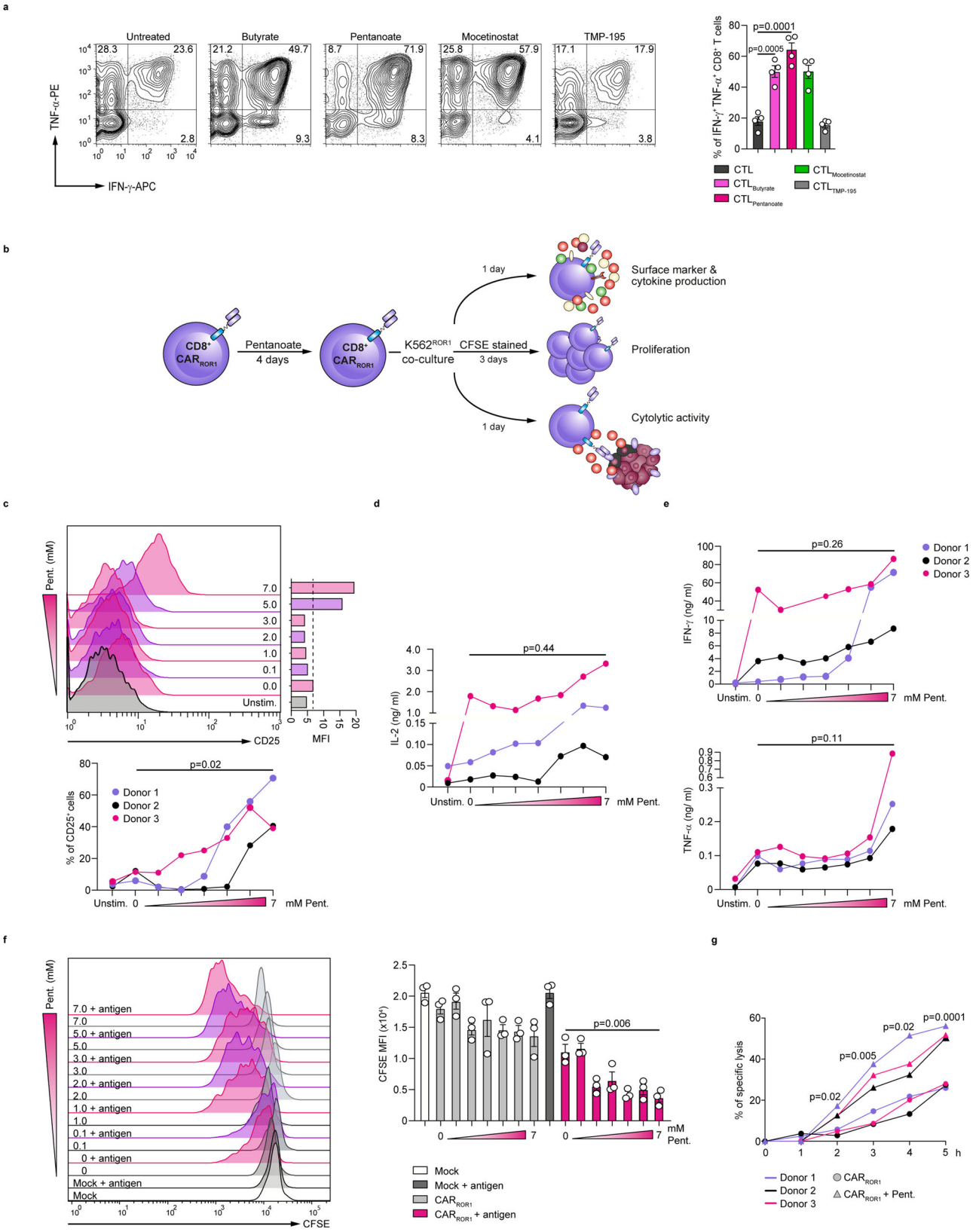

was also able to induce in vitro CD4$^+$ CTL differentiation in human CD4$^+$ T cells with similar phenotype[39], suggesting a predominant role for HDAC inhibitory activity over metabolic effects for SCFA-treated T cells. Interestingly, although the specific class I and class II HDAC inhibitors mocetinostat and TMP-195 were not capable of increasing the phosphorylation of mTOR and its target protein S6, the pan-HDAC inhibitor TSA was shown to increase mTOR activity in T cells[13], suggesting a certain level of interdependence between HDAC inhibition and metabolic effects. In the future, the complex cross-talk between SCFA-mediated epigenetic changes and their multiple effects on the cellular metabolism of CTLs should be investigated in more detail.

Fig. 5 Pentanoate enhances the functional status of human CAR T cells. a CD8$^+$ T cells were isolated from peripheral blood of healthy donors were differentiated into CTLs in presence or absence of butyrate (1 mM), pentanoate (4 mM), mocetinostat (HDAC class I inhibitor, 300 nM) or TMP-195 (HDAC class II inhibitor, 2.5 μM). Representative contour plots (left) and graphs (right) show the frequency of IFN-γ$^+$ TNF-α$^+$ CD8$^+$ T cells. (n = 4 combined from four independent experiments). **b** Experimental setup for the functional analysis of pentanoate-treated ROR1-specific human CD8$^+$ CAR T cells (CAR_{ROR1} T cells). **c** The surface expression of CD25 was measured following pentanoate treatment by flow cytometry. **d** The secretion of IL-2 was detected in supernatants of pentanoate-treated CAR_{ROR1} T cells by ELISA. **e** The secretion of IFN-γ and TNF-α was analyzed in supernatants of pentanoate-treated CAR_{ROR1} T cells by ELISA. **f**, **g** Proliferation of CAR_{ROR1} T cells was determined by CFSE labeling (**f**). CAR_{ROR1} T cells pretreated with pentanoate were stained with CFSE and subsequently co-cultured with $K562^{ROR1}$ cells in the absence of pentanoate. CD8$^+$ T cells without the CAR construct were used as mock control cells. The cytolytic activity of CAR_{ROR1} T cells was examined by analysis of specific lysis following encounter with luciferase-expressing $K562^{ROR1}$ cells (**g**). The percentage of lysed target cells was determined in 1 h intervals (effector-to-target cell (E:T) ratio = 2.5:1). Data points shown in the graphs represent CAR_{ROR1} T cells derived from three different donors (**c**–**g**). Following pentanoate pretreatment, the stimulation was mediated by co-culture of CD8$^+$ CAR_{ROR1} T cells with ROR1-expressing K562 ($K562^{ROR1}$) cells in the absence of pentanoate. The groups in **a** and **c**–**g** were compared by two-tailed unpaired Student's *t*-test, data shown as mean ± s.e.m. Source data are provided as a Source data file.

SCFAs can regulate the activity of immune cells not only by triggering metabolic and epigenetic changes, but also by binding to cognate receptors on the surface of cells. SCFAs serve as ligands for GPR41 and GPR43 on intestinal Tregs and epithelial cells, leading to activation mitogen-activated protein kinase signaling and secretion of chemokines and cytokines[11,40]. As most SCFAs have agonist activity for GPR41 and GPR43[41], we treated CTLs lacking these both SCFA-receptors with pentanoate. We did not observe any detectable influence of GPR41 and GPR43 on SCFA-mediated regulation of CTL activity. One plausible explanation might be a low expression of both molecules on T cells isolated from spleen and LNs. Only CD4$^+$ T cells derived from intestinal lamina propria, but not that from other tissues, have been demonstrate to express high levels of these SCFA-receptors[13]. We could also observe that penatoate enhanced the expression of CD25 and IL-2 in CTLs. During activation of T cells, IL-2 is consumed in an autocrine manner, which might have impact on the persistence and activity of adoptively transferred CTLs in the microenvironment of solid tumors. Interestingly, the pentanoate-mediated upregulation of CD25 in CTLs was completely abrogated upon co-treatment of cells with 2-DG, indicating that pentanoate-mediated enhancement in glycolytic activity might be responsible for observed effects. Recently, CD25 was shown to be the upstream molecule inducing mTOR signaling in T cells[42], suggesting a possible positive feedback triggered by pentanoate treatment.

Genetic modification with a CAR endows T cells with a new antigen-specificity target and eliminate tumor cells. In contrast to CD19, the first clinically approved molecule for CAR T cells, which is present on the cell surface of CD19-positive lymphoma and leukemia, the orphan receptor ROR1 is expressed on many epithelial tumors and is also a target for CAR T cells[32,43]. The potential effects of metabolites produced by the gut microbiota on the efficacy of human CAR T cells has thus far been unknown. In this study, we demonstrated that the SCFAs pentanoate and butyrate improved the efficacy of murine CAR T cells by increasing the expression of CTL-associated effector molecules in ROR1-specific CAR T cells. Most importantly, pentanoate also enhanced the efficacy of human CAR T cells suggesting that microbial metabolites could be therapeutically employed.

Our study illustrates one potential embodiment to exploit the beneficial effect of pentanoate and butyrate on CTL function, i.e. SCFA-treatment during CTL manufacturing, which can readily be implemented in clinical-grade GMP manufacturing processes[44]. Another potential embodiment is the administration of pentanoate, butyrate or other SCFAs, or the transfer of a bacterial consortium that produces these SCFAs to patients that have received adoptive cell therapy. However, the clinical implementation of this embodiment will require careful additional investigations to determine the optimal route, dosing, and schedule in order to balance the stimulation of effector vs. regulatory immune cell subsets in favor of the desired therapeutic outcome.

Methods

Mice. Rag1-deficient mice, *FIR* × *tiger* reporter animals, and WT mice on a C57BL/6 background were maintained under SPF conditions at the Biomedical Research Center, Philipps-University of Marburg. *Ffar2*$^{-/-}$*Ffar3*$^{-/-}$mice (on a C57BL/6 background) were kindly provided by Dr. Stefan Offermanns (Max Planck Institute for Heart and Lung Research, Bad Nauheim, Germany). Female 8–12-week old CD45.1 OT-I and CD45.2 WT mice were used for in vivo experiments. The work in animal facility such as daily animal care, breeding and offspring separation, was carried out under SPF or GF conditions. Mice were kept at 21-23 °C and 40% humidity with a 12 h light/12 h dark light cycle. The sterile conditions for GF animals were routinely tested (twice a week) by culturing feces in thioglycollate medium under aerobic and anaerobic conditions for at least two weeks. All animal work was approved by the regional animal care and use committee of the government bureau Gießen, Hesse, Germany (Study Nr. G24/2019, Regierungspräsidium Gießen, Landgraf-Philipp-Platz 1-7, 35390 Gießen, Germany). All animal experiments were performed in accordance with the German law guidelines of animal care.

Tumor models and adoptive transfer of T cells. For adoptive transfer experiments, mice were subcutaneously (s.c.) injected with 1×10^6 B16-OVA or 1.5×10^6 PancOVA cells. At day 5 after tumor injection, 750,000 (in PancOVA model) or 1×10^6 (in B16OVA model) of CD45.1 OT-I CTLs were transferred intraperitoneally (i.p.) into CD45.2 mice. To analyze T cells in tumors, mice were sacrificed 10–20 days after the adoptive transfer of cells. In a subset of experiments, transferred T lymphocytes were sorted from tumors for indicated analyses.

In vivo persistence of pentanoate-treated CTLs. CD8$^+$ T cells expressing either CD45.1 or CD45.2 derived from congenic mice were isolated as described above and activated for three days in absence or presence of 2.5 mM pentanoate. 1.5×10^6 CD45.1$^+$ untreated control CTLs were mixed with 1.5×10^6 CD45.2$^+$ pentanoate-treated CTLs, 0.5×10^6 Foxp3$^+$ Tregs (FACS-sorted from *FIR* × *tiger* reporter mice) as well as 2.5×10^6 Foxp3-CD4$^+$ T cells and adoptively transferred into Rag1-deficient mice. On day 15 after the transfer, LNs and spleen were analyzed for the CTL ratio, proliferation, and expression of CD25 by FACS analysis.

In vitro T cell differentiation. T lymphocytes were purified from LNs and spleens of mice using the kit for negative isolation (Miltenyi Biotec) with a high purity (90–95%). Purified CD8$^+$ T cells were activated with plate-bound anti-CD3 (5 μg/ml, clone 145-2C11) and soluble anti-CD28 (1 μg/ml, clone 37.51) in the presence of 50 U/ml IL-2 and anti-IFN-γ (10 μg/ml, clone XMG1.2) to obtain suboptimal CTL conditions. In specific experiments, T cells were treated with indicated concentrations of sodium pentanoate, sodium butyrate, sodium propionate, sodium acetate, sodium valproate or TSA (all substances, Sigma-Aldrich). Furthermore, some CTLs were cultivated in the presence of 300 nM mocetinostat and 2.5 μM TMP-195, respectively. The water-soluble fraction of small intestinal, caecal, and colonic luminal content was filter-sterilized (0.2 μm filter, Millipore) and diluted (1:40) in RPMI medium before treating the CD8$^+$ T cells.

Antibodies and flow cytometry. After three days of the cell culture, CD4$^+$ and CD8$^+$ T lymphocytes were restimulated for 4 h with PMA (50 ng/ml)/ionomycin (750 ng/ml) in the presence of 10 mg/ml Brefeldin A (all reagents, Sigma-Aldrich). Following treatment with fluorochrome-labeled antibodies, T cells were fixed with 2% formaldehyde for intracellular cytokine staining. For Annexin V staining, T cells were washed with HBSS buffer and resuspended in a HBSS solution containing FITC-labeled AnnexinV (eBioscience). The FACS measurements were performed by ARIA III and *FACSCalibur* flow cytometers (both BD) followed by analysis using FlowJ_V10 software (TreeStar). The following antibodies were used

for the FACS staining: anti-CD3 (145-2C11, 1:300), anti-CD4 (RM4-5, 1:300), anti-CD8 (53-6.7, 1:300), anti-CD19 (clone 1D3/CD19, 1:300), anti-CD45.1 (A20, 1:300), anti-CD25 (PC61.5, 1:300), anti-IFN-γ (XMG1.2, 1:300), anti-TNF-α (MP6-XT22, 1:300) and anti-granzyme B (16G6, 1:300). Transcription factors were detected using the Foxp3 staining kit (eBioscience) as well as anti-Eomes (Dan11mag, 1:200) and anti-T-bet (eBio4B10, 1:200) antibodies. For human T cells, anti-human IFN-γ (4S.B3, 1:50), anti-human CD25 (M-A251, 1:50), anti-human CD69 (FN50, 1:50), anti-human CD8 (SK1, 1:100) and anti-human/mouse granzyme B (QA16A02, 1:50) were used. For phospho-stainings, anti-phospho-STAT5 (Tyr694) (SRBCZX, 1:20), anti-phospho-mTOR (Ser2448) (MRRBY, 1:20) and anti-phospho-S6 (Ser235/236, 1:20) (cupk43k, 1:20) were used. All antibodies were purchased from eBioscience, BD Biosciences, Invitrogen or BioLegend. The gating/sorting strategies for the FACS analysis of T cells are provided in Supplementary Fig. 10. For data collection, Cell Quest Pro version 5.1 and BD FACSDiva 6.1.3 were used. Analysis of flow cytometry data was performed with FlowJoV10.

Intracellular phospho-staining. $CD8^+$ T cells were isolated as described above and activated for three days in absence or presence of 2.5 mM pentanoate. Cells were harvested, washed in PBS and rested for 4 h in RPMI at 37 °C. After 4 h resting, cells were kinetically incubated with 50 U/ml IL-2. The reaction was stopped by washing the samples with cold PBS on ice and subsequent fixation with 2% formaldehyde solution for 10 min at 37 °C. Permeabilisation was performed for 30 min by slow addition of 98% methanol (−20 °C) to a final concentration of 90% on ice. The samples were pelletized and washed in phospho-washing buffer (PBS, 2% FCS, 0.2% Tween-20). The cells were stained by incubation with the respective antibody for 45-60 min at RT. 1 ml of phospho-washing buffer was added for 10 min at RT prior to washing and further analysis.

Measurement of ECAR. Murine CTLs were cultured with or without pentanoate (2.5 mM) for three days. ECAR was measured with the XF96 Analyzer (Seahorse Biosciences). 2×10^5 CTLs/well were used for ECAR analysis. Basal ECAR reading was carried out with T cells grown in base DMEM without addition of glucose. ECAR was measured under basal conditions and in response to glucose (10 mM), oligomycin (2 μM, Seahorse Biosciences), and 2-deoxy-glucose (2-DG, 100 mM).

ELISA. TNF-α secretion from murine T cell cultures was detected by the mouse TNF-α Mouse ELISA kit (Invitrogen) according to the manufacturer's instructions. For human $CD8^+$ T cells, IL-2, IFN-γ, and TNF-α secretion was detected by ELISA (Biolegend). Absorbance was measured using a FLUOstar Omega ELISA plate reader (BMG Labtech).

Generation of a ROR1-expressing pancreatic tumor cell line. Panc02 cells were cultured in RPMI. The cells were harvested and 1×10^5 cells in 500 μl medium with 5 μg/ml polybrene seeded in 24-well plates. Lentivirus was added to a final MOI of 10. The cells were washed 48 h after transduction and expanded for 7 days. $ROR1^+$ cells were sorted and expanded for experiments.

Production of retroviral supernatant. The R11-ROR1-specific CAR containing the IgG4 hinge-CH2-CH3, CD28 transmembrane domain, and a signaling module comprising the cytoplasmatic domains of 4-1BB and CD3z was described earlier[45]. A similar ROR1 CAR except containing the murine CD28, 4-1BB, and CD3ζ was constructed. As a transduction marker, a tCD19 marker separated from the CAR by a T2A ribosomal skip element was used. The sequence was cloned into the MP71 retroviral vector to create MP71-R11-CD19t. For production of retroviral supernatant, Platinum-E cells for retroviral packaging were co-transfected with MP71-R11-CD19t and the retroviral packaging construct pCL-10A1, using the Effectene transfection reagent (QIAGEN) according to the manufacturer's instructions. Supernatants were collected 2 and 3 days after transfection.

Murine CAR T cell generation. $CD8^+$ T lymphocytes were purified from spleens of C57/BL6 mice by positive selection with CD8a (Ly-2) Microbeads (Miltenyi Biotec) with high purity (90–95 %). T cells were activated with plate-bound anti-mouse CD3ε (2 μg/ml, clone 145-2C11) and anti-mouse CD28 (2 μg/ml clone 37.51) antibodies in presence of 50 U/ml IL-2. 24 h and 48 h after activation, T cells were transduced in retroviral supernatant supplemented with 10 μg/ml polybrene by centrifugation at 2500 rpm for 90 min at 32 °C. For expansion, CAR T cells were cultured in medium supplemented with 50 U/ml IL-2, IL-7 (10 ng/ml) and IL-15 (10 ng/ml). CAR-modified T cells were enriched by immunomagnetic selection using anti-mouse CD19-PE antibody (clone 1D3/CD19) and anti-PE microbeads (Miltenyi Biotec).

Human CAR T cell generation. T cells for CAR modification were isolated from the peripheral blood of healthy donors. All participants provided written informed consent to participate in research protocols approved by the Institutional Review Board of the University of Würzburg (146/17-me). Peripheral blood mononuclear cells (PBMCs) were isolated by Ficoll-Paque density gradient centrifugation. $CD8^+$ T cells were isolated by magnetic-bead separation ($CD8^+$ T cells Isolation Kit, Miltenyi Biotech). 1×10^6–2×10^6 isolated $CD8^+$ T cells were stimulated with CD3/CD28 Dynabeads (Thermo Fisher Scientific) at a 1:1 bead to cell ratio in presence of 50 U/ml IL-2. Two days post-activation, nucleofection of the cells was performed by addition of 1 μg of the sleeping beauty vector pT2/HB (Addgene #26557) containing the CAR construct and 0.5 μg minicircle DNA encoding the SB100X transposase to the transfection medium. Electroporation was performed according to the manufacturer's protocol using the 4D-Nucleofector™ (Lonza, program CL-120). The electroporated cells were then transferred to a 48-well plate with 0.9 ml pre-warmed CTL medium and a half medium change with CTL supplemented with 100 U/ml recombinant human IL-2 was performed after 3 h. CD3/CD28 Dynabeads were removed magnetically five days after transfection. Transfection efficiency was assessed the day after bead removal by flow cytometry via staining of the EGFRt transfection marker with AF647-conjugated anti-EGFRt mAb (Cetuximab, Eli Lilly; conjugated in-house, 1:100). A scheme illustrating the structure of the CAR construct is provided in Supplementary Fig. 11.

Enrichment and antigen-independent expansion of human CAR T cells. Two days after removal of the CD3/CD28 Dynabeads, CAR^+ T cells were enriched by positive selection of the EGFRt transfection marker via immunomagnetic bead separation. $EGFRt^+$ T cells were frozen or used directly for antigen-independent expansion. Following enrichment, 1×10^5 CAR T cells, 5×10^6 irradiated TM-LCL and 3×10^7 irradiated PBMCs were mixed and seeded in 25 cm^2 cell culture flasks with OKT3 (f.c. 30 ng/ml) in a total volume of 20 ml and incubated at 37 °C. CAR T cells were expanded for 10 days applying full and half medium changes.

Functional analysis of human CAR T cells. After expansion, CAR T cells were treated with increasing concentrations of pentanoate. 4 days after treatment, the cells were washed and stained with 0.1 μM CFSE prior to co-culture with irradiated (80 Gy) ROR1-expressing K562 target cells at 4:1 E:T ratio for 72 h. Finally, proliferation was analyzed by flow cytometry. In order to determine cytokine secretion and surface marker expression, pretreated CAR T cells were co-cultured with target cells for 24 h. at 4:1 E:T ratio at 37 °C. Subsequently, the production of IL-2, IFN-γ, and TNF-α was analyzed in the supernatants by ELISA (Biolegend) according to the factory protocol. Surface marker expression was investigated by antibody staining followed by flow cytometry. The cytotoxic capacity of CAR T cells was determined by using a biophotonic assay based on the lysis of firefly luciferase/GFP (ffluc/GFP) transduced target cells. CAR T cells and 5×10^3 $ffluc^+/GFP^+$ target cells were plated in different E:T ratios in 96-well white flat bottom plates with LCL medium containing 150 μg/ml D-luciferin substrate. The plate was incubated for 24 h at 37 °C while the luminescence signal was measured at different time points using the Infinite 200 PRO plate reader (Tecan, Männedorf, Switzerland). Lysis mediated by CAR T cells was calculated as the reduction of luminescence signal by effector cells compared to mock transfected cells: Specific Lysis [%] = Mean ((lysis by mock cells) − Single value (lysis by CAR T cells)/Mean (lysis by mock cells)) × 100.

Bacterial culture and cell-free supernatant collection. Pure cultures *of Escherichia coli* NCIMB 12210, *Enterococcus faecalis* NCIMB 13280, *Bacteroides fragilis* DSM 2151, *B. vulgatus* DSM 1447, *B. ovatus* DSM 1896, *Megasphaera massiliensis* DSM 26228, *M. elsdenii* NCIMB 8927, *M. massiliensis* NCIMB 42787, *Bifidobacterium breve* DSM 20213, *B. longum subsp. longum* DSM 20219, *Faecalibacterium prausnitzii* DSM17677, *Anaerostipes hadrus* DSM 3319, *Blautia coccoides* DSM 935, *Dorea longicatena* DSM 13814, *Parabacteroides distasonis* DSM 20701, *Faecalicatena contorta* DSM3982 *and Ruminococcus gnavus* ATCC29149 were grown anaerobically in YCFA + broth [Per litre: casein hydrolysate 10.0 g, yeast extract 2.5 g, sodium hydrogen carbonate 4.0 g, glucose 2.0 g, cellobiose 2.0 g, soluble starch 2.0 g, di-potassium hydrogen phosphate 0.45 g, potassium di-hydrogen phosphate 0.45 g, resazurin 0.001 g, L-cysteine HCl 1.0 g, ammonium sulphate 0.9 g, sodium chloride 0.9 g, magnesium sulphate 0.09 g, calcium chloride 0.09 g, haemin 0.01 g, SCFAs 3.1 ml (acetic acid 2.026 ml/L, propionic acid 0.715 ml/L, n-valeric acid 0.119 ml/L, iso-valeric acid 0.119 ml/L, Iso-butyric acid 0.119 ml/L), vitamin mix 1: 1 ml (biotin 1 mg/100 ml, cyanocobalamine 1 mg/100 ml, p-aminobenzoic acid 3 mg/100 ml, pyridoxine 15 mg/100 ml), vitamin mix 2:1 ml (thiamine 5 mg/100 ml, riboflavin 5 mg/100 ml), vitamin mix 3:1 ml (folic acid 5 mg/100 ml)] until they reached their stationary growth phase. Cultures were centrifuged at 5000 × *g* for 10 min and the cell-free supernatant (CFS) was filtered using a 0.45 μm followed by a 0.2 μm filter (Millipore). 1 mL aliquots of the CFS were stored at −80 °C until further use. In some experiments, filter-sterilized supernatant of *Megasphaera massiliensis* DSM 26228 were used at 1:40 or 1:20 supernatant to cell media ratio to treat CTLs.

Measurement of fatty acids in bacterial supernatants. The composition of SCFAs and MCFAs in bacterial supernatants was determined by MS Omics APS, Denmark. Following acidification with hydrochloride acid, internal standards with deuterium labeling were administered. All samples were randomized prior to analysis. The experimental setup comprised of a high-polarity column (Zebron™ ZB-FFAP, GC Cap. Column 30 m × 0.25 mm × 0.25 μm) inserted in a gas chromatograph (7890B, Agilent) connected to a quadropole detector (5977B, Agilent) under system control of the Agilent ChemStation. The Agilent ChemStation was

further used to convert raw data into netCDF format prior to processing in Matlab R2014b (Mathworks, Inc.) using the PARADISe software as described previously[46].

Pan-HDAC and specific HDAC activity assays. Murine or human CD8$^+$ T cells were harvested in the lysis buffer, and 100 µl of cell lysates were subjected to HDAC inhibition by adding 5 mM of SCFAs (or 500 nM TSA) for 15 min. Following initial inhibition of HDACs by SCFAs, the peptide substrate Ac-Arg-Gly-Lys(Ac)-AMC (300 µM, Bachem, Bubendorf, Switzerland) was added to the reaction tubes for 30 min. The cleavage of the deacetylated substrate was achieved by addition of 100 µl of the developer solution (10 mg/ml trypsin in 50 mM Tris-HCl, pH = 8, 100 mM NaCl, 2 µM TSA) for 30 min at 37 °C. The fluorescence intensity of free AMC was measured at Ex/Em = 355 nm/460 nm. For the impact of bacterial supernatants and SCFAs on specific HDAC isoforms, the fluorogenic assay for each HDAC enzyme (HDAC1-3, HDAC4-6, HDAC9) was used (BPS Bioscience). Assays were performed according to the manufacturer's instructions and all measurements were conducted in triplicate using the Omega series Software V5.5, MARS 3.32 R5.

Statistical analysis. Means of two groups were analyzed by using an unpaired Student's *t*-test (GraphPad Prism 8). *P* values of $p < 0.05$ were considered significant. Where appropriate, data are presented as mean ± s.e.m. For comparison of multiple experimental groups, data were analyzed using a linear-mixed effects model with Tukey correction.

Reporting summary. Further information on research design is available in the Nature Research Reporting Summary linked to this article.

Data availability

The authors declare that data supporting the findings of this study are available within the Article and its Supplementary information files. Source data are provided with this paper.

Received: 6 April 2020; Accepted: 8 June 2021;
Published online: 01 July 2021

References

1. Sivan, A. et al. Commensal Bifidobacterium promotes antitumor immunity and facilitates anti-PD-L1 efficacy. *Science* **350**, 1084–1089 (2015).
2. Matson, V. et al. The commensal microbiome is associated with anti-PD-1 efficacy in metastatic melanoma patients. *Science* **359**, 104–108 (2018).
3. Routy, B. et al. Gut microbiome influences efficacy of PD-1-based immunotherapy against epithelial tumors. *Science* **359**, 91–97 (2018).
4. Zitvogel, L., Ma, Y., Raoult, D., Kroemer, G. & Gajewski, T. F. The microbiome in cancer immunotherapy: diagnostic tools and therapeutic strategies. *Science* **359**, 1366–1370 (2018).
5. Wang, Y., Ma, R., Liu, F., Lee, S. A. & Zhang, L. Modulation of gut microbiota: a novel paradigm of enhancing the efficacy of programmed death-1 and programmed death ligand-1 blockade therapy. *Front. Immunol.* **9**, 374 (2018).
6. Vetizou, M. et al. Anticancer immunotherapy by CTLA-4 blockade relies on the gut microbiota. *Science* **350**, 1079–1084 (2015).
7. Tanoue, T. et al. A defined commensal consortium elicits CD8 T cells and anti-cancer immunity. *Nature* **565**, 600–605 (2019).
8. Skelly, A. N., Sato, Y., Kearney, S. & Honda, K. Mining the microbiota for microbial and metabolite-based immunotherapies. *Nat. Rev. Immunol.* **19**, 305–323 (2019).
9. Mager, L. F. et al. Microbiome-derived inosine modulates response to checkpoint inhibitor immunotherapy. *Science* **369**, 1481–1489 (2020).
10. Arpaia, N. et al. Metabolites produced by commensal bacteria promote peripheral regulatory T-cell generation. *Nature* **504**, 451–455 (2013).
11. Smith, P. M. et al. The microbial metabolites, short-chain fatty acids, regulate colonic Treg cell homeostasis. *Science* **341**, 569–573 (2013).
12. Furusawa, Y. et al. Commensal microbe-derived butyrate induces the differentiation of colonic regulatory T cells. *Nature* **504**, 446–450 (2013).
13. Park, J. et al. Short-chain fatty acids induce both effector and regulatory T cells by suppression of histone deacetylases and regulation of the mTOR-S6K pathway. *Mucosal Immunol.* **8**, 80–93 (2015).
14. Park, J., Goergen, C. J., HogenEsch, H. & Kim, C. H. Chronically elevated levels of short-chain fatty acids induce T cell-mediated ureteritis and hydronephrosis. *J. Immunol.* **196**, 2388–2400 (2016).
15. Kespohl, M. et al. The microbial metabolite butyrate induces expression of Th1-associated factors in CD4+ T Cells. *Front. Immunol.* **8**, 1036 (2017).
16. Marino, E. et al. Gut microbial metabolites limit the frequency of autoimmune T cells and protect against type 1 diabetes. *Nat. Immunol.* **18**, 552–562 (2017).
17. Mathewson, N. D. et al. Gut microbiome-derived metabolites modulate intestinal epithelial cell damage and mitigate graft-versus-host disease. *Nat. Immunol.* **17**, 505–513 (2016).
18. Trompette, A. et al. Dietary fiber confers protection against flu by shaping Ly6c(−) patrolling monocyte hematopoiesis and CD8(+) T cell metabolism. *Immunity* **48**, 992–1005.e1008 (2018).
19. Bachem, A. et al. Microbiota-derived short-chain fatty acids promote the memory potential of antigen-activated CD8(+) T cells. *Immunity* 51, 285–297.e5. (2019).
20. Luu, M. et al. The short-chain fatty acid pentanoate suppresses autoimmunity by modulating the metabolic-epigenetic crosstalk in lymphocytes. *Nat. Commun.* **10**, 760 (2019).
21. Yuille, S., Reichardt, N., Panda, S., Dunbar, H. & Mulder, I. E. Human gut bacteria as potent class I histone deacetylase inhibitors in vitro through production of butyric acid and valeric acid. *PLoS ONE* **13**, e0201073 (2018).
22. Padmanabhan, R. et al. Non-contiguous finished genome sequence and description of *Megasphaera massiliensis* sp. nov. *Stand. Genomic. Sci.* **8**, 525–538 (2013).
23. Koh, A., De Vadder, F., Kovatcheva-Datchary, P. & Backhed, F. From dietary fiber to host physiology: short-chain fatty acids as key bacterial metabolites. *Cell* **165**, 1332–1345 (2016).
24. Chang, C. H. et al. Posttranscriptional control of T cell effector function by aerobic glycolysis. *Cell* **153**, 1239–1251 (2013).
25. Peng, M. et al. Aerobic glycolysis promotes T helper 1 cell differentiation through an epigenetic mechanism. *Science* **354**, 481–484 (2016).
26. Qiu, J. et al. Acetate promotes T cell effector function during glucose restriction. *Cell Rep.* **27**, 2063–2074 (2019). e2065.
27. Cham, C. M. & Gajewski, T. F. Glucose availability regulates IFN-gamma production and p70S6 kinase activation in CD8+ effector T cells. *J. Immunol.* **174**, 4670–4677 (2005).
28. Kim, M., Qie, Y., Park, J. & Kim, C. H. Gut microbial metabolites fuel host antibody responses. *Cell Host Microbe* **20**, 202–214 (2016).
29. Balmer, M. L. et al. Memory CD8(+) T cells require increased concentrations of acetate induced by stress for optimal function. *Immunity* **44**, 1312–1324 (2016).
30. Coutzac, C. et al. Systemic short chain fatty acids limit antitumor effect of CTLA-4 blockade in hosts with cancer. *Nat. Commun.* **11**, 2168 (2020).
31. Spolski, R., Li, P. & Leonard, W. J. Biology and regulation of IL-2: from molecular mechanisms to human therapy. *Nat. Rev. Immunol.* **18**, 648–659 (2018).
32. Srivastava, S. et al. Logic-gated ROR1 Chimeric antigen receptor expression rescues T cell-mediated toxicity to normal tissues and enables selective tumor targeting. *Cancer Cell* **35**, 489–503.e488 (2019).
33. Hudecek, M. et al. Receptor affinity and extracellular domain modifications affect tumor recognition by ROR1-specific chimeric antigen receptor T cells. Clinical cancer research: an official journal of the American Association for. *Cancer Res.* **19**, 3153–3164 (2013).
34. Wallstabe, L. et al. ROR1-CAR T cells are effective against lung and breast cancer in advanced microphysiologic 3D tumor models. *JCI Insight* **4**, e126345 (2019).
35. Nicolas, G. R. & Chang, P. V. Deciphering the Chemical Lexicon of Host-Gut Microbiota Interactions. *Trends Pharmacol. Sci.* **40**, 430–445 (2019).
36. Haenen, D. et al. A diet high in resistant starch modulates microbiota composition, SCFA concentrations, and gene expression in pig intestine. *J. Nutr.* **143**, 274–283 (2013).
37. Dorrestein, P. C., Mazmanian, S. K. & Knight, R. Finding the missing links among metabolites, microbes, and the host. *Immunity* **40**, 824–832 (2014).
38. Haghikia, A. et al. Dietary Fatty Acids Directly Impact Central Nervous System Autoimmunity via the Small Intestine. *Immunity* **44**, 951–953 (2016).
39. Preglej, T. et al. Histone deacetylases 1 and 2 restrain CD4+ cytotoxic T lymphocyte differentiation. *JCI Insight* **5**, e133393 (2020).
40. Kim, M. H., Kang, S. G., Park, J. H., Yanagisawa, M. & Kim, C. H. Short-chain fatty acids activate GPR41 and GPR43 on intestinal epithelial cells to promote inflammatory responses in mice. *Gastroenterology* **145**, 396–406 (2013). e391-310.
41. Brown, A. J. et al. The Orphan G protein-coupled receptors GPR41 and GPR43 are activated by propionate and other short chain carboxylic acids. *J. Biol. Chem.* **278**, 11312–11319 (2003).
42. Ray, J. P. et al. The interleukin-2-mTORc1 kinase axis defines the signaling, differentiation, and metabolism of T helper 1 and follicular B helper T cells. *Immunity* **43**, 690–702 (2015).
43. Mestermann, K. et al. The tyrosine kinase inhibitor dasatinib acts as a pharmacologic on/off switch for CAR T cells. *Sci. Transl. Med.* **11**, eaau5907 (2019).
44. Prommersberger, S. et al. CARAMBA: a first-in-human clinical trial with SLAMF7 CAR-T cells prepared by virus-free Sleeping Beauty gene transfer to treat multiple myeloma. *Gene Ther.* https://doi.org/10.1038/s41434-021-00254-w (2021).

45. Hudecek, M. et al. The nonsignaling extracellular spacer domain of chimeric antigen receptors is decisive for in vivo antitumor activity. *Cancer Immunol. Res.* **3**, 125–135 (2015).
46. Johnsen, L. G., Skou, P. B., Khakimov, B. & Bro, R. Gas chromatography—mass spectrometry data processing made easy. *J. Chromatogr. A* **1503**, 57–64 (2017).

Acknowledgements

We would like to thank Anne Hellhund for excellent technical support and research group A. Beilhack for providing us with OT-I mice. The technical expertise in breeding and maintaining of SPF and GF animals by staff of animal facility, Biomedical Research Center, Philipps-University of Marburg, is gratefully acknowledged. We also thank Suchita Panda, Christoph Mörtelmaier, and Iain Robertson from 4D Pharma Research Ltd. for their technical support. We are grateful to Michael Lohoff (Philipps-University of Marburg), Julia Benzel (DKFZ Heidelberg), Felix Schneider (Philipps-University of Marburg), Wolfgang Bywalez and Andrew Kaiser (Miltenyi Biotec GmbH) for helpful discussions. This project is supported by the Von Behring-Röntgen-Stiftung (Maik Luu and Ulrich Steinhoff), Stiftung PE Kempkes (Maik Luu), German Cancer Aid (Deutsche Krebshilfe e. V., Max Eder Program, grant no. 70110313 to Michael Hudecek), FAZIT-Stiftung (Hanna Leister and Alexander Visekruna) and the German Research Foundation (grants DFG-KFO325 to Thomas M Gress, Matthias Lauth, Christian A Bauer, Felix Picard, Magdalena Huber and Alexander Visekruna, DFG SFB1292 TP01 to Tobias Bopp, as well as DFG SFB/TRR 221, project no. 324392634 to Michael Hudecek).

Author contributions

A.V., U.S., M. Hudecek, I.E.M., T.B., and T.M.G. designed and planned the study. M. Hudecek, T.N., Z.R., M. Luu, and A.V. wrote the article. M. Luu, N.R., S. Y., M.K., A.W., H.L., H.R., K.M., K.O., and C.A.B. performed in vitro experiments and analyzed the data. M. Luu, Z.R., R.R., F.P., F.F., M. Huber, and M. Lauth designed and carried out in vivo experiments. T.N and A. Baldrich performed the experiments with human CAR T cells. A. Busetti conducted the GC-MS analysis. Z.R. and A. Baldrich contributed equally to the manuscript.

Funding

Open Access funding enabled and organized by Projekt DEAL.

Competing interests

M.L., M. Hudecek, and A.V. are inventors on a patent application related to the use of pentanoate that has been filed by Philipps-University Marburg and Julius-Maximilians University Würzburg (WO2021/058811A1). The title of the patent application is the following one: "Short-chain fatty acid pentanoate as enhancer for cellular therapy and anti-tumor therapy". All other authors have no competing interests.

Additional information

Supplementary information The online version contains supplementary material available at https://doi.org/10.1038/s41467-021-24331-1.

Correspondence and requests for materials should be addressed to M.H. or A.V.

Peer review information *Nature Communications* thanks Reno Debets and the other, anonymous reviewer(s) for their contribution to the peer review of this work. Peer review reports are available.

Reprints and permission information is available at http://www.nature.com/reprints

Publisher's note Springer Nature remains neutral with regard to jurisdictional claims in published maps and institutional affiliations.

Open Access This article is licensed under a Creative Commons Attribution 4.0 International License, which permits use, sharing, adaptation, distribution and reproduction in any medium or format, as long as you give appropriate credit to the original author(s) and the source, provide a link to the Creative Commons license, and indicate if changes were made. The images or other third party material in this article are included in the article's Creative Commons license, unless indicated otherwise in a credit line to the material. If material is not included in the article's Creative Commons license and your intended use is not permitted by statutory regulation or exceeds the permitted use, you will need to obtain permission directly from the copyright holder. To view a copy of this license, visit http://creativecommons.org/licenses/by/4.0/.

© The Author(s) 2021